Earth-Space Cross-Pollination: *Synergies between the terrestrial raw materials value chain and the development of space resources. Links to Sustainability.*

Aaron Sediles Martinez – Geologist & Raw Materials Sustainability MSc

ajsedilesm.un@gmail.com

Introduction

From the limestones in the pyramids of Egypt, to the gold in the James Web Space Telescope, everything we do ultimately relies on resources that for now, have come all from the Earth. Our material reliance has grown together with the advancement of society. The increased variety of technology-based products and services that each new generation has enjoyed, has in turn implied an increased variety or materials needed. Moreover, the current context of green transition exacerbates the issue of our dependence on Earth materials. Several critical materials will be needed to sustain our modern society. However, extracting such materials can pose risks to the environment and new low impact solutions are needed. This has sparked numerous innovations in one of the oldest industries on Earth, the Raw Materials industry.

Looking up to the realm of space resources can provide a scene of mutual benefit for two industries with great points in common. Here are showcased the terrestrial resources value chain and some recent sustainability innovations and challenges which can be expanded to possible commonalities with the space resources field. From resource exploration to material refining, passing through dust control and the use of bacterium for resource recovery, highlighting how these could be useful for the Space resources field.

Similarly, we will explore how the terrestrial resources industry can potentially benefit from the advances in space resources. Space is arguably the toughest and most difficult environment humans have ever attempted to operate in. Being far from the security of our planet gives little to no room for waste or failure and has meant the development of the most advanced approaches in terms of autonomous operations and robotics, safety, and resource efficiency to name a few. Making progress in space technologies can help us land impactful breakthroughs for society on Earth as well, the sole concept of In-Situ Resource Utilization holds potential of improving the way we manage the materials we use to enable all in our daily lives.

Space resources and Earth resources, both resources for the advancement of human civilization. In the same way we developed out of the stone age to what we are today, the realm of space can build upon the knowledge already created on Earth and launch us to new heights.

Terrestrial Raw Materials Value Chain:

The raw materials value chain. The loop represents the circular economy (EIT Raw Materials 2018)

Earth resources challenges:

- Water intensity
- Dust control
- Release of pollutants
- Social license to operate
- Increasingly lower grades and more challenging environments
- Energy consumption
- Invasive operations

Recent sustainability approaches Bioleaching:

Traditionally, there are two routes to the extraction process of elements from ores (minerals containing the element of interest) a hydrometallurgy route generally associated with oxides, which involves the dissolution of ores in acids; and a pyrometallurgical route, generally utilized to extract metals from insoluble sulfides, currently the standard process in copper production for example. This last route, however, requires a great amount of water for the flotation process and produces big amounts of waste that needs to be stored in dams, and most importantly, it is very energy intensive in the smelting stage. The use of Bacteria consortia to process these kind of minerals is now a proven alternative, although some time constrains have been noted.

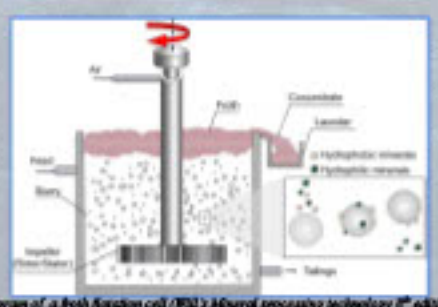

Diagram of a flotation cell (Wills' Mineral processing technology 8th edition)

Resource recovery from waste

As seen in the value chain diagram, all the stages of the raw materials life-cycle produce some kind of waste. This is a persistent issue that has always existed and the recovery of value from waste is a field of constant development. Some examples include the utilization of metallurgical slag to produce construction materials, which in some cases have even proved to store carbon within their structure. Another example is the extraction of Rare Earth Elements from minerals contained in tailings from mines, minerals that before were not considered valuable.

Mining as a service

A change in business model has been proposed by distinct academics and industry experts. A shift from shareholders centrism to stakeholders' centrism where mining operations are run thinking not only thinking on revenue and with a mega scale mentality but in a manner where modular smaller operations are possible that considers the interest of all those affected by the operation.

Dry mineral processing

In order to extract metals from ores, it is first necessary to do size reduction to liberate the mineral of interest from the non target minerals and then separate the ore from the gangue. This two processes, comminution and flotation can be water intense. A current area of research to decrease the water need includes things like gravity separation, magnetic separation, electrostatic separation,

Ore particles after comminution (Wills' Mineral Processing Technology 8th edition)

Full life cycle perspective

Thinking of the materials involved in everything we do with a life cycle perspective allows to detect hot spots of environmental impact in areas beyond global warming. This is possible through the establishment of specific system boundaries, a unit to make impact calculations and the investigation on the different impact categories.

Automation in waste sorting and recycling.

The shift to a circular economy where all the resources are kept in a looping system will be a crucial step for humanity to continue to exist. Materials do not stop being resources after a product has been made or after it has completed its service life. This same approach should be carried to space. Automatic material identification and sorting systems exist today to separate complex streams of waste for adequate recycling, using for example combinations of Xray scanning, photography and AI. As do things here on Earth Space infrastructure and devices, eventually reach an end of life, making the recycling approaches in place here, relevant for space.

Space Resources Utilization General Flowchart

(A universal framework for Space Resource Utilization (SRU)-Hadler et al. 2020)

Space resources challenges examples

- Most challenging environment ever attempted
- Different gravity and atmospheric characteristics
- Cyclic temperature variations
- Electrostatically properties of regolith
- Value chain at the initial stages
- Big scale continuous operation in space has many unknowns
- High costs involved
- Need for human presence?
- Remote Maintenance
- Consumables?
- Space environmentalism

Potential Cross-Pollination opportunities:

In an environment where scarcity is at its highest, the advances already made on Earth will turn crucial for space and vice versa, the expansion of such techniques in space will mean giant leaps on Earth. Additionally, being space the hardestt environment we have ever ventured to, where no waste can be allowed and where there is little room for errors, the development of the Space Resources Field will sure bring back to Earth a multitude of benefits.

Areas of potential knowledge exchange

- ISRU vs Not in my backyard
- Resource exploration and extraction
- Robotics, automation and safety
- Clean energy
- Water use reduction
- Increasee of autonomous & non-invasive operations
- Challenging operational environments
- Dust control
- Innovation in construction

Robotic dog and drone used in mining in the north of Sweden by LKAB (image taken from MiningDig.com)

SINReM

Let's Connect!

Linked in

In-Situ Propellants for Electric Propulsion

Adam Parks, Vlad George-Tirila and Dr Charlie Ryan, University of Southampton
A.Parks@soton.ac.uk

The focus of this project is to design, manufacture and test Hall effect thrusters, a type of electric propulsion technology, using propellants that can be obtained in-situ on the Moon.

Hall Effect Thrusters
- Most used spacecraft propulsion type
- High Isp: low propellant consumption
- Uses electrical power

Applications
- Interplanetary tranfers
- Attitude and orbit control
- Moon-Earth transfers

Magnesium and calcium have been identified as the best-performing propellant options. The fact that these are stored as a solid presents additional difficulties compared to typical gaseous propellants such as xenon and krypton. The propellant must be vaporised and fed into the thruster propellant distributer without condensing, requiring the use of heaters. Calcium has never been tested in a Hall thruster, and test data using magnesium is very limited.

Hall thruster working principle

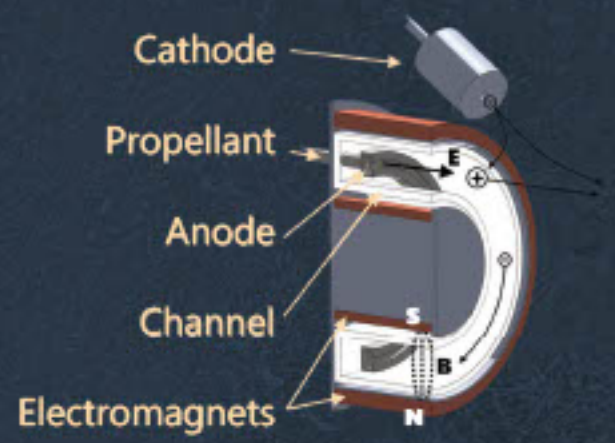

Primary propellant candidates

	Magnesium	Calcium
Lunar regolith %wt	~5%	~5%
Atomic mass	24	40
First ionisation energy	7.6 eV	6.1 eV
Peak cross section	5.3 Å²	8.7 Å²
Density STP	1.7 g/cm³	1.6 g/cm³
Melting point	650°C	842°C
Vapour pressure @m.p.	384 Pa	211 Pa
Possible extraction	FFC Cambridge process	

Example mission scenario:
15-year lunar gateway orbit maintenance

	Xe	Kr	Ca	Mg
Propellant mass (kg)	1600	1273	876	681
Propellant volume (L)	769	1415	565	392
Ideal Isp (s)	3025	3786	5474	7032
Ideal thrust (mN)	404	323	223	174

Hall Thruster set up to use propellants stored in solid form

Hall thruster operating on magnesium propellant

University of Southampton esa

LUXEMBOURG SPACE RESOURCES WEEK 2023

New Technological Approach for Improving the Thermionic Energy Conversion Efficiency for Space-Power Applications and Deep Space Exploration

Alexander Lukin

Western-Caucasus Research Center, Tuapse, 352808, Russian Federation

AIAA Solid Rockets Technical Committee

E-Mail: lukin@wcrc.ru

HARNESSING ENERGY IN SPACE

Abstract

For a number of space applications require power sources that deliver high power in reliable and sustained ways over long periods of time. The direct conversion of heat into electricity without any intermediate steps or moving parts remains one of the most promising but challenging methods of energy generation. The objective of the presented research is to solving a scientific problem - increasing the energy efficiency of the method of thermionic conversion of thermal energy into electrical energy through the creation and use of a new type of emission nanomaterials - multilayer carbyne-enriched 3D-shaped nano-interfaces and fine-tuning of their topological, physicochemical and functional characteristics.

Based on recently discovered fundamental phenomenon of collective atomic vibrations, manifested within transition domains of multilayer nanostructures, called phonon waves, we developed the new concept for improving the efficiency of thermionic energy converters by predictive functionality unlocking of the 2D-ordered linear-chain carbon-based multilayer emitters through excitation and fine-tuning the collective atomic vibrations and nanoarchitecture. For predictive excitation and adjustment, the interface effects, phonon waves propagation, energy exchange and synergistic effects provided by the multilayer nano-enhanced interfaces we propose using a combination of a set of techniques. The developed approach opens up the possibility of creating devices for thermionic energy conversion of a new type, the energy efficiency of which can significantly (by orders of magnitude) exceed the efficiency of existing plasma thermionic converters. Electricity generating sources based on a thermionic conversion are considered as basic options for the development of Lunar and Martian research missions.

Background

Despite having a huge potential as an efficient direct energy conversion device, the progress in vacuum-based thermionic energy converters development has always been hindered by the space charge effect and unavailability of materials with low work function. The creation of low work function materials is critical for power conversion and electron emission applications. The work function is, in fact, a measure of how intensely a particular material is able to hold its electrons. Emission electrons carry away a significant amount of thermal energy from the emitter, but only a part of it can be directly converted into electrical energy. Over the past few decades, carbon-based nanomaterials and, specifically, low-dimensional nanocarbon allotropes have revolutionized the field of materials science.

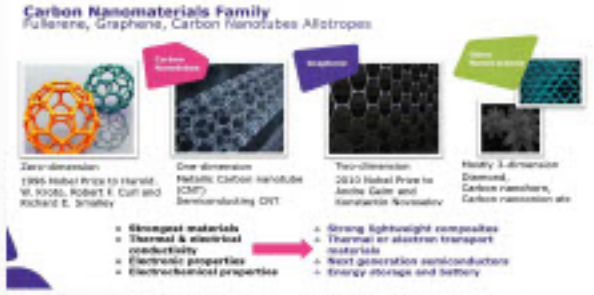

The "holy grail" of low-dimensional carbon allotropes, carbyne, represents a one-dimensional chain of carbon atoms.

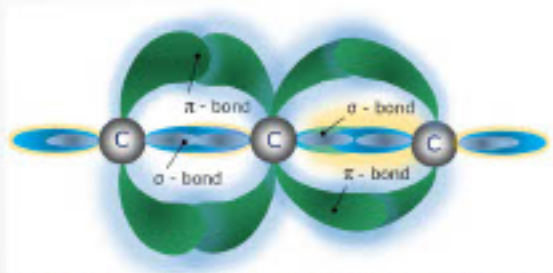

Fig. 1. The electronic structure of a fragment of a linear-chain carbon molecule section.

The advantage of carbyne for field emission applications is the high mobility of charge carriers and the strong anisotropy of the electrical resistance along the chains of carbon atoms and between the chains. Carbyne carbon chains are efficient electron emitters, and the crystalline phase has a low electron work function. The anomalously low work function of carbyne microcrystals can be explained by the superposition of the internal micro-fields of the carbon chains that make up the crystals. The growth of the macroscopic crystals of carbyne is inhibited by the instability and high reactivity of this allotropic form of carbon.

Relatively recently, an original route to compensate for the high reactivity of the carbon chains was found. In particular, a technique to encapsulate the oriented linear chains of carbon atoms into the matrix of amorphous carbon during the ion-assisted pulse-plasma deposition, was developed. In accordance with the features of the obtained spatial topology, the grown nano-matrix was named as an 2D-ordered linear-chain carbon. This new nanomaterial behaves as an excellent electron-field emitter owing to its exceptional properties and offers several benefits compared to traditional cathodes.

New Approaches and Methods

Since the origin of the physicochemical properties and functional characteristics of nanomaterials is at the atomic scale, the predictive manipulation of collective atomic vibrations within nanolayers is the key to designing multilayer emission nano-systems with unique properties. Based on recently discovered fundamental phenomenon of collective atomic vibrations, manifested within transition domains of multilayer nanostructures, called phonon waves, we developed the new concept for improving the efficiency of thermionic energy converters by predictive functionality unlocking of the 2D-ordered linear-chain carbon-based multilayer emitters through excitation and fine-tuning the collective atomic vibrations and nanoarchitecture.

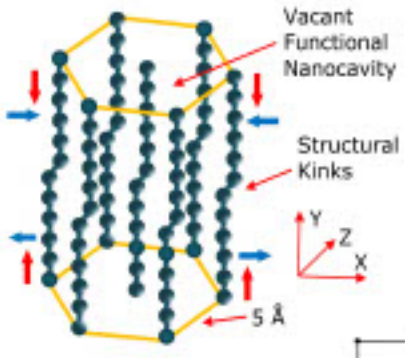

Fig. 2. Geometric characteristics of the two-dimensionally ordered linear-chain carbon nano-matrix.

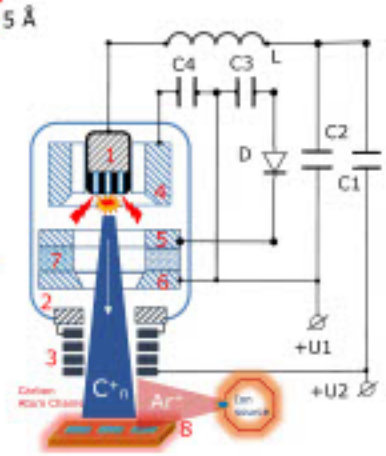

Fig. 3. Schematic representation of the pulse-plasma carbon generator that installed in the reactor of the experimental set-up.

The performance of devices for energy conversion is intimately linked to the ability of materials to form complex heterogeneous 3D-shaped interfaces. Planar nano-interfaces are considered as a "basis" that can be modified or upgraded to 3D-shaped nano-interfaces. Using the surface acoustic waves (SAW) allows to generate 3D-shaped nano-interfaces with complex geometry. For fine-tuning and programming of the nano-interface-based and synergistic effects (self-synchronization of collective atomic vibrations, phonon waves propagation, energy exchange) within the multilayer 3D-shaped nano-enhanced interfaces we developed a set of tool-kits: - initiation and programming of phase transformations in grown nano-layers by combining ion and electron irradiation with different doses; - heteroatomic doping with clusters of atoms of various chemical elements; - stimulation of the growing zone by surface-acoustic waves; - stimulation of the growing zone by remote exposure to high-frequency electromagnetic fields; - initiation in the zone of growing the phenomenon of "explosive" directional self-assembly of carbyne-enriched nanostructures; - the use of data-driven digital twins-based nanoscale manufacturing approach.

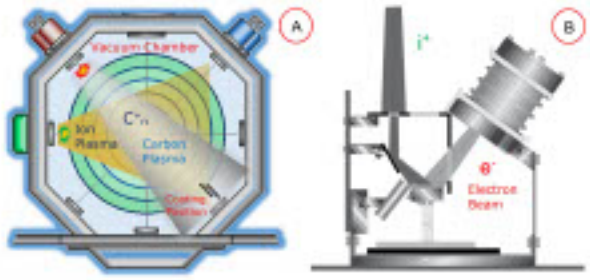

Fig. 4. Schemes of the experimental set-ups for concurrent electron beam and ion- irradiation of the 2D-ordered linear-chain carbon-based multilayer nano-enhanced interfaces: (A) - pulse-plasma deposition reactor; (B) – combination of the ion sputtering of a graphite target simultaneously with electron beam irradiation using an electron gun.

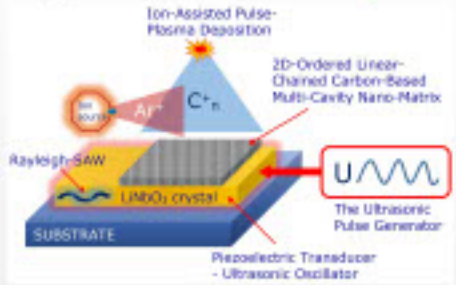

Fig. 5. Schematic representation of application of the inverse piezoelectric effect during the ion-assisted carbon pulse-plasma deposition.

Results

The scientific novelty of the research lies in the development of a new strategy for growing samples of emission nanomaterials of a new type - data-driven information technology tools and the development of advanced technological methods and methods for growing new types of multilayer emission nanomaterials with a programmable complex of unique structural and physicochemical properties that will become the basis to create promising systems for direct energy conversion.

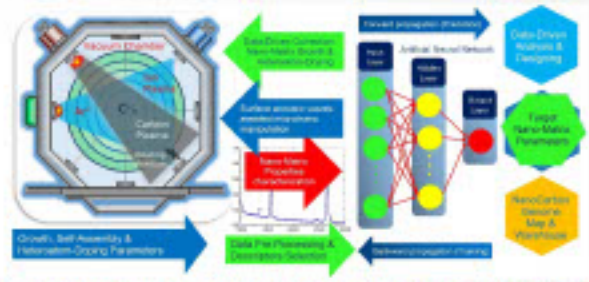

Fig. 6. Machine learning-based fine-tuning of the 3D-shaped nano-interfaces with complex geometry: a scheme of tracking and tailoring the key descriptors and linkages for incorporating into the data-driven carbon nanomaterials genome approach.

A set of interacting 3D-shaped nano-interfaces can be considered as nanodevices. The schematic representation of interactions of the effects and phenomena used for fine-tuning the artificially structured multi-layered transition nano-enhanced interfaces properties is presented in Figure 7.

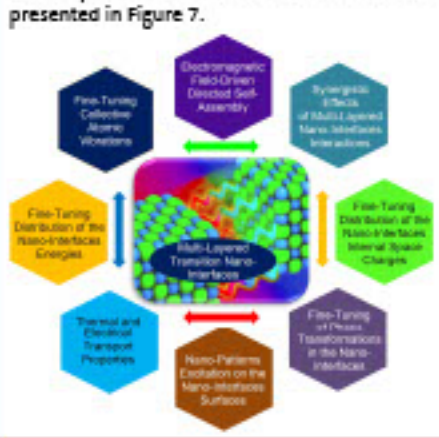

Fig. 7. Fine-tuning the artificially structured multi-layered transition 3D-shaped nano-enhanced interfaces properties and their synergistic effects.

Conclusion

We developed the new concept for improving the efficiency of thermionic energy converters by predictive unlocking the multilayer low-dimensional nano-carbon allotropes-based emitters functionality through excitation and fine-tuning the collective atomic vibrations, functionalities and nanoarchitecture. In particular, we propose using 2D-ordered linear-chain carbon-based multilayered nano-enhanced interfaces as well as their synergistic effects.

For predictive excitation and adjustment of the nano-interface-based and synergistic effects such as self-synchronization of collective atomic vibrations, phonon waves propagation and energy exchange within the multilayer 3D-shaped nano-enhanced interfaces we developed a set of tool-kits. In particular, these tool-kits include combination of a set of techniques:

- the energy-driven initiation of the allotropic phase transformations at concurrent electron beam and ion irradiation required for manipulating phonon waves propagation;
- the surface acoustic waves-assisted micro/nano- manipulation during the ion-assisted pulse-plasma growing combined with heteroatom doping;
- initiating directed self-assembly through application external high-frequency electromagnetic fields;
- using the data-driven digital twins-based nanoscale manufacturing approach.

The developed approach opens up the possibility of creating the thermionic energy conversion systems of a new type, the energy efficiency of which can significantly (by orders of magnitude) exceed the efficiency of existing systems.

Acknowledgments

The research work is jointly supported and funded by the Scientific and Technological Research Council of Turkey (TÜBİTAK) and the Russian Foundation for Basic Research (RFBR) according to the research project № 20-58-46014.

Questions? Please, kindly send at: lukin@wcrc.ru

WCRC.RU Western-Caucasus Research Center TUAPSE

Trade-off study for critical lunar infrastructure – landing pads

Authors: Alexandra ADIACONITEI, Aidan COWLEY

Corresponding: Alexandra ADIACONITEI, alexandra.adiaconitei@esa.int

Introduction

On the Moon surface, the critical infrastructure elements are exposed to the harsh environmental conditions:

- high temperature variations
- vacuum
- micrometeoroids
- radiation

Effects:
- ↗ Increased complexity of all manufacturing process
- ↘ Decreased survivability, sustainability and the operability of the critical infrastructure

Objectives

Landing pad – indispensable facility to a permanent Moon base ensuring a safe landing and take-off – and mitigating the dust plume problem [1].

- embody previous research on the topic into a functional solution;
- develop and investigate concepts with low-TRL and low-cost processes that can provide efficient results;
- Provide a concept based on a holistic level

Methods:

Process definition:

SITE SELECTION Select a suitable location that is relatively flat, stable, and free from obstacles

SITE PREPARATION Excavate, level and compact the soil to create a flat surface for the landing pad

ISRU PROCESS Utilize in situ lunar resources for constructions

→Reinforcement to provide additional stability and withstand the harsh lunar environment (metal or polymer rods, or by mixing fibbers or other additives with the regolith)

→Assembling - modular or prefabricated components

Trade-off Analysis criteria:

Pre-Manufacturing Phase criteria:
- Landing location
- Dependency on Earth resources
- ISRU difficulty level
- Power required

Manufacturing Phase criteria:
- Heritage/TRL
- Process complexity level
- Power required
- Manufacturing time
- Scalability

Post-Manufacturing Phase criteria:
- Performance
- Reusability
- Sustainability
- Maintenance

References:
[1] Metzger, P.T., Dust Transport and Its Effect Due to Landing Spacecraft (2020), LPI Contribution No. 214, id.5040

Compression of Deep Neural Networks for Space Autonomous Systems

Carl Shneider*, Nilotpal Sinha, Michele Jamrozik, Marcella Astrid, Peyman Rostami, Anis Kacem, Abdelrahman Shabayek, Djamila Aouada

Computer Vision, Imaging, and Machine Intelligence Research Group (CVI²)

Summary: Efficient compression techniques are required to deploy deep neural networks (DNNs) on edge devices for space resource utilization tasks. Two approaches are investigated.

DNNs for Space Edge AI with Computational Constraints

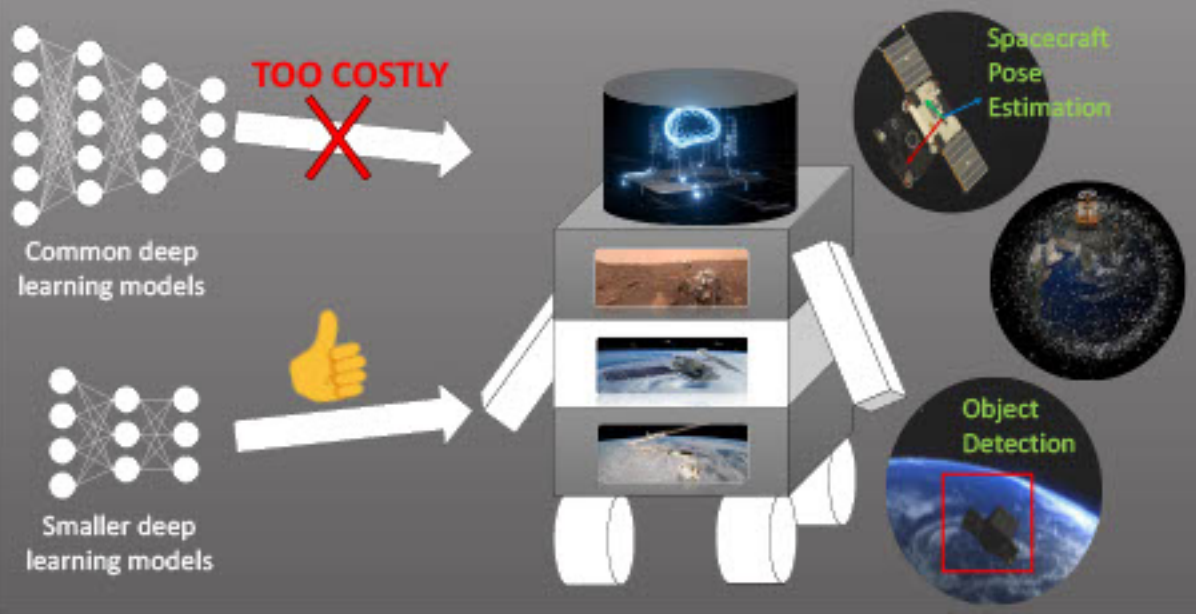

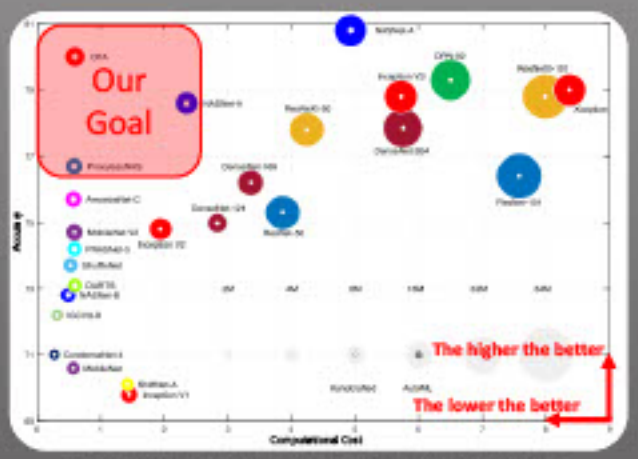

L. Deng, G. Li, S. Han, L. Shi and Y. Xie, "Model Compression and Hardware Acceleration for Neural Networks: A Comprehensive Survey," in *Proceedings of the IEEE*, vol. 108, no. 4, pp. 485-532, April 2020.

Efficient Compression Techniques

Pruning

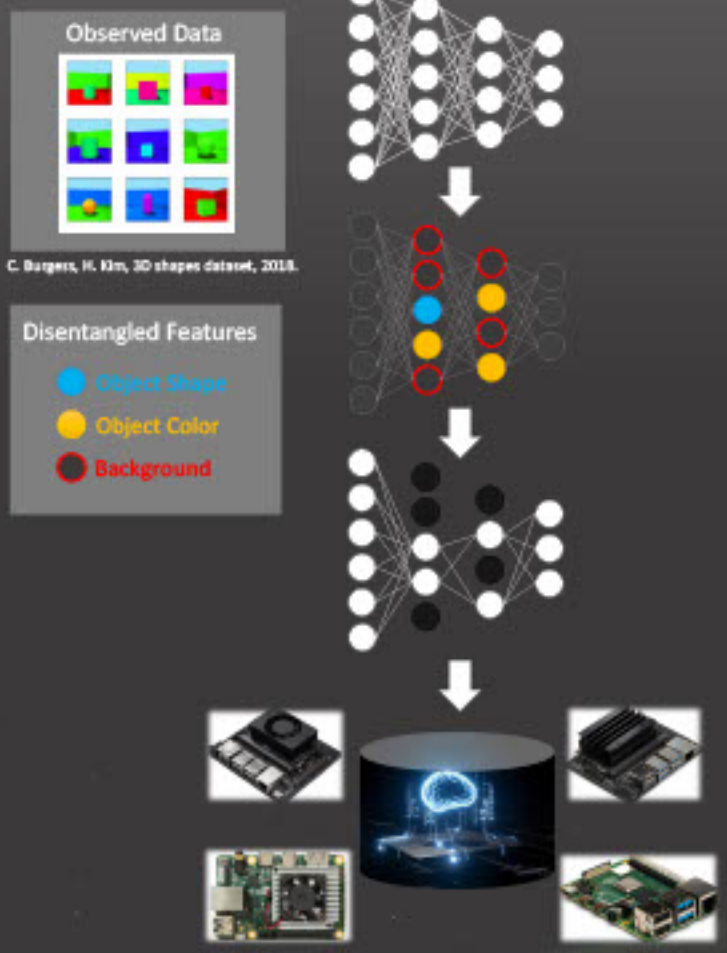

Neural Architecture Search (NAS)

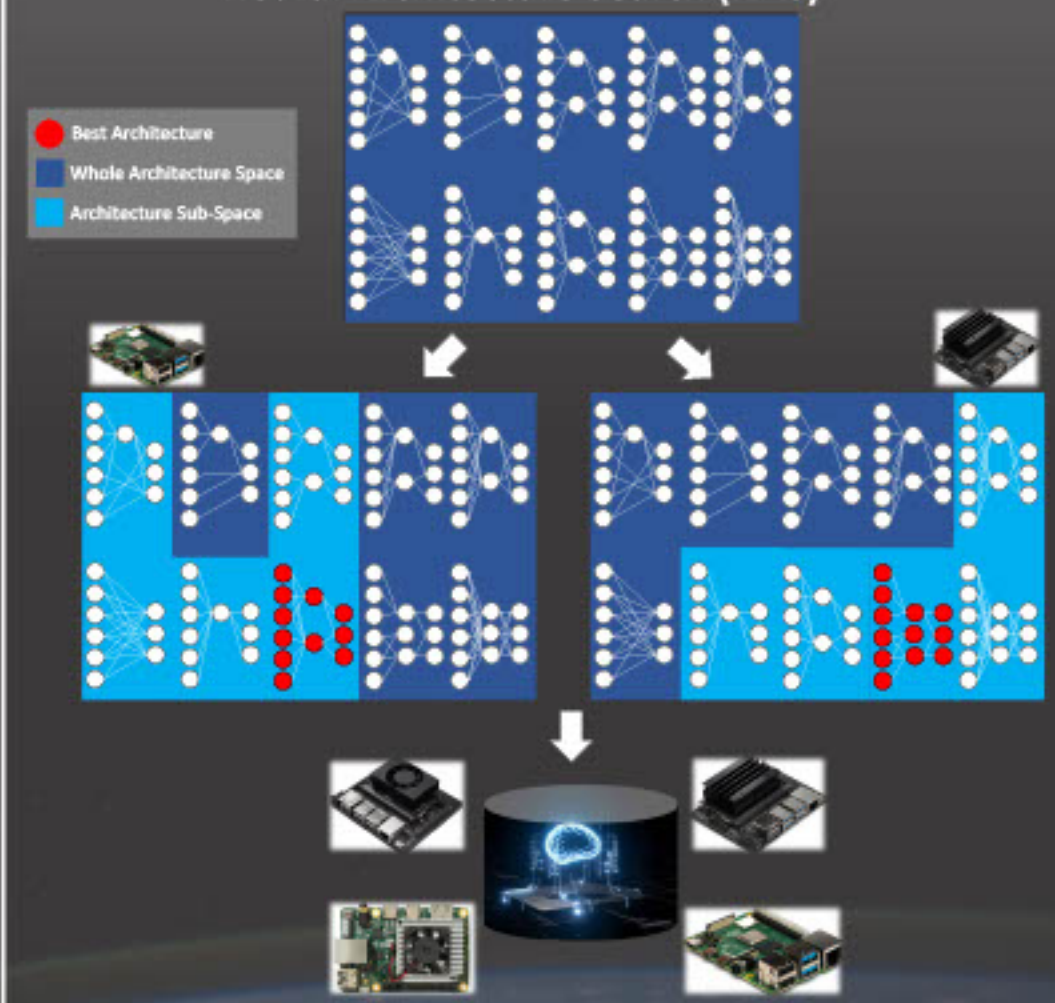

Implementation & Future Work

CONTACT US

Acknowledgement
This work was funded by the Luxembourg National Research Fund (FNR) under the project reference ELITE.

*carl.shneider@uni.lu

In-situ and *post-operando* investigations of Additively Manufactured pure Lunar Regolith simulants parts

Caterina Iantaffi [a,b], George Maddison [e], Elena Ruckh [a,b], Samy Hocine [a,b], Marta Majkut [d], CLA Leung [a,b], Martina Meisnar [d], Thomas Rohr [e], Peter D. Lee [a,b]

caterina.iantaffi.19@ucl.ac.uk, peter.lee@ucl.ac.uk

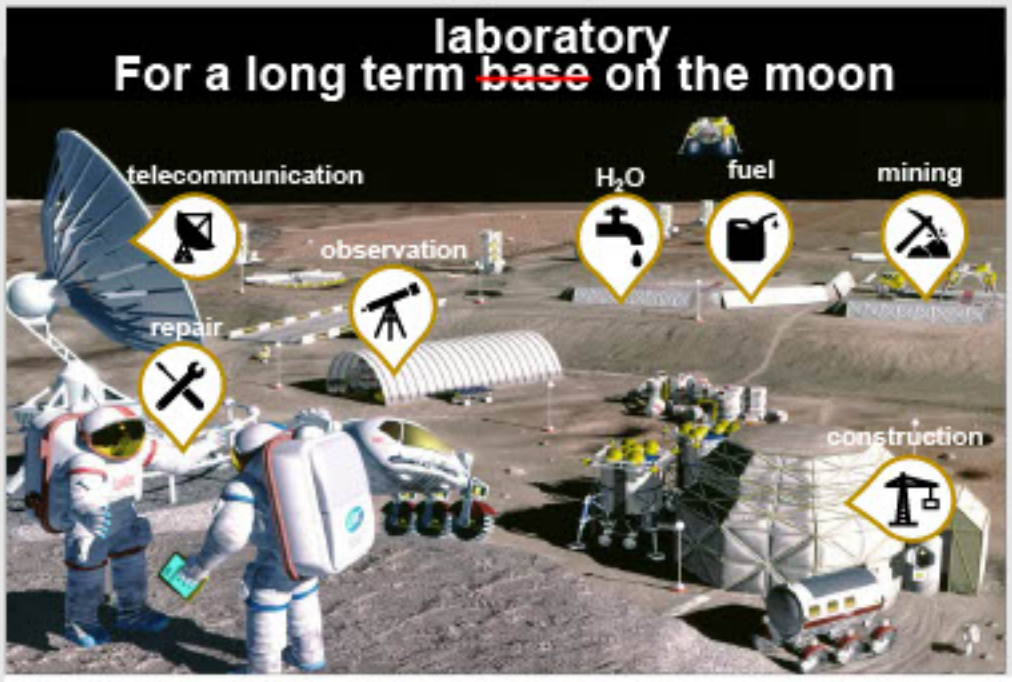

Laboratory on earth

Comparative characterisation of EAC-1A (ESA) and LMS1 (Exolith Ltd.) powder Mare Regolith simulants.

Definition of processability window by laser Additive Manufacturing (LAM) for densified regolith parts.

In-situ synchrotron x-ray imaging experiments for understanding laser melting and sintering mechanisms and the influence of laser parameters on process stability and defects formation.

Laser printability

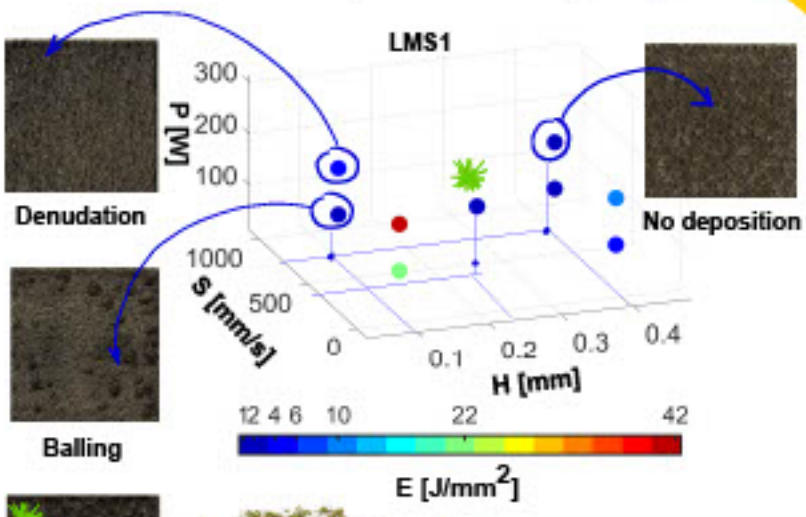

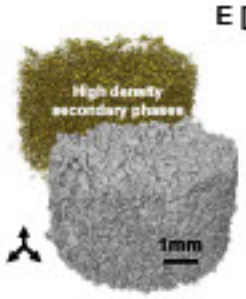

By generating a process map, the optimal conditions for densification were outlined. However, the processability window is very narrow.

Characterisation

Spreadability

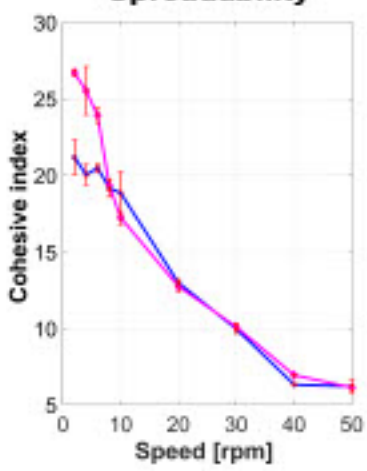

At low rotating speed, LMS1 has lower cohesiveness than EAC-1A promoting an homogenous powder bed spreading.

Optical

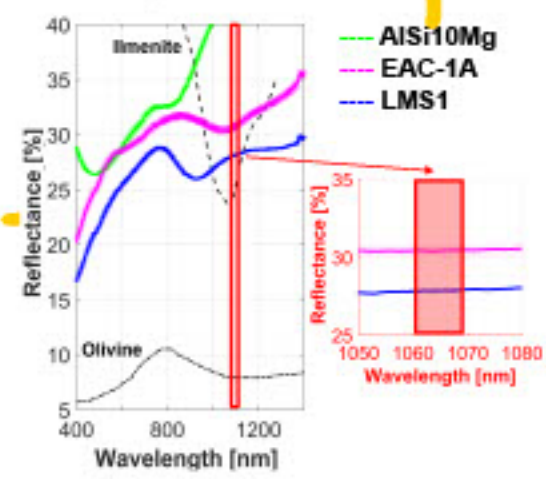

At laser wavelength 1064 nm, EAC-1A reflectance is only 8 % higher than LMS1.

In-situ observation

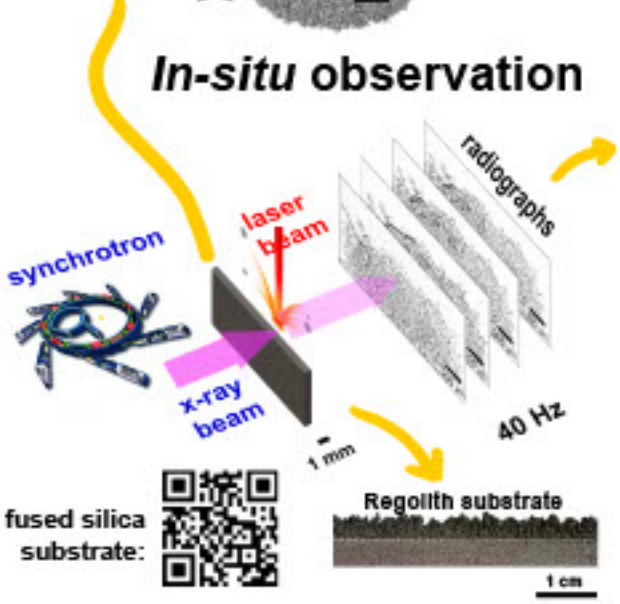

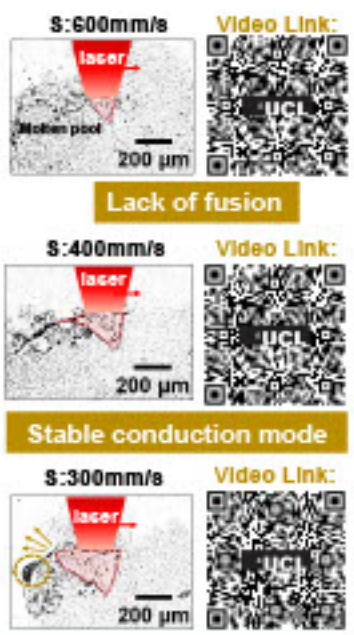

Different substrates materials have been tested; AlSi10Mg is Regolith compatible.

Conclusions

LMS1 and EAC-1A simulants have different multi-physics properties.

For densified Regolith part low laser energy is required. The optimal build conditions for densification: P:145W, s:400mm/s, h:0.25mm.

Change in molten pool morphology (e.g. depth, width) with process parameters are quantifiable.

Just the beginning

- Multi-physics models calibration
- New printing strategies
- Regolith blending materials

a Mechanical Engineering, University College London, WC1E 7JE, UK
b Research Complex at Harwell, Harwell Campus, Didcot, , OX11 0FA, UK
c European Synchrotron Radiation Facility, 71 Avenue des Martyrs, F-38000 Grenoble, France
d ESA-RAL Advanced Manufacturing Laboratory, Harwell Campus, OX11 0FD, UK
e European Space Agency, ESTEC, Noordwijk, The Netherlands

LUNAR CARGO

C. KOSMAS[1], LUNAR CARGO PC, charis.kosmas@lunarcargo.space

SCAN to get the URL of the animation of MACEDONAS

SCAN to get the URL of the animation of OPLONAS

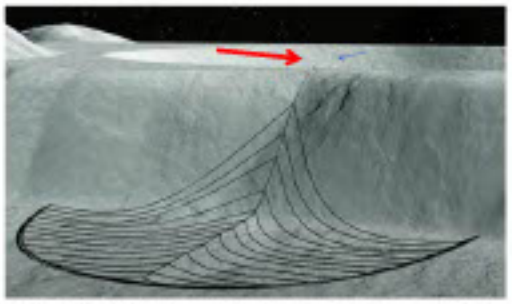

FIG 1: Parcel approaching target catcher (after being ejected by assumed spacecraft)

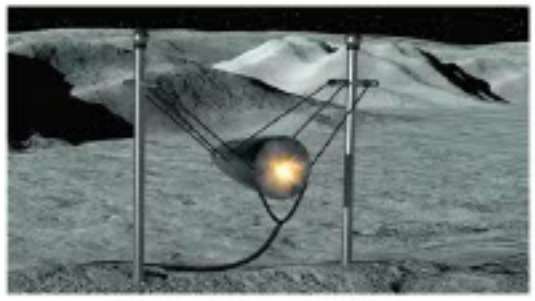

FIG 2: Parcel hits target and arrested by catcher

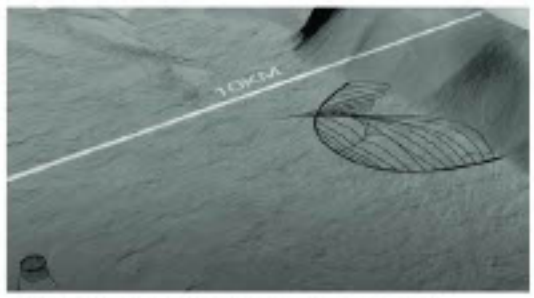

FIG 3: Target catcher with arrested parcel fly away due to momentum

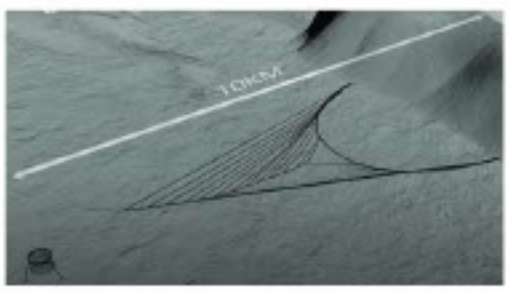

FIG 4: Momentum is transferred to the "dendritic" system and speed decays

The MACEDONAS (Momentum Absorption Catcher for Express Deliveries on Non Atmospheric Somata), is a Lunar surface parcel catching system for arresting decelerating and guiding in a safety net, parcels that are ejected by orbiting, parcel storage depos. Repositioning through a winch based system permits its reuse every 111 minutes.

FIG 5: Safety net secures from free fall.

FIG 6: OPLONAS approaches tangentially. Pre-spins to achieve smooth contact

The OPLONAS (Oversized payload Lander on Non Atmospheric Somata), is a wheel shaped spacecraft for landing and decelerating a cylindrical (payload containing & bus) hub, at the plateau Oceanous Procellarum. The hup is upcycled as habitat and the tethers around the hub and the rim are upcycled to create a MACEDONAS. Load capacity > 12 tones)

FIG 7: Roll friction erodes the momentum.

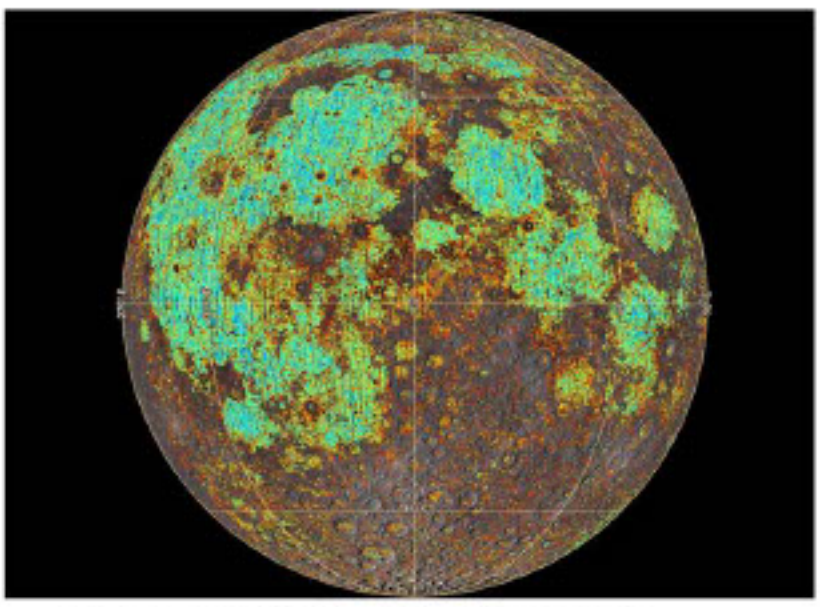

FIG 8: Areas in Blue – Blue green with inclination lower to 5 degrees. Suitable for OPLONAS landing.

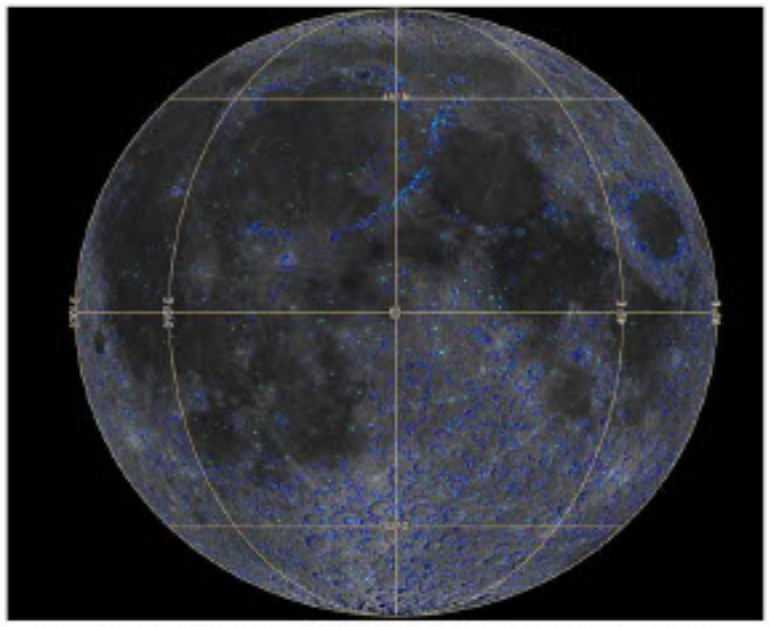

FIG 9: Spots in Blue – Blue white locations with high elevation and inclination. Suitable for installing MACEDONAS.

Up to 70 % cost reduction possible with respect to current cost projections.

NO USE OF FUEL.

OPLONAS is a wheel looking apacecraft, of 60 m overall diameter, with a cylindrical payload-containing hub in the centre. Between the perimetric rim and the hub, high tensile strength axial ropes hold in place the rim when it rotates with 8.62 rev / sec. This specific rotational speed matches the speed of the spacecraft, so that the only friction component upon tangential contact of OPLONAS to the ground, to be the roll friction. Considering the low gravity on the Moon the rolling of the OPLONAS spacecraft will last for tens of minutes and will run for a significant part of the 2500 stretch of the Oceanus Procellarum (Fig 8).

OPLONAS Point design Engineering data : 60 m diameter of wheel. Cylindrical hub 6 m diameter 9 meters height with inertial syatem. Axial tethers 754 (in 2 planes), thickness of axial Zylon® 253.3 mm. RIM & RIBS thickness of core for the 9 rings 0.25 cm. Thickness of skin from gum metal 125mm. Breaking Mass (RIBS & RINGS)= 259 kg. Total mass of **axial tethers 8,776 kg. TOTAL inert mass for upcycling 9,035 kg. Payload 3,872 kg.**

MACEDONAS Point Design Catcher at 100 m height, deceleration duration 10.9 sec, strip length 9,175 m, deceleration 15.75 g.

MACEDONAS Highly reconfigurable to accommodate parcels of varying mass . The material for building a MACEDONAS can derive from up-cycling the flexible elements of OPLONAS. The catcher of the MACEDONAS needs to be stationed at high grounds (Fig 9).

Space Resources Week 2023 (Luxembourg)

lunar cargo

Space Resources Week, Luxembourg, 2023

Patrick Harkness, Xuan Li, Andrew Scott-George, and Kevin Worrall

The electromechanical footprint of the drillstring is often a limiting factor in planetary subsurface exploration. This poster reports on some aligned concepts, currently under development at the University of Glasgow, which seek to reduce weight-on-bit, rotational speed, and downhole torque requirements accordingly.

The authors note their appreciation to UKRI and UKSA, as well as the University of Glasgow, for funding offered in support of the concepts discussed in this poster.

Contact: patrick.harkness@glasgow.ac.uk

LOWER WEIGHT, SPEED, AND TORQUE IN DRILLING

Reduced weight-on-bit. Ultrasonically-assisted drilling (UAD) is a process whereby a rotating bit is caused to resonate at a high frequency (20kHz), with an amplitude of just a few microns. This assembly may then be mounted on a rail facing a target, with a force transducer, linear actuator, and bang-bang controller such that a target weight-on-bit may be maintained during drilling [1].

Sonication amplitudes of 0 μm (black), 9.2 μm (blue), 18.2 μm (cyan), 27.4 μm (green), and 36.6 μm (red) are applied. The results (Fig. 1) show that, in limestone, high vibrational amplitudes can be as effective as tripling weight-on-bit.

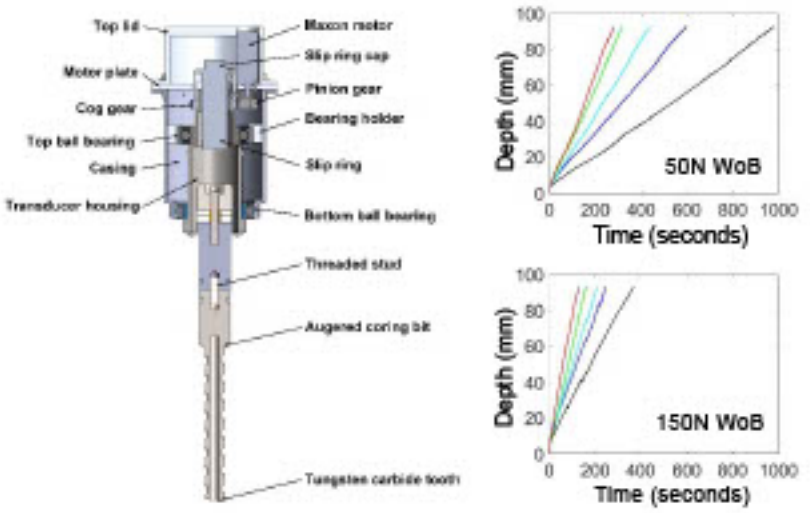

Fig. 1: An ultrasonically-assisted drill rig, with performance in limestone.

Reduced speed. Sonication is known to reduce the force required to insert penetrators into granular media so, in rotary augering (which depends on there being lower friction on the auger flights than on the borehole walls) the same effect could reduce the rotation speed required to achieve uplift [2].

To investigate this possibility, an auger was designed to resonate at 20kHz and introduced to glass microspheres, as shown in Fig. 2. Increasing the sonication amplitude maintained the 'spoil' mass flow rate, even as the rotation speed was reduced [3].

The ultrasonic auger can also be held stationary inside a rotating tube. This is an extension to the 'Olds Elevator' concept, and it holds out the potential for enhanced auger feeding performance.

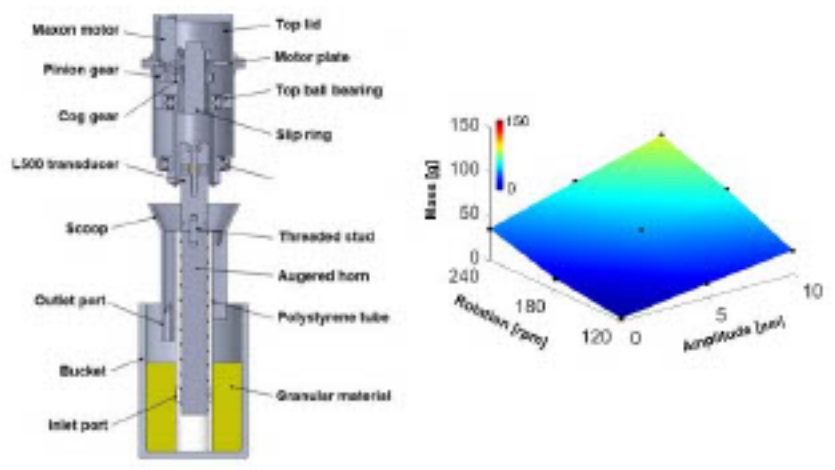

Fig. 2: An ultrasonically-assisted auger rig, with performance in spheres.

Reduced torque. Despite sonication, the auger still has a non-zero torque requirement. A superior drillstring would be one with no internal moving parts and zero torque requirement.

To address this requirement, the pulse-elevator [4] is proposed. This is a combination of the Tesla valve [5] and the vibro-conveyor, machined into a non-rotary bit, as shown in Fig. 3. This architecture works by simple percussion. Any material at the bottom of the hole falls into the pulse-elevator scoops, and each oscillation catapults the material in one scoop up to the next. Computer simulations in device-frame illustrate the concept.

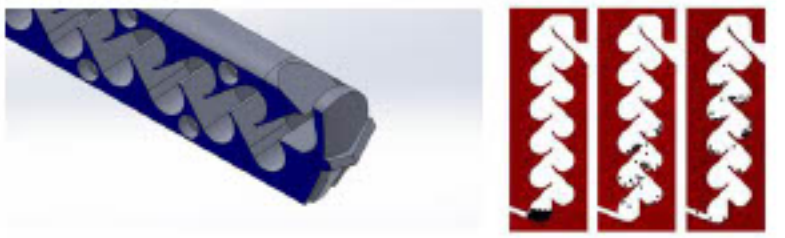

Fig. 3: A pulse-elevator, with simulated performance in device-frame.

In laboratory conditions, the performance of the pulse-elevator is extraordinarily repeatable, as shown in Fig. 4.

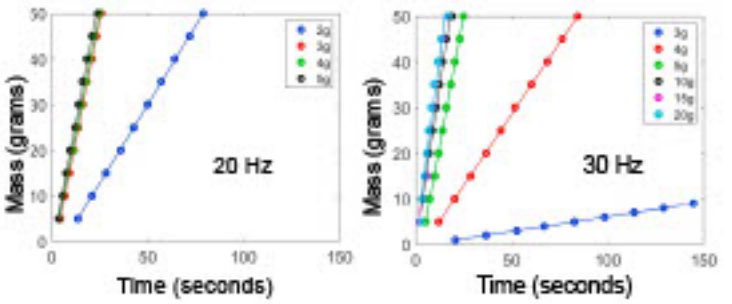

Fig. 4: Pulse elevator uplift performance in glass microspheres.

Using this concept, a hammering drill can be made that does not require gross rotation, and yet can still extract spoil from the bottom of the hole. A simple demonstrator has excavated a hole 160mm deep (more than five bit diameters), in tuff, in just ten minutes. Spoil was successfully uplifted from the bottom of the hole throughout, with no requirement for augering at all.

The pulse-elevator architecture can also be modified to permit horizontal transport of granular materials, perpendicular to the excitation. This has the effect of enabling uplift and transit using a single solid-state device.

Conclusions. Sonication and vibration can facilitate both rock-cutting and the subsequent spoil management processes, increasing rate-of-progress and reducing the electromechanical footprint of the exploration hardware.

References. [1] Li, X. and Harkness, P., 2022. Autonomous and ultrasonically assisted drilling in a range of rocks and ice. Ultrasonics, 125, p.106803. [2] Firstbrook, D., et al., 2017. An experimental study of ultrasonic vibration and the penetration of granular material. Proceedings of the Royal Society A, 473(2198), p.20160673. [3] Li, X., et al., 2022. Ultrasonic augers for improved transport of granular materials. Acta Astronautica, 201, pp.1-11. [4] Li, X., et al., 2022. The pulse-elevator: A pump for granular materials. Acta Astronautica, 200, pp.33-41. [5] Tesla, N., 1920. US Patent 1,329,559.

Review of Water Capturing Devices for Lunar ISRU

Christoph Kalis[1,2], Luca Kiewiet*[1], Mart Heitkamp[1], Henning Wache[1], Alessandra Menicucci[2] and Paul Zabel[1]

[1]German Aerospace Center (DLR), Institute of Space Systems, Bremen, Germany
[2]Delft University of Technology, Faculty of Aerospace Engineering, Delft, Netherlands
*luca.kiewiet@dlr.de

1. Introduction

The use of resources present on celestial bodies, known as In-Situ Resource Utilization (ISRU), is becoming more and more important in space exploration due to the high cost of launching mass into orbit. ISRU would enable long-term manned operations and permanent (robotic) presence on extra-terrestrial bodies. Water is considered to be one of the most important resources for further space exploration and is currently investigated for extraction and purification on the future manned Lunar base envisioned around 2025. Previous research focused on the extraction of water from regolith but little work has been done to find ways on how to capture and liquefy the water vapour after its extraction.

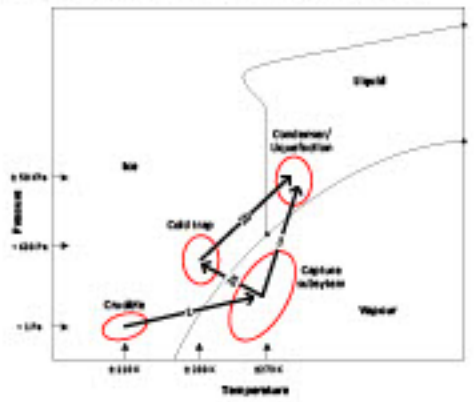

Figure 1: Schematic phase diagram with process overview. Path 2 shows how water can be captured as a solid, and path 3 as a liquid.

Thermal extraction is currently the preferred method for winning water, meaning heat is applied to the water ice regolith mixture resulting in the sublimation of ice and outgassing of the water vapour. This vapour is then captured and liquefied, as can be seen in figure 1. If sufficient temperature and pressure is present in the reaction chamber, a collection as liquid on the bottom of the chamber is theoretically possible. Unfortunately, the regolith has a high saturation with liquid water of around 16%. The residual water in the regolith would be too high and thus efficiency of the collection is likely too low. See figure 2 for the setup to test this.

Figure 2: Test-setup water in lunar regolith (saturation occurs at around 16%).

2. Potential Solutions

A cold trap is a cold surface to which the water vapour coming from the extraction system can deposit onto as a solid, after which it can be considered captured and secured. In this scenario, liquid water occurs after the capturing in a solid state. The gathered ice needs to be in an environment where liquid water can exist. Whether this change in pressure and temperature takes places directly in the capturing system (internal liquefaction) or whether the ice is detached from the capturing system and processed in another location (external liquefaction) needs to be decided.

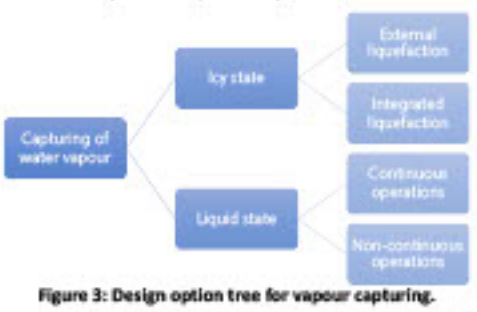

Figure 3: Design option tree for vapour capturing.

The options for capturing in liquid state can be divided in continuous and non-continuous operations. For continuity, a constant flow of water vapour to the condensing surface at sufficient pressure and temperatures above the triple point is needed. This could be realized with a pump between the extraction subsystem and the capturing subsystem, since the liquid phase is undesired in the extraction subsystem. A high pressure in the crucible is unwanted since the water should only be in solid or gas state during extraction. These options are visualized in figure 3.

3. Preliminary Design of LUWEX

In Figure 4 an overview of the entire LUWEX experiment design is presented. A needle valve between the cold trap chamber and the vacuum chamber controls the vapour flow towards the actual cold trap itself and prevents the pressure rising too much. A slider separates the cold trap chamber from the liquefaction chamber to have a contained environment during liquefaction. In Figure 5 a preliminary CAD drawing of the relevant systems is presented. In the crucible, the water vapour has a temperature of around 273K after heating the regolith. This refers to a saturation pressure of 470 Pa which is then also present in the cold trap and liquefaction. Present volatiles in the icy-regolith sample are water ice, methanol, ethanol, CO2. The cold trap has to withstand these volatiles and is designed in such a way, that these volatiles are not deposited on the cold fingers.
The design was driven by volume constraints of the chamber and size of the slider which separates the cold trap and the liquefaction.
The goals of this baseline design were as follows:

1. As much cold trap area as possible for maximal ice mass and thus water vapour capturing.
2. Long residence time of the vapour for lower losses leading to a higher efficiency.
3. High liquefaction volume to lower the need for melting cycles for a higher total collection rate.

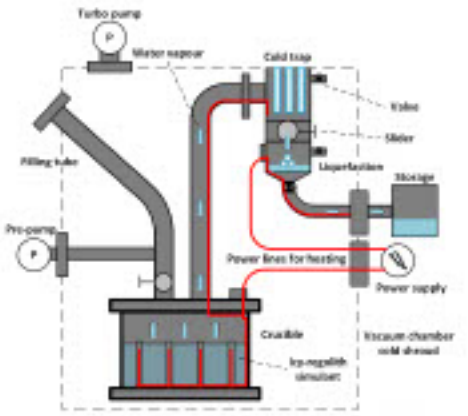

Figure 4: Schematic of the LUWEX experiment inside the TVAC.

The main reason for the decision of capturing as a solid, meaning cold trapping, was less complexity, since there is no need to rise the pressure between the crucible and the capturing system.. The condenser needs pumps and valves with pressure control to function efficiently and optimally. Besides, the condenser needs to maintain a higher temperature than the cold trap for it to work. The cold trap can make use of the cold Lunar environment. Also, less heat and control schemes are required to achieve the desired temperature and pressure ranges. Yet, the system is less controllable because pressure is more sensitive to unwanted condensation.

In future systems with cold trapping, the liquefaction might not occur directly after the capturing, so the intermediate storage could be in icy state. This reduces the storage complexity and favours the design with a cold trap.

Figure 5: Model of the cold trap and liquefaction.

4. Cold Trap Experiment

Since there is little experience about capturing water vapour in low pressure environments, and specifically so for the purpose of In-Situ Resource Utilization, a small-scale test was conducted to see how effective it would be to capture water vapour on the Moon using a cold trap. Figure 6 shows the setup of this experiment.

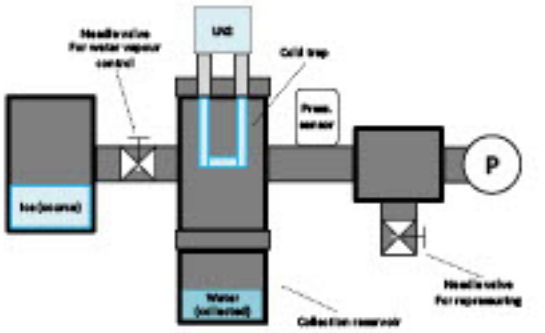

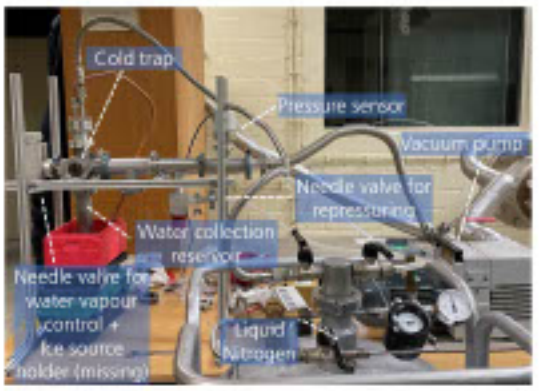

Figure 6: Schematic experiment setup above and the actual setup below.

The experiment was designed to test the effectiveness of the cold trap when the vacuum pump is running ("constant" low pressure). This would be analogous to the cold trap being exposed to the "atmosphere" of the Moon. In table 1 the results are presented.

Table 1: Results of the cold trap experiment under low pressure.

Run #	Sublimated [g]	Captured [g]	Efficiency
1	9.34	7.11	76.12%
2	4.45	3.18	71.46%

Figure 7: Cold trap without ice (left) and with ice (right).

Secondary to this, experience and insights were gained along the way about cold traps and working with these test setups.
The collection efficiency was surprisingly high, despite the shape of the cold trap not being optimized.

5. Conclusion

The challenge of this research project is the lack of data and previous research done in the field of water capture for ISRU. Nevertheless, these outcomes provide a solid foundation for LUWEX and future research. Many different ways to capture water vapour are envisioned, and this work provides an initial overview in some of the possibilities. Future works will investigate what the most optimal way to capture water would be for different scenarios.

Visit https://luwex.space/ or scan the QR code!

This work is part of the DLR internally funded young investigator group "Synergetic Material Utilization" (SMU) established 2021 at the Institute of Space Systems in Bremen, Germany. The group focuses on research and development of ISRU technologies for Moon and Mars exploration.

The project LUWEX is funded through the Horizon Europe framework program of the European Union with the grant number 101081937.

Funded by the European Union

Enabling Infrastructure Ecosystem for Space Resources

Erik Kulu, erik.kulu@factoriesinspace.com
Space Resources Week 2023, April 19-21

Factories in Space is the largest public database of commercial entities in the in-space economy, space resources and microgravity manufacturing. Directory started in 2018 and has over 700 entries.

Enabling ecosystem for space resources would include most of the in-space economy startups, from technologies to customers. Enabling infrastructure ecosystem is narrower but still very broad.

Cambridge Dictionary defines infrastructure as "the basic system and services, such as transport and power supplies, that a country or organization uses in order to work effectively".

Compared to the 10 categories for in-space economy at Factories in Space, leaving out Human Spaceflight, Space Stations, In-Space Manufacturing (ISRU is still included) and Miscellaneous. While they can be helpful, they are not strictly an enabling infrastructure.

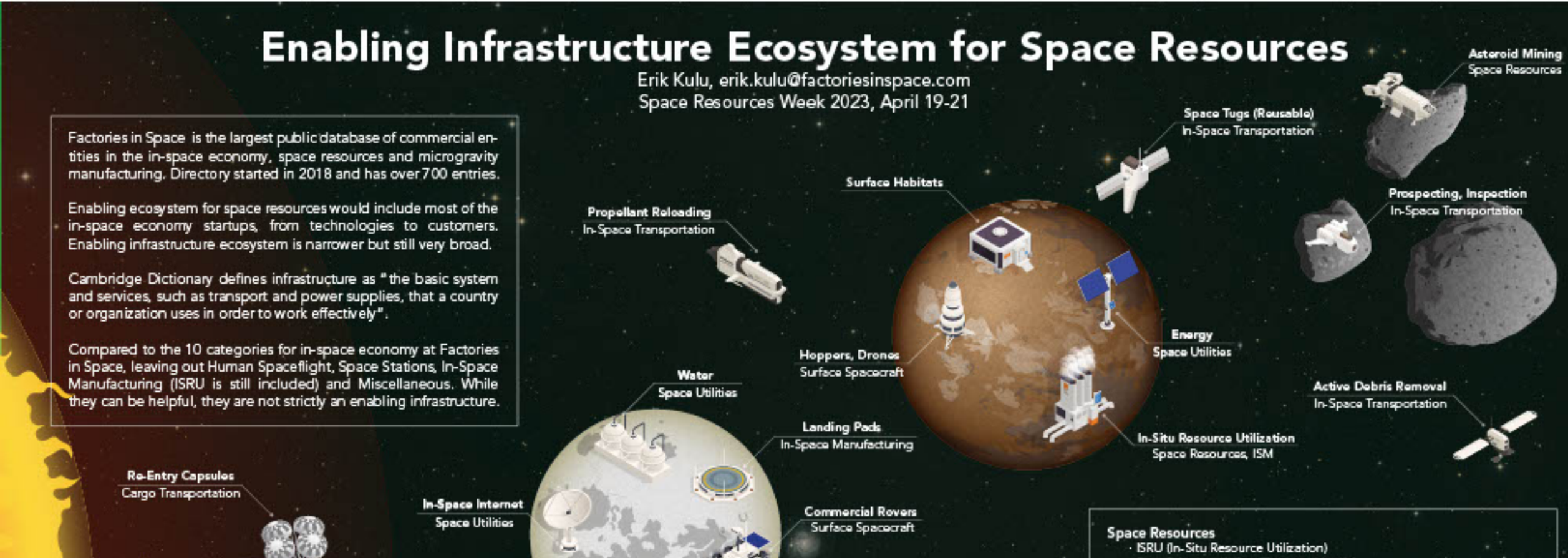

Launch & Landers
- Reusable Low-Cost Launchers
- Robotic Landers (Moon, Mars)
- Re-Entry Capsules (Earth, Mars)

Launchers, landers and re-entry vehicles are enabling infrastructure.

Surface Spacecraft
- Robotic Rovers
- Drones, Hoppers

Surface spacecraft are required for prospecting, mining & transportation.

In-Space Transportation
- Space Tugs, Orbital Transfer Vehicles (OTV)
- Propellant Reload Stations, Active Debris Removal

Spacecraft for transportation, docking and other close operations.

Space Resources
- ISRU (In-Situ Resource Utilization)
- Pure Substances (Ice, Oxygen, Metals)
- Space Mining, Lunar Mining, Asteroid Mining
- Prospecting, Processing, Beneficiation, Recycling

Space resources is a category for directly space mining related activities.

Space Utilities
- Energy, Power-Beaming
- In-Space Internet, Data Relay
- Navigation, Water, Propellant

Utilities are required for transportation, mining and processing.

Surface Facilities

Surface habitats and structures are required for storage and processing.

Last update 2023-04-12

Electrowinning of metals from lunar regolith by using new types of ionic liquids

A. Dietz[1], E. Moustafa[1]
[1]Fraunhofer Institute for Surface Engineering and Thin Films IST

Fraunhofer IST

Fraunhofer Institute for Surface Engineering and Thin Films IST

Introduction

For the colonisation of the moon, the production and permanent supply of oxygen is essential for survival and is being intensively investigated using a wide variety of methods. However, other materials are also needed, for example to produce tools or other components for infrastructure. By means of electrolytic processes in ionic liquids, it was possible to deposit iron and aluminum, which are the important metal components in lunar regolith. For this purpose, the lunar regolith, which consists of the oxides of different metals, was chemically dissolved and then electrochemically deposited as pure metal (cathodic process). The production of oxygen (anodic process) is also possible, but has not yet been intensively investigated.

The benefit of the electrowinning of metals from dissolved regolith is the possibility, to separate the metals by applying different electrochemical potentials. Iron, for example, is electrochemically more noble than aluminum and is therefore easier to separate via electrolysis. Furthermore, this process works at moderate temperatures between 20 °C and 100 °C.

The upscaling of electrochemical deposition processes can be used for production for the material and is well known, such as the process for aluminum production.

Electrodeposition (-winning) of iron in ionic liquids EMIM Cl

Electrodeposition (-winning) of aluminum in ionic liquids EMIMCl

The challenge

Conventional ionic liquids that are commercially available, such as EMiM Cl, showed only a slight tendency to dissolve regolith chemically. The reason for this is the fact that regolith consists of a mixture of different minerals such as ilmenite or olivine, which are chemically very stable. However, by using so-called ionic liquids trichlorides (IL-TriCl) it was possible to dissolve chemically some components of the regolith.
IL-TriCl are common ionic liquids that have been treated with gaseous chlorine. This makes them strong oxidising agents capable of partially dissolving regolith simulant [1]. From this solution, it has then been possible to deposit metallic iron electrochemically.

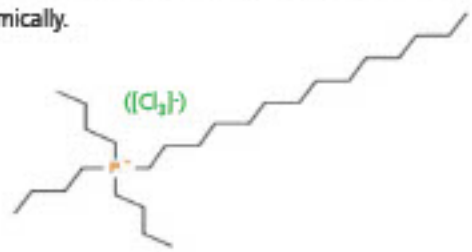

Example for IL-TriCl: Tributyltetradecylphosphonium-trichloride

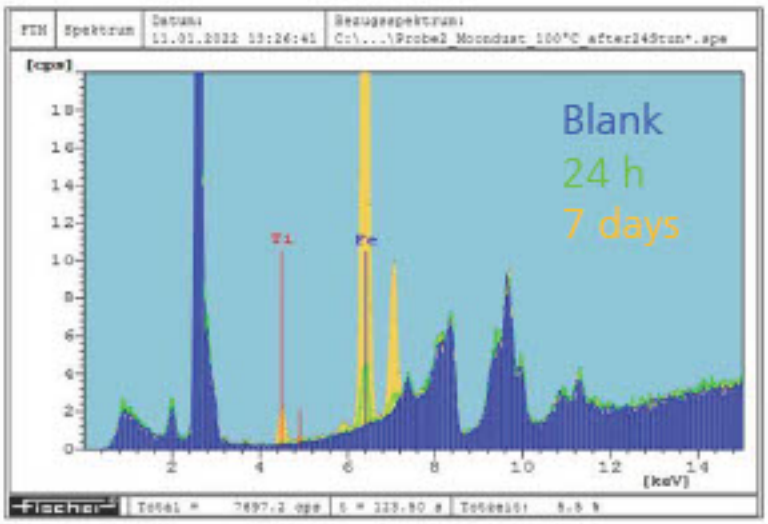

XRF-Measurement of the dissolution of regolith simulant in IL-TriCl at increased temperature (100 °C)

Dissolution of regolith and electrodeposition of iron

A lunar regolith simulant (TUBS-M, TU Braunschweig) was treated with Tributyltetradecylphosphonium-trichloride at 100 °C. The XRF-measurement from the filtered electrolyte shows the chemical dissolution of the iron contained in the regolith simulant. From this electrolyte, it has been possible to electrochemically deposit iron.

IL-TriCl without regolith (left) and with dissolved regolith simulant (right)

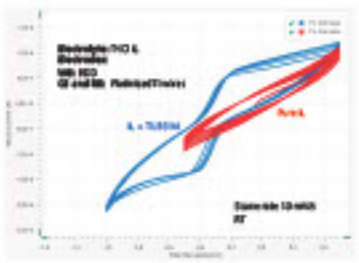

Cyclic voltammograms of pure IL-TriCl (red) and with dissolved TUBS-M (blue)

Electrodeposited iron on copper substrate
Electrolyte: IL-TriCl with dissolved regolith simulant

Contact

Dr. Andreas Dietz
Electroplating
Phone: +49 531 2155 646
Mobile +49 178 2155 011
andreas.dietz@ist.fraunhofer.de
Fraunhofer IST
Bienroder Weg 54e
38108 Braunschweig
www.ist.fraunhofer.de

1 Xiaohua Li, Arne Van den Bossche, Tom Vander Hoogerstraete, Koen Binnemans; Ionic liquids with trichloride anions for oxidative dissolution of metals and alloys; Chem. Commun., 2018, 54, 475–478

Supported by:
Federal Ministry for Economic Affairs and Climate Action
on the basis of a decision by the German Bundestag

Welcome to #*TheMoon*

#TheMoon is Europe's largest fully privately financed Moon environment. #The Moon stretches over 90m² and is filled with 40 tons of regolith RS-1. It`s derived from the well-known TUBS-M simulant, which fulfills all scientific needs for realistic lunar surface experiments.

The large rectangular size of the testbed is ideally suited for vehicles and terrain modelling. It can be completely darkened and illuminated with a professional lighting system e.g., to mimic the lunar pole regions. A gantry can be used for gravity assist for an even more complete Moon simulation.

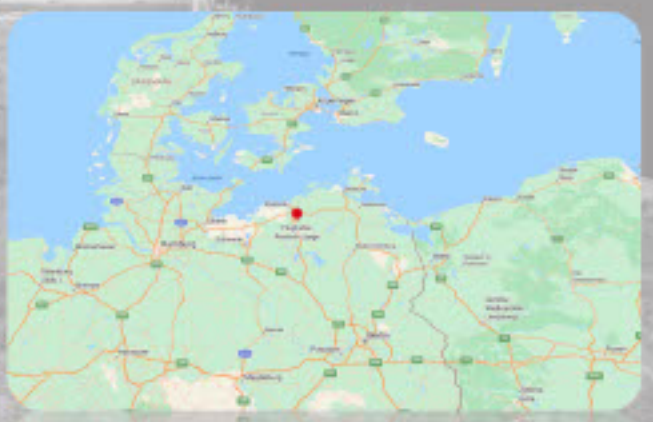

#TheMoon is conveniently located in the airport of Rostock-Laage. Test equipment and can be shipped to #TheMoon by plane, truck or ship, as the airport is located at the motorway to the harbor of Rostock, Hamburg and Berlin.

#TheMoon is open to research institutes, industry, universities, media business, …. No science justification or paperwork is needed, just book your slot at https://TestingFor.Space
It's like Airbnb, just a little bit more "*spacy*" ...

Orbit Recycling
Wertstoff aus dem All

PTS

spaceport rostock
#TheMoon

Resource Mapping of the Moon's South Pole

Author: Freja Thoresen and Aidan Cowley
Corresponding: Freja Thoresen, freja.thoresen@esa.int

Learning about the Moon Mineralogy

Information about the Moons mineralogy is needed, especially at the south pole. Mineral mapping can be used for analysis of ISRU technologies. Machine learning methods have proven to be a powerful tool for analysis of hyperspectral images.

→ **Problem:** Supervised learning may not be feasible due to the lack of labelled data in the lunar environment.

→ **Solution:** Unsupervised clustering of images to learn about the Moons mineralogy.

Exploring hyperspectral images of the Moon

The Moon mineralogy mapper from the Indian mission Chandrayaan-1 mapped 97 % of the entire Moon's surface with 85 spectral bands ranging from near-visible to infrared light [1]. Wavelengths over 2.5 microns excluded, since additional corrections would be needed to correct thermal additions [2].

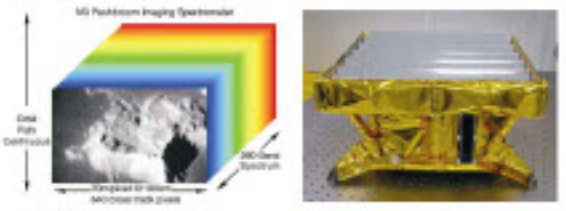

Pieters et al. (2009)

Implementation of State-of-the-art AI solutions

An unsupervised deep neural network learns the most important features of the image to reconstruct the image entirely.

→ **Recent studies:** Clustering methods improve when the data is reduced to low-dimension extracted features.

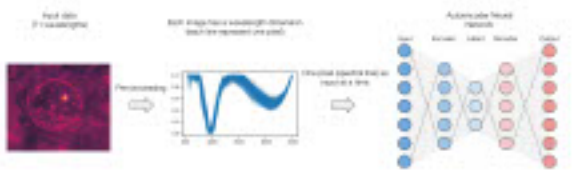

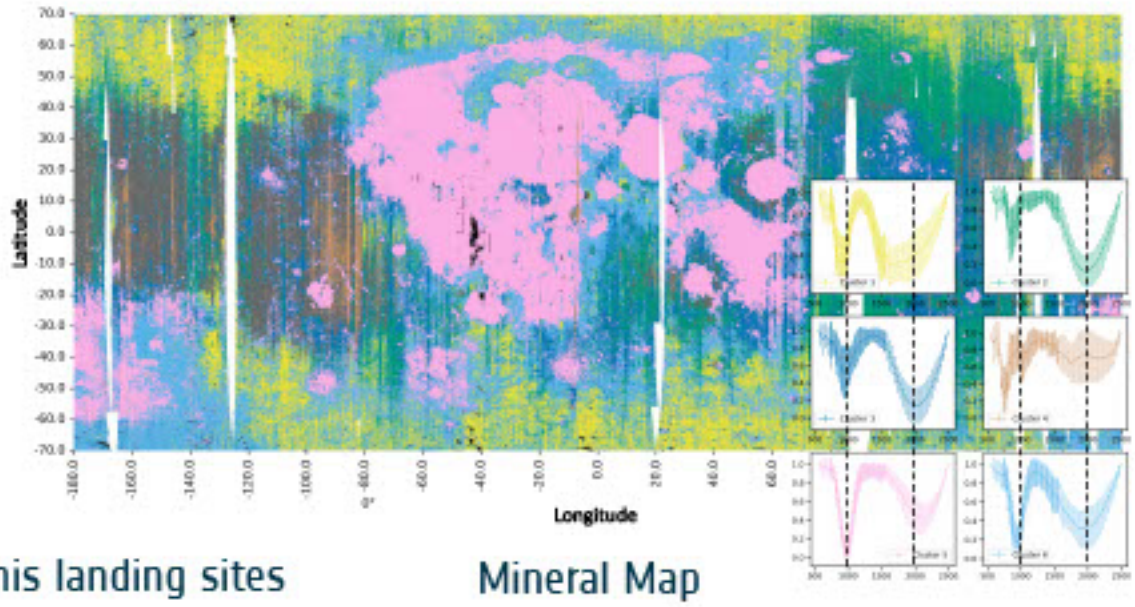

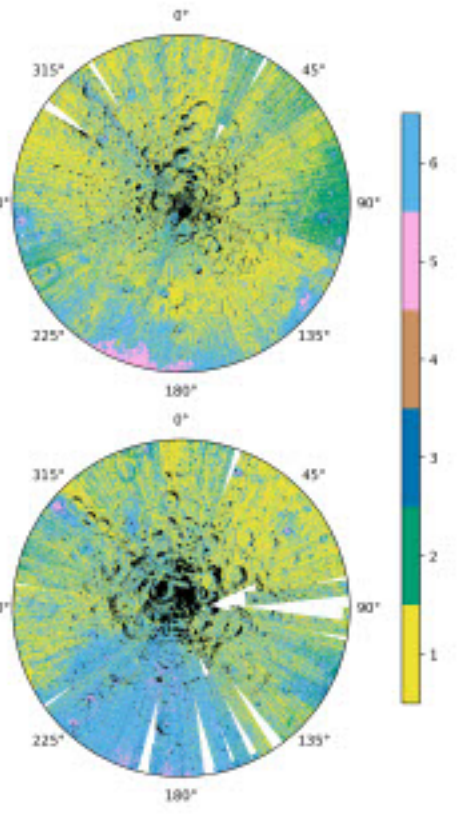

Artemis landing sites

→ Mineral map at the Artemis landing site candidates.

→ Primarily composed of cluster 1 and 6, which corresponds to mainly plagioclase

→ Minor deposits of cluster 5 (Mare)

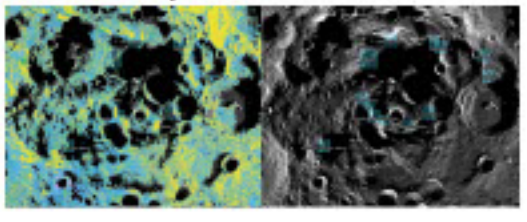

Mineral Map

→ The latent variables from the neural network are clustered into 6 categories.

→ Grey areas: Excluded (featureless)

→ Black areas: Reflectance of zero

→ Clusters are compared to reflectance of known minerals

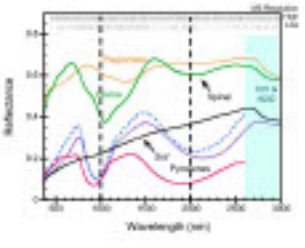

References

[1] Pieters, C. et al. (2009), The Moon Mineralogy Mapper (M3) on Chandrayaan-1, Current Science 96, 500-505. [2] Li, S., & Milliken, R. E. (2016). An empirical thermal correction model for Moon Mineralogy Mapper data constrained by laboratory spectra and Diviner temperatures. Journal of Geophysical Research: Planets, 121(10), 2081–2107.

Acknowledgments: Supported by Spaceship EAC, as part of the European Astronaut Centre, belonging to the European Space Agency (ESA)

Holistic system modeling: Towards the design of scalable ISRU architectures

Space Resources Week 2023
Francisco J. Guerrero-Gonzalez[1] (f.guerrero@tum.de), Philipp Reiss[1]

Scan QR code to download poster

Context

Holistic and multidisciplinary modeling approaches are key when developing complex new In-Situ Resource Utilization (ISRU) systems to assess their scalability, optimize their architectures, and make high-level pondered decisions from their conception.
Individual modeling efforts of ISRU architectures can be found in the literature [1, 2, 3]. Direct comparisons and trade-offs are only possible when such efforts are collected under a single universal framework.

ISRULib

The Technical University of Munich has an extensive legacy of developing tools for the analysis and simulation of human spaceflight systems. The Life Support Trade-Off Tool (LSTOT) combines multi-criteria and equivalent system mass analyses whereas the Virtual Habitat (V-HAB) is capable of dynamically simulating individual processes and matter and energy flows across systems. Although both tools have been occasionally used to model ISRU components [4, 5], their main focus has been the analysis and simulation of life support systems. Therefore, ISRU models are lacking within these tools.

Scan QR code to find out more about ISRULib

ISRULib is a new database of component- and system-level ISRU readable and easily-understandable models that can be incorporated into these specific analysis and simulation tools and be used by the entire community to carry out high-level technological trade-offs and preliminary architectural definitions.

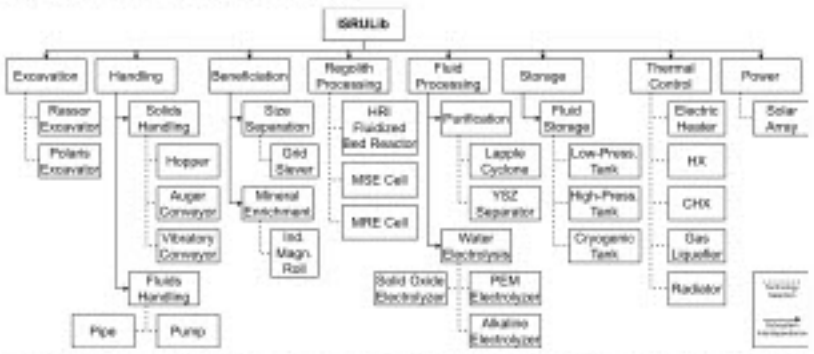

Fig. 1: Issue tree of ISRULib models. The models are based on analytical parametric calculations, extrapolated experimental results, surrogate models from numerical simulations, and already existing ISRU hardware.

The goal is to keep ISRULib constantly updated. The models are written in Jupyter Notebooks (Python 3.0) and stored in an open-source Gitlab project that includes a model template and its coding guidelines to facilitate the inclusion of new models in the database. The proposed models will be subject to a peer review before being finally included in ISRULib.

Results

Fig. 3 exemplifies how the Hydrogen Reduction of Ilmenite (HRI) fluidized bed reactor mass and power budgets are modeled. This model is used in the system study described in Fig. 2a. Sensitivity analyses were carried out for the initial ilmenite and anorthite concentrations in regolith (Fig. 4). The salt ratio of the MSE process and the degradation rate of the MRE reactor are identified as key parameters that determine the feasibility of these ISRU processes. When both the metal and oxygen production rates are accounted for, HRI and carbonylation require a feedstock with a mineral composition between the one of Highlands and high-Ti Mare (7.5 wt.% $FeTiO_3$ and 55 wt.% $CaAl_2Si_2O_8$) to become more effective than the production of Al–Si alloys through MSE and vacuum distillation.

Fig. 3: High-level schematic of the HRI fluidized bed reactor model. User inputs are mapped to model outputs.

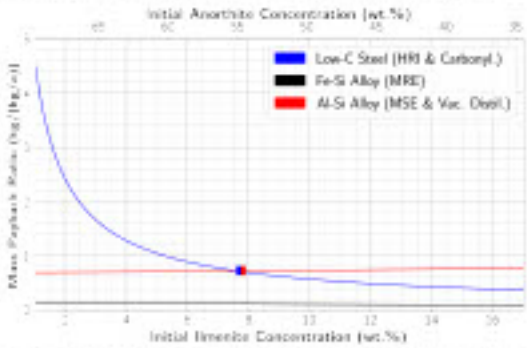

Fig. 4: Sensitivity of the mass payback ratios (kg of hardware/kg of product/a), of the three ISRU production plants to the mineral composition of lunar regolith. The solid lines represent the total payback ratios, including oxygen and metal production. The smaller the payback ratio, the less mass must be brought from Earth to produce a certain amount of product on-site.

References

[1] Schreiner, S.S. et al. (2016) Adv. Space Res. 57, 1585-1603. [2] Hinterman, E. et al. (2021) IEEE Aerospace Conference (50100). [3] Linne, D. et al. (2021) J. Aerosp. Eng. 34 (4), 04021043. [4] Kaschubek, D. et al. (2021) Act. Astronaut. 186, 33-49. [5] Guerrero-Gonzalez, F.J. and Zabel, P. (2023) Act. Astronaut. 203, 187-201.

ISRU metal and O_2 production modeling

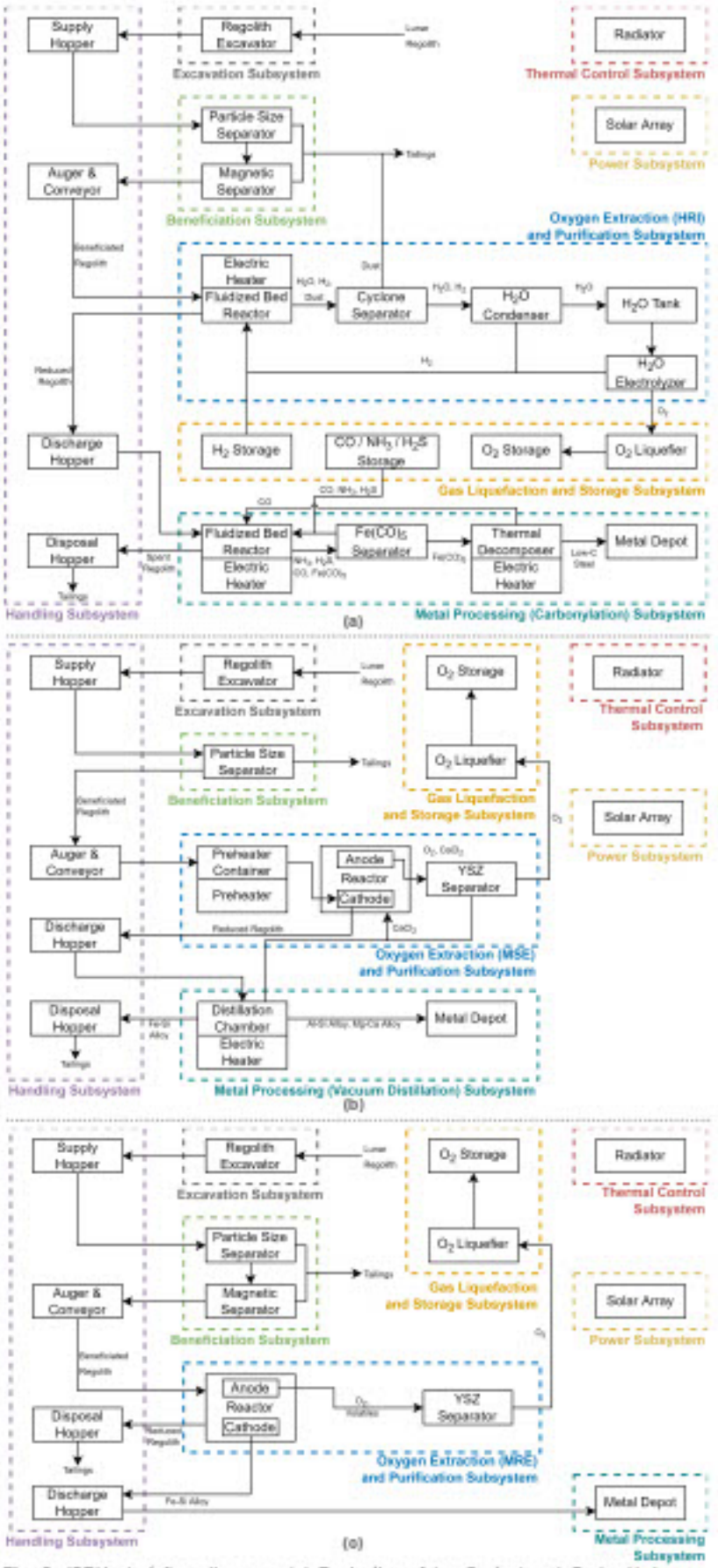

Fig. 2: ISRU plant flow diagrams. (a) Production of low-C steel and O_2 by Hydrogen Reduction of Ilmenite (HRI) and carbonylation. (b) Production of Al-Si alloys and O_2 by Molten Salt Electrolysis (MSE) and vacuum distillation. (c) Production of Fe-Si alloys and O_2 by Molten Regolith Electrolysis (MRE).

Using the models available in ISRULib, we have conducted in Ref. [5] a system study to compare the performance of 3 different ISRU production plants that extract metals and oxygen from regolith at the lunar South Pole. Fig. 2. schematically represents the selected processes that have been modeled holistically, including excavation, beneficiation, handling, oxygen extraction and purification, metal processing, gas liquefaction and storage, thermal control, and power. These models have been used to determine the overall ISRU mass and power budgets. Some of the study results can be found on the left.

Scan QR code to download system study

[1] Technical University of Munich, Professorship for Lunar and Planetary Exploration Technologies, Lise-Meitner-Str. 9, 85521 Ottobrunn, Germany

esric
powered by LSA, ESA & LIST

LIST

GEO-SPATIAL INFORMATION REQUIREMENTS for Lunar Resources Utilization

Abstract: The development of a geospatial information ontology can improve the exchange and use of information between stakeholders involved in lunar exploration through its implementation on the ESRIC Knowledge Sharing Platform. Through a qualitative mixed method using the Protégé application, the creation of a geospatial ontology adapted to the needs of the Luxembourg lunar exploration community was carried out. The conclusions of the study may lead to a standardized framework for the exchange and analysis of geospatial data in the context of lunar exploration and resource utilization.

Ivan Sánchez Alva, ESRIC [1] ivan.sanchez@esric.lu

Introduction:

This poster presents the concept of geospatial information for lunar resource utilization and the development of a framework for geospatial information sharing and analysis in the ESRIC Knowledge Sharing Platform. Geospatial ontologies can provide a standardized framework for integrating and analyzing geospatial data.

Aim:

This research aims to evaluate the potential utilization of geospatial information for lunar resource management and create a geospatial information ontology to assist individuals involved in lunar exploration by improving information sharing and utilization.

Ontology

Geospatial Information

Geospatial Information ontology is a formal representation of knowledge about geospatial information, including spatial relationships, geometry, and location-based concepts. It provides a common vocabulary and structure for organizing and sharing geospatial information across different systems and applications.

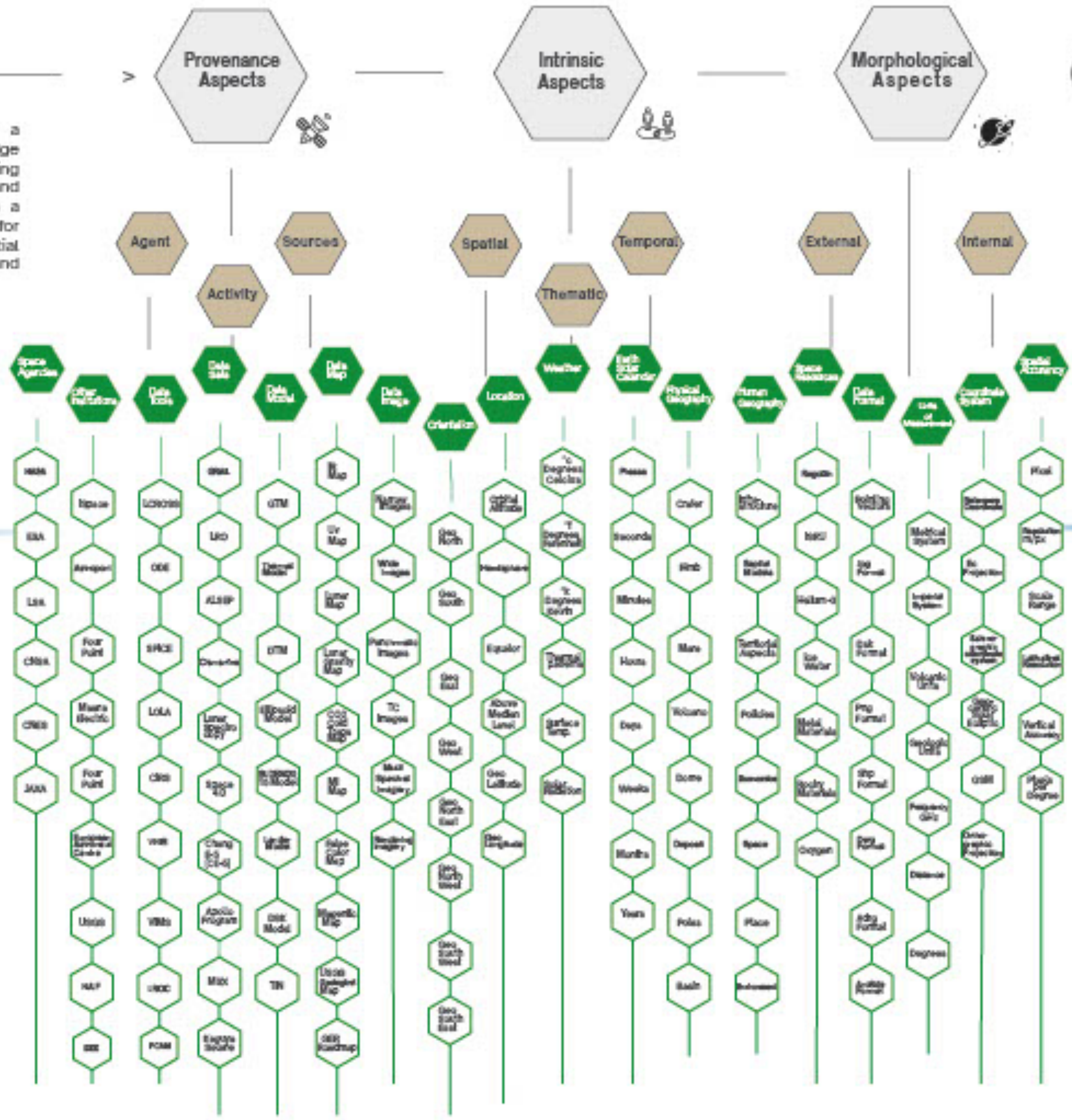

Findings:

The geospatial information ontology created in this study categorizes data related to provenance, intrinsic and morphological properties that we can observe. In this study **98** scientific articles were reviewed, of which only **26** contained information related to the topic of interest obtaining **768** concepts, which were classified into entities, classes and individuals, obtaining **335** concepts that were related by axioms using the Protégé application.

Discussion:

- Geospatial information ontology in the ESRIC platform standardizes vocabulary for knowledge sharing and functionality among stakeholders in lunar exploration around the world.
- Practical applications are the implementation of the concepts in the ESRIC Knowledge Sharing Platform to improve collaboration and information sharing among stakeholders involved in lunar exploration being useful for government and private organizations in developing more efficient and effective strategies for exploring and utilizing the Moon's resources.

Conclusion:

The development of a geospatial ontology integrated into the ESRIC platform can improve information sharing and utilization among stakeholders in lunar exploration and resource management around the world, promoting collaboration and innovation in the field.

References:

- Crawford, I.A., M. Anand, C.S. Cockell, H. Falcke, D.A. Green, R. Jaumann, and M.A. Wieczorek. 2012. 'Back to the Moon: The Scientific Rationale for Resuming Lunar Surface Exploration'. Planetary and Space Science [illegible]
- Dassereto, Federico, Laura Di Rocco, Giovanna Guerrini, and Michela Bertolotto. 2020. 'Evaluating the Effectiveness of Embeddings in Representing the Structure of Geospatial Ontologies'. In Geospatial Technologies for Local and Regional Development, [illegible] Lecture Notes in Geoinformation and Cartography. Cham: Springer International Publishing. [illegible]
- Di, Kaichang, Zhaoqin Liu, Wenhui Wan, Man Peng, Bin Liu, Yexin Wang, Sheng Gou, and Zongyu Yue. 2020. 'Geospatial Technologies for Chang'e-3 and Chang'e-4 [illegible]
- 'ESRIC KSP - Home Page'. 2022. 2022. https://knowledge.esric.lu/.
- 'ISO 19115 Geographic Information -- Metadata Workbook'. 2013.

Pantone:

Font: Open Sauce One

Regular (Content - Size 32)

Bold (Subtitles - Size 36)

ExtraBold (Titles - Size 42)

esa LUXEMBOURG SPACE AGENCY

LUXEMBOURG SPACE RESOURCES WEEK

Simulating Simulants

Joe Louca - Bristol Robotics Laboratory
Antonia Tzemanaki - Bristol Robotics Laboratory
Kerstin Eder - Bristol Robotics Laboratory
John Vrublevskis - Thales Alenia Space (UK)

Virtual modelling of lunar regolith behaviour can test tool designs and train robot operators for reduced gravity scenarios

Background

Future technology demonstration missions will collect lunar regolith

Lunar regolith is challenging due to **high friction** and **inter-particle cohesion**

Regolith simulants used for tests on Earth are often expensive and hazardous

Testing in reduced gravity is still difficult

Previous work[1] proposed a lunar regolith model with adjustable parameters: **gravity, density, friction** and **cohesion**

How can the model be **scaled up** and adapted to use as a **virtual simulant?**

Methodology

Updated algorithm only checks for collisions between particles in neighbouring cells

Computation time for the updated algorithm increases linearly with number of particles

Time complexity: $O(n)$ vs $O(n^2)$

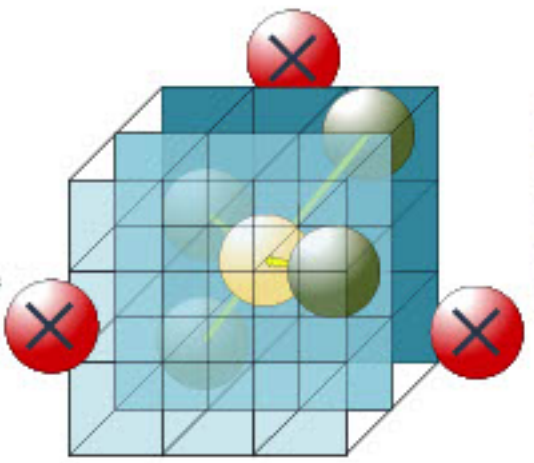

Scalability of Updated Simulation

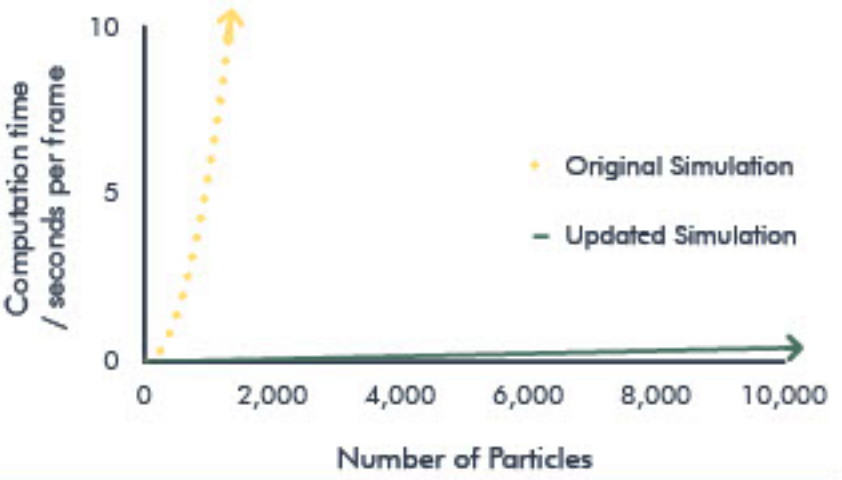

Results

Pouring through a funnel

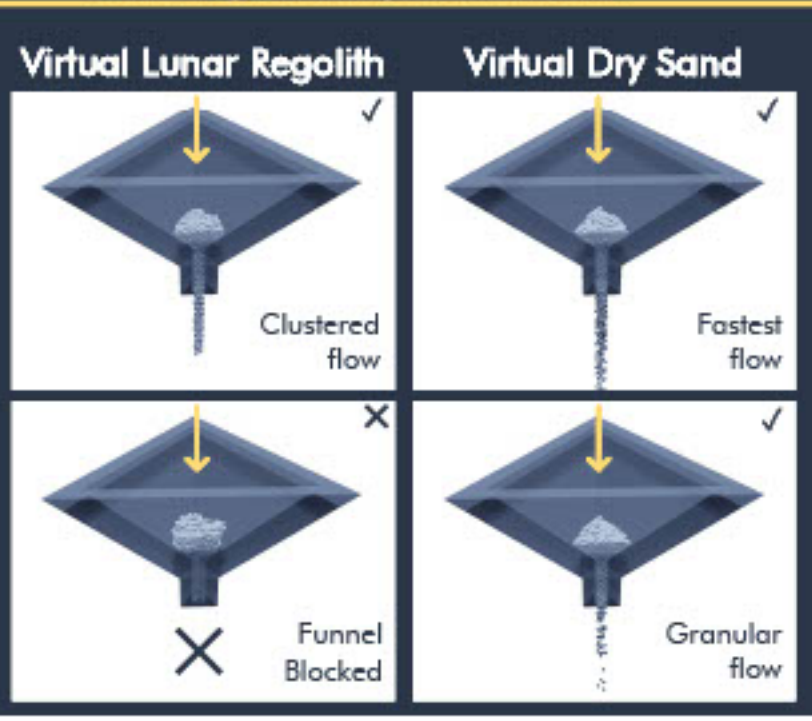

Collecting with brushes

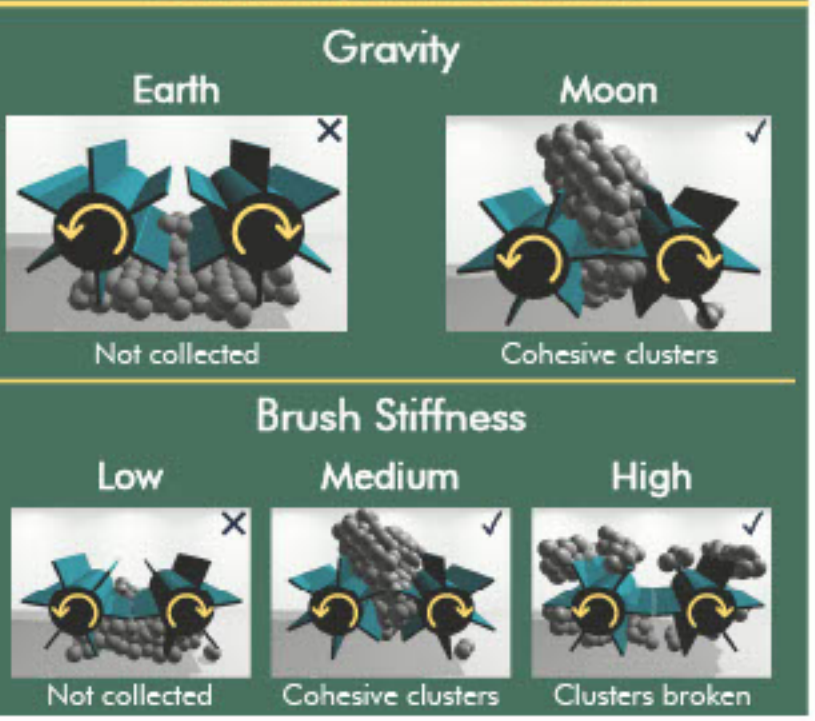

[1]Pereira, Aaron, and Annika Schmidt. "Efficient haptic rendering of regolith." 2021 IEEE International Conference on Robotics and Automation (ICRA).

SPACE RESOURCES WEEK 2023

brl Bristol Robotics Laboratory

University of BRISTOL

UWE Bristol University of the West of England

EPSRC Engineering and Physical Sciences Research Council

ThalesAlenia Space

Lunar Ejecta Assessment for Natural Landing Pad Selection

J.D. Menges[1] and Kevin M. Cannon[1]
[1]Colorado School of Mines, Space Resources Program
Golden, CO 80401
jdmenges@mines.edu

Background

As more permanent infrastructure and presence are established in pursuit of lunar resources, we must develop strategies to acquire and maintain access to regions of interest (ROI), including priority landing sites. Plume Surface Interaction (PSI) presents a challenge regarding safety near natural landing sites (sites with no constructed landing pad). Regolith particles, primarily less than a millimeter in diameter, traveling at high speeds (possibly exceeding lunar escape velocity) can directly impact and damage nearby terrain and existing infrastructure.

Historically, this phenomenon occurred when regolith ejected from the Apollo 12 lander resulted in significant pitting and erosion of the Surveyor III lander, approximately 155m away [1]. Figures 1 and 2 show the resulting damage to Surveyor III.

Figure 1. Pitting and cracking shown in color differences in returned portions of Surveyor 3 [1]

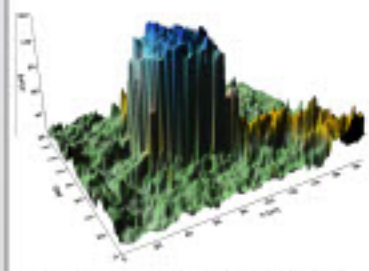

Figure 2. An example pit modeled from returned portion of Surveyor 3 [1].

This project aims to develop a tool that will provide a safety index in the product form of an aerial map overlay. Given a landing location, the overlay will show the comparative risk from a lander within a given radius of the landing site. Inversely, if we have a location we wish to protect, the overlay can show all landing locations that minimize the ejecta risk within a given radius of the protected site.

In the absence of constructed landing pads to mitigate ejecta, this tool would allow for the optimization of natural landing pad selection as well as the selection of sites for planned infrastructure development.

Results

Our index model aims to take the 2-dimensional cross-section seen in Figure 4 and apply it 360° around the landing location and radially outward to a specified radius of analysis. We restrict the DTM array to only the points (pixels) within the radius (Figure 5a). Using a particle distribution with a set number of bins, we look at the size and corresponding velocity of the smallest particle in each bin. We use a set trajectory angle of 3° to determine the trajectory model of each sized particle. Comparing this trajectory model to the elevation at every point within the radius allows us to determine if a particle of a certain size will travel to or beyond that point. If it does not, we further restrict the array to include only the points where a particle of that size could land (Figure 5b).

For our index model, we have chosen to assess the index as a function of impact momentum. Impact momentum is defined as the product of a particle's mass and velocity. Assuming a spherical particle and a grain density of 3100 kg/m^3, we associate each particle size with a momentum value. The total momentum at a given pixel would be the sum of the product of the number of particles landing in that pixel and their momentum value. We could estimate the total number of particles blasted by Apollo 12 using [4], but to decrease the computational complexity, we assume a total of 1e6 particles.

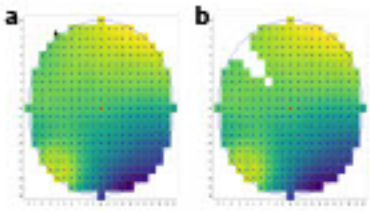

Figure 5. (a) DTM is restricted to points within 20m of A12. (b) DTM restricted to points accessible to 320μm particle at 3° launch angle.

The updated index product is an overlay of the ejecta assessment within the specified radius (Figure 6). The index values are the log of the summed momentum values at each pixel. A higher index value represents higher damage potential from ejecta.

Inversely, the index tool also provides the ability to protect locations. Figure 7 is centered on Surveyor III. Each pixel's index value now represents the ejecta damage potential to Surveyor III from landing at that point.

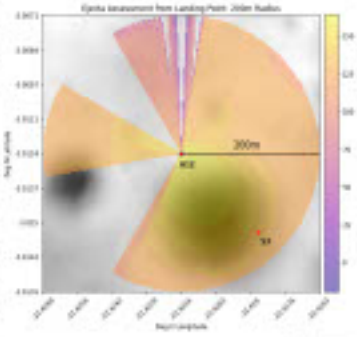

Figure 6. (left) Centered on the Apollo 12 landing site, the index overlay shows the potential damage done by regolith ejecta within 200m of the landing site.

Figure 7. (right) Centered on Surveyor III, the inverse index shows the damage done to S3 from landers landing at any point within 200m of S3. The optimal landing locations are those with no index value presented.

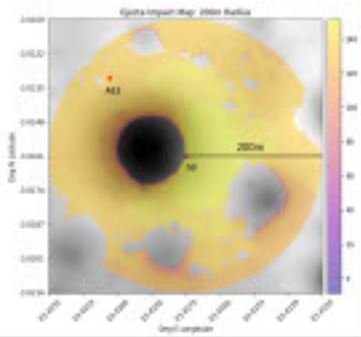

Initial Model Setup: Digital Terrain Model & 2D Cross-Section

Using the Apollo 12 landing scenario as a proof of concept for our index tool, we acquire the high-resolution Digital Terrain Model (DTM) of the Apollo 12 landing site from LRO NAC [5]. We estimate the particle size distribution from [3] & [4] and the initial particle velocity from [2] & [4]. We assume an isotropic distribution of particles radially from the landing site and a velocity distribution as a function of particle size estimated from [2]. We used a simplified ballistic trajectory model, treating the regolith as a collection of individual spherical particles that follow ballistic trajectories without complex interactions such as collision with other particles or plume entrainment.

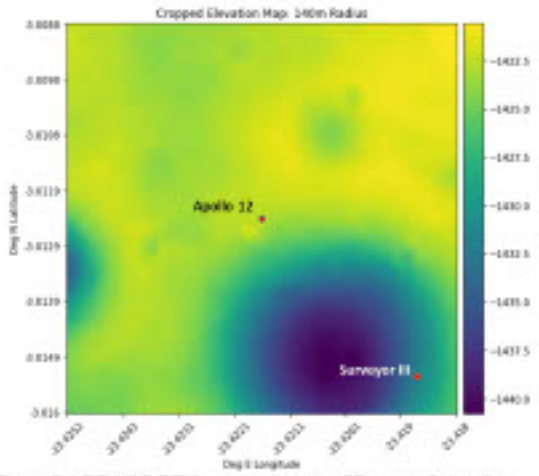

Figure 3. LRO NAC DTM constructed as a 2D array of elevation values. LRO NAC spatial resolution is 2 meters per pixel (mpp).

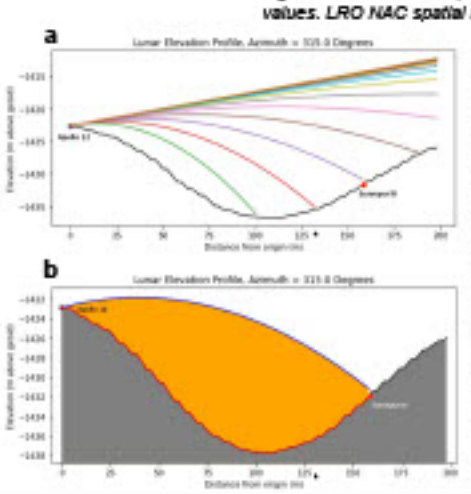

Figure 4. (right) (a) Trajectories of 20 different particle sizes between 0.6μm and 1.2cm launched at a directional azimuth of 315° at a launch trajectory angle of 3°. (b) Trajectory of particles binned between 2.6 – 4.3mm. Red outline shows the ground surface susceptible to impact damage from particles of these sizes launched at 3°.

After constructing an array of the DTM (Figure 3), we determine whether the trajectories of particles, by size, are impeded by existing terrain. Figure 4a shows a cross-section of particles ranging from 0.6μm to over 1cm launched at an angle of 3° at a 315° azimuth, replicating the estimated trajectory angle and direction of ejecta toward Surveyor III. Figure 4b, shows the potential ground surface damage of particles binned between 2.5 – 4.3mm.

Discussion

Current trajectory models, even simplified ballistic models, are computationally intensive and therefore time consuming. The creation of an index tool that can efficiently map the comparative safety and hazards presented by PSI ejecta will visually assist planners in the downselection of landing sites within a desired distance from resource-rich ROIs and eventually extraction and processing infrastructure.

Inputting a particle size distribution currently poses a challenge, as such distributions can only be accurately estimated from returned lunar samples. [7] is currently working on a thermophysical model that would derive a global lunar map of regolith properties, including grain radius.

This tool also provides the capability of visually showing the benefits or drawbacks of infrastructure placement. Since the DTM is a simple 2D array of elevation values, we can simulate infrastructure by manipulating the elevation values in the array. For example, building a 10m long by 2.5m tall berm directly southeast of the Apollo 12 landing site would result in the overlay shown in Figure 8 with no apparent damage to Surveyor III. This could be optimized to show the minimum height of berms required to protect infrastructure or the maximum height of buildings allowed that would minimize their exposure to ejecta.

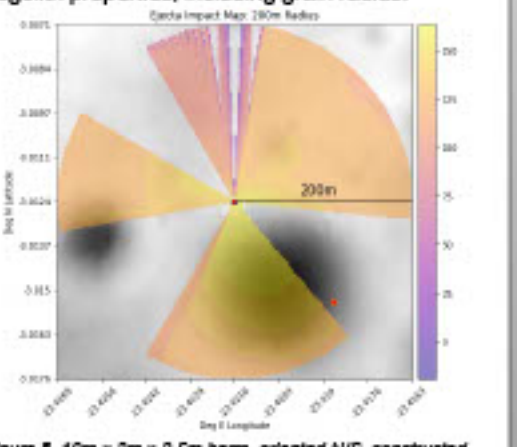

Figure 8. 10m x 2m x 2.5m berm, oriented N/S, constructed 10m SE of A12 landing site. A berm constructed at this location would have minimized damage to Surveyor III.

Conclusion

This index tool aims to provide mission planners with a simplified method of downselecting potential natural landing sites optimized toward minimizing localized erosion risks to terrain, infrastructure, and equipment. Ideally, a finalized version of this proposed tool would present a user interface that allows users to input the coordinates for the potential landing or protected site and the desired radius of analysis.

The tool would also allow for the construction of simulated infrastructure (e.g., berms or habitats) to analyze the benefits and drawbacks of protected and unprotected structures. If building material is known, the estimated penetration depth of pitting ejecta into infrastructure could also be estimated and used as an additional indicator of risk [6] (Figure 9). Another variable to consider as an input is lander type, which can influence the number of particles blasted from the landing site as a function of thrust [4].

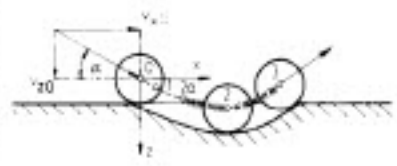

Figure 9. The path of a singular regolith grain penetrating infrastructure as modeled in [6].

References

[1] Immer et al. (2011), *Icarus, 211(2)*, 1089-1102. [2] Lane & Metzger (2015), *Acta Geophysica, 63(2)*, 568-599. [3] Graf (1993), *NASA Reference Publication 1265*. [4] Katzan & Edwards (1991), *NASA Contractor Report 4404*. [5] Henriksen et al. (2017), *Icarus, 283*, 122-137. [6] Beckmann & Gotzmann (1981), *Wear, 73(2)*, 325-353. [7] Bürger et al. (2023), *54th LPSC Abs. 1185*.

National Aeronautics and Space Administration

LUNAR DEVELOPMENT & TEST FACILITY

NASA-JSC BLDG. 351

NASA-JSC-EP offers lunar environmental test capabilities for subsystem and system hardware and assemblies at JSC Building 351. This capability complements existing Agency resources for both ambient dust testing and dirty thermal vacuum capability.

Component Test Lab Features

- 3-ft. dirty thermal vacuum chamber: 10^{-7} torr, LN_2 cooled shroud
- Ambient settling dust chamber for quick and easy functional testing with agitated simulant
- Vacuum glove box for convenient manipulation for testing
- On-site expertise available for successful vacuum operations with prepared simulant samples and test articles

Dust Containment & Preparation Lab

Regolith Simulant Test Bin Features

- 48" x 96" surface area for larger test articles or mobility testing
- 8" maximum fill depth
- Interior baffles for partial filling at full depth and efficient use of simulant
- Filled and prepared in dust containment and prep lab to keep other equipment clean

15-foot Chamber Features

- 15-ft. Φ Spherical with ~78-in. Φ clear entry for easy access
- Vacuum: ~10^{-6} torr, Thermal: -196°C to +120°C
- Air, GN_2 pressurization
- Feed-throughs for high-power electrical connections and high-channel count data
- Control automation enabling low-cost operations
- Ambient dust containment room for regolith control and testing
- Hardware exposure testing to dust/regolith
- Regolith bin for design and test of excavation, processing, or construction technology

Deploying Lunar In-Situ Resource Utilisation Plant with Explicit Consideration of Uncertainty

Kosuke Ikeya[1], Michel-Alexandre Cardin[2], Jan Cilliers[1], Stanley Starr[1], Kathryn Hadler[3]

1. Imperial College London, Department of Earth Science and Engineering
2. Imperial College London, Dyson School of Design Engineering
3. European Space Resources Innovation Centre

1. Introduction

To deploy efficient and feasible In-Situ Resource Utilisation (ISRU) plants on the moon, some critical decisions need to be made carefully.

Examples of Decisions

- Scale of the plant 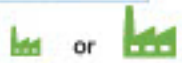 small or large
- Resource extraction technology

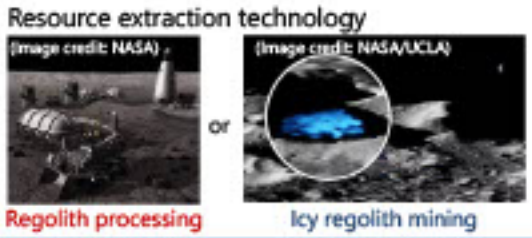

Regolith processing | Icy regolith mining

However, **operational and environmental uncertainty** makes this decision-making challenging.

Source of Uncertainty

- Resource content 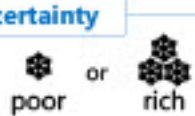 poor or rich
- Operational availability

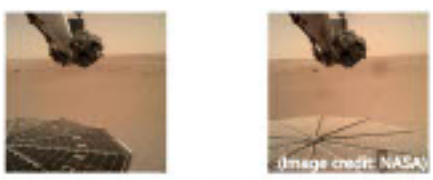

Solar arrays of InSight covered with Martian regolith.

Aim: Estimate the **value and risk of each decision** by explicitly considering the distribution of **uncertain parameters** and their effect on the performance of ISRU plants.

Method:
1) Monte-Carlo Simulations
2) Bayesian Decision Analysis

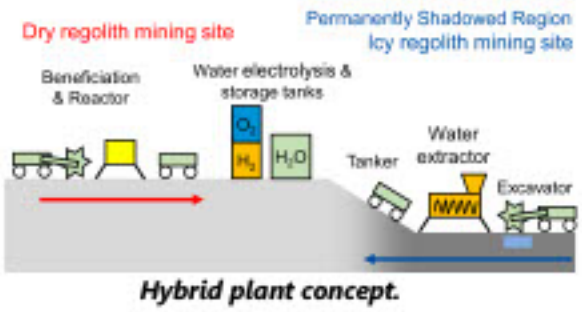

Hybrid plant concept.

2. Method

Plant Mass and Power Estimation

- Dry regolith processing (Carbothermal reduction)
  - Carbothermal reduction reactor sizing based on Ref. [1]
  - Oxygen yield calculation based on Ref. [2]
  - Lunar highland regolith composition [3]
- Ice mining
  - Auger dryer [4]
  - Oxygen yield based on resorption & desorption model [5]

Lunar Auger Dryer ISRU (LADI). [4]

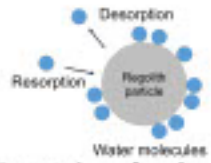

Desorption and Resorption of molecular water.

Monte-Carlo Simulation

Excerpt of Monte-Carlo variables and distributions.

Variable	Average	Standard deviation	Distribution	Refs.
SiO_2 content	45.2 %	0.93 %	normal	[3]
Water content	1 %	0.5 %	lognormal	[6, 7]
Operational availability	225/365	2.5%	lognormal	[1, 8]

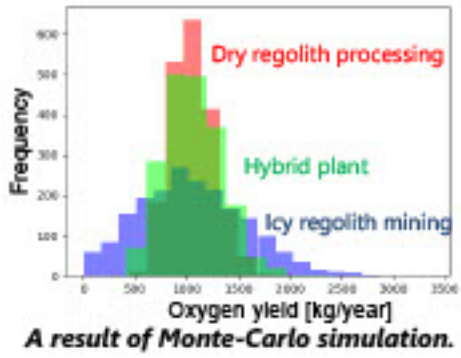

A result of Monte-Carlo simulation.

Bayesian Decision Analysis

Bayesian decision trees provide the value of each decision from various outcomes and the probability of each outcome happening.

1st decision: O_2 extraction technology
1st chance: O_2 yield of pilot plant (1 yr. operation)
2nd decision: Scale of full-sized plant
2nd chance: O_2 yield of full-sized plant (3 yrs. operation)

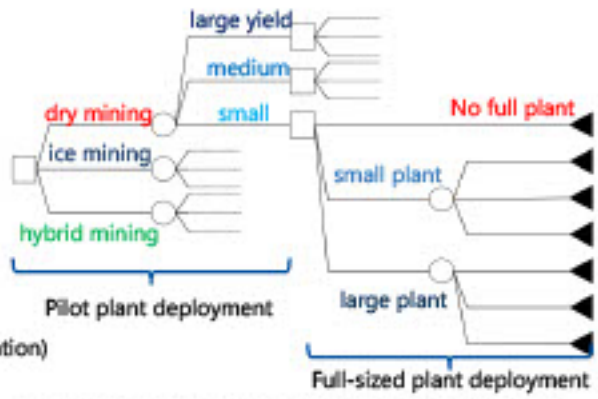

Decision tree of deploying Lunar ISRU plants.

3. Results

Expected values of each decision based on multiple criteria.

Criterion	Decisions: Plant technology	Decisions: Plant size	Score
Oxygen yield m_{O_2}	Dry regolith processing	Big plant	36,000 t
	Ice mining	**Big plant**	**75,900 t**
	Hybrid mining	Big plant	75,600 t
Oxygen yield ratio $\frac{m_{O_2}}{m_{regolith}}$	**Dry regolith processing**	**Small plant**	**6.8e-3**
	Ice mining	Small plant	5.3e-3
	Hybrid mining	Small plant	5.6e-3
Sustainability indicator $\frac{m_{O_2}}{m_{system}}$	Dry regolith processing	Big plant	13.1
	Ice mining	Big plant	31.7
	Hybrid mining	**Big plant**	**34.8**

The best combination of decisions changes depending on the criterion.

4. Discussion & Future Work

Sensitivity Analysis

The storage capacity turns out to be a sensitive parameter for plants with icy regolith mining.

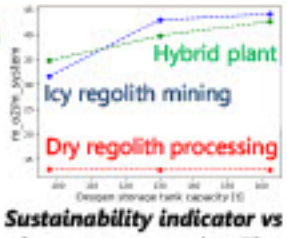

Sustainability indicator vs the storage capacity. The change in the best plant architecture can be seen.

Future Work

- Optimisation of each plant design.
- Improvement of mass and power estimation.

5. Conclusion

The expected performance of ISRU plants based on each decision is analysed considering three plant architectures: **carbothermal reduction of dry regolith**, **water extraction from icy regolith**, and a new **hybrid plant** of them. The preliminary result indicates ice mining is expected to produce more oxygen while dry regolith processing is expected to generate more oxygen per excavated regolith mass. The hybrid architecture is expected to outperform the others regarding oxygen yield per system mass.

References

[1] Sirina, D. L., Schuler, J. M., Ohkita, L., Kleinhans, J. E., Colletta, A. J., J Rasmussen, K., Olsson, S. R., Sutvik, N. K., and Moore, L. "Lunar Production System for Extracting Oxygen from Regolith." Journal of Aerospace Engineering, Vol. 34, No. 4, 2021, p. 04021045. https://doi.org/10.1061/(ASCE)AS.1943-5525.0001255

[2] Reid, I., Lungh, S., and Lovegra, M. "Oxygen Extraction from Lunar Dry Regolith: Thermodynamic Numerical Characterization of the Carbothermal Reaction." Acta Astronautica, Vol. 169, 2020, pp. 133–154. https://doi.org/10.1016/j.actaastro.2020.01.031

[3] Wiley, W. I., Reid, A. M., Warner, J. L., Brown, R. W., Gooley, R., and Donaldson, C. (1970). Glass compositions in Apollo 12 soils 12021 and 12051 Proceedings of the Abstract Science Conference, 309-321

[4] Sirina, D. L., Kleinhans, J. E. and Ilka, A. "Lunar Water Plant Plant Conceptual Design." AIAA 2020-4250 AIAA/AHS 2020 November 2020.

[5] Reiss, P. "A Combined Model of Heat and Mass Transfer for the In Situ Extraction of Volatile Water from Lunar Regolith." Icarus, Vol. 308, 2018, pp. 1–15. https://doi.org/10.1016/j.icarus.2018.01.020.

[6] Hayne, P. O., Hendrix, A., Sefton-Nash, E., Siegler, M. A., Lucey, P. G., Retherford, K. D., Williams, J.-P., Greenhagen, B. T., and Paige, D. A. "Evidence for Exposed Water Ice in the Moon's South Polar Regions from Lunar Reconnaissance Orbiter Ultraviolet Albedo and Temperature Measurements." Icarus, Vol. 255, 2015, pp. 58–69. https://doi.org/10.1016/j.icarus.2015.03.032.

[7] Colaprete, A., Schultz, P., Heldmann, J., Wooden, D., Shirley, M., Ennico, K., Hermalyn, B., Marshall, W., Ricco, A., Elphic, R. C., Goldstein, D., Summy, D., Bart, G. D., Asphaug, E., Korycansky, D., Landis, D., and Sollitt, L. "Detection of Water in the LCROSS Ejecta Plume." Science, Vol. 330, No. 6003, 2010, pp. 463–468. https://doi.org/10.1126/science.1186986.

[8] Cilliers, J. J., Kleyn, J.N., and Hadler K., Estimating the scale of Space Resource Utilisation (ISRU) operations to satisfy lunar oxygen demand (2020), Planetary and Space Science, 180, 104749

Review of Water Capturing Devices for Lunar ISRU

Christoph Kalis[1,2], Luca Kiewiet*[1], Mart Heitkamp[1], Henning Wache[1], Alessandra Menicucci[2] and Paul Zabel[1]

[1]German Aerospace Center (DLR), Institute of Space Systems, Bremen, Germany
[2]Delft University of Technology, Faculty of Aerospace Engineering, Delft, Netherlands
*luca.kiewiet@dlr.de

1. Introduction

The use of resources present on celestial bodies, known as In-Situ Resource Utilization (ISRU), is becoming more and more important in space exploration due to the high cost of launching mass into orbit. ISRU would enable long-term manned operations and permanent (robotic) presence on extra-terrestrial bodies. Water is considered to be one of the most important resources for further space exploration and is currently investigated for extraction and purification on the future manned Lunar base envisioned around 2025. Previous research focused on the extraction of water from regolith but little work has been done to find ways on how to capture and liquefy the water vapour after its extraction.

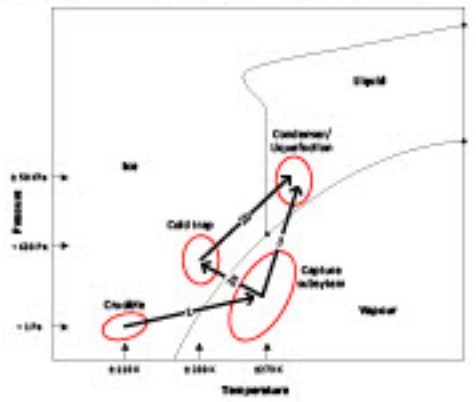

Figure 1: Schematic phase diagram with process overview. Path 2 shows how water can be captured as a solid, and path 3 as a liquid.

Thermal extraction is currently the preferred method for winning water, meaning heat is applied to the water ice regolith mixture resulting in the sublimation of ice and outgassing of the water vapour. This vapour is then captured and liquefied, as can be seen in figure 1. If sufficient temperature and pressure is present in the reaction chamber, a collection as liquid on the bottom of the chamber is theoretically possible. Unfortunately, the regolith has a high saturation with liquid water of around 16%. The residual water in the regolith would be too high and thus efficiency of the collection is likely too low. See figure 2 for the setup to test this.

Figure 2: Test-setup water in lunar regolith (saturation occurs at around 16%).

2. Potential Solutions

A cold trap is a cold surface to which the water vapour coming from the extraction system can deposit onto as a solid, after which it can be considered captured and secured. In this scenario, liquid water occurs after the capturing in a solid state. The gathered ice needs to be in an environment where liquid water can exist. Whether this change in pressure and temperature takes places directly in the capturing system (internal liquefaction) or whether the ice is detached from the capturing system and processed in another location (external liquefaction) needs to be decided.

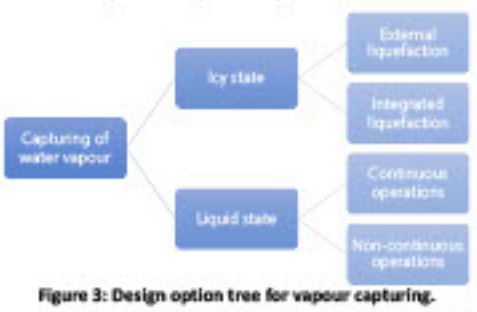

Figure 3: Design option tree for vapour capturing.

The options for capturing in liquid state can be divided in continuous and non-continuous operations. For continuity, a constant flow of water vapour to the condensing surface at sufficient pressure and temperatures above the triple point is needed. This could be realized with a pump between the extraction subsystem and the capturing subsystem, since the liquid phase is undesired in the extraction subsystem. A high pressure in the crucible is unwanted since the water should only be in solid or gas state during extraction. These options are visualized in figure 3.

3. Preliminary Design of LUWEX

In Figure 4 an overview of the entire LUWEX experiment design is presented. A needle valve between the cold trap chamber and the vacuum chamber controls the vapour flow towards the actual cold trap itself and prevents the pressure rising too much. A slider separates the cold trap chamber from the liquefaction chamber to have a contained environment during liquefaction. In Figure 5 a preliminary CAD drawing of the relevant systems is presented. In the crucible, the water vapour has a temperature of around 273K after heating the regolith. This refers to a saturation pressure of 470 Pa which is then also present in the cold trap and liquefaction. Present volatiles in the icy-regolith sample are water ice, methanol, ethanol, CO2. The cold trap has to withstand these volatiles and is designed in such a way, that these volatiles are not deposited on the cold fingers.
The design was driven by volume constraints of the chamber and size of the slider which separates the cold trap and the liquefaction.
The goals of this baseline design were as follows:

1. As much cold trap area as possible for maximal ice mass and thus water vapour capturing.
2. Long residence time of the vapour for lower losses leading to a higher efficiency.
3. High liquefaction volume to lower the need for melting cycles for a higher total collection rate.

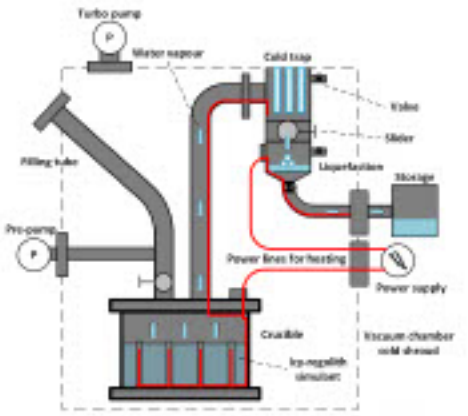

Figure 4: Schematic of the LUWEX experiment inside the TVAC.

The main reason for the decision of capturing as a solid, meaning cold trapping, was less complexity, since there is no need to rise the pressure between the crucible and the capturing system.. The condenser needs pumps and valves with pressure control to function efficiently and optimally. Besides, the condenser needs to maintain a higher temperature than the cold trap for it to work. The cold trap can make use of the cold Lunar environment. Also, less heat and control schemes are required to achieve the desired temperature and pressure ranges. Yet, the system is less controllable because pressure is more sensitive to unwanted condensation.

In future systems with cold trapping, the liquefaction might not occur directly after the capturing, so the intermediate storage could be in icy state. This reduces the storage complexity and favours the design with a cold trap.

Figure 5: Model of the cold trap and liquefaction.

4. Cold Trap Experiment

Since there is little experience about capturing water vapour in low pressure environments, and specifically so for the purpose of In-Situ Resource Utilization, a small-scale test was conducted to see how effective it would be to capture water vapour on the Moon using a cold trap. Figure 6 shows the setup of this experiment.

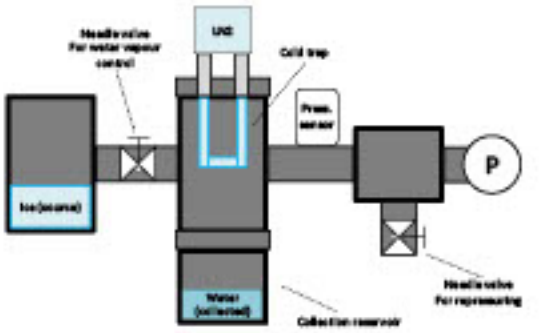

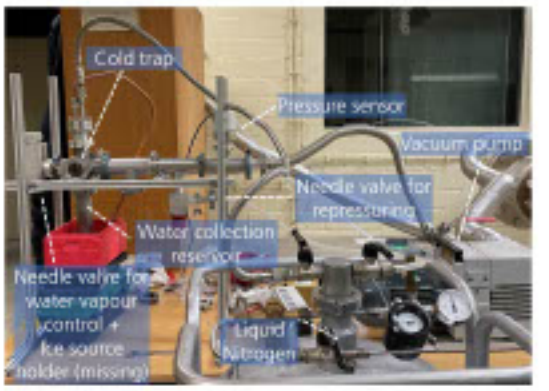

Figure 6: Schematic experiment setup above and the actual setup below.

The experiment was designed to test the effectiveness of the cold trap when the vacuum pump is running ("constant" low pressure). This would be analogous to the cold trap being exposed to the "atmosphere" of the Moon. In table 1 the results are presented.

Table 1: Results of the cold trap experiment under low pressure.

Run #	Sublimated [g]	Captured [g]	Efficiency
1	9.34	7.11	76.12%
2	4.45	3.18	71.46%

Figure 7: Cold trap without ice (left) and with ice (right).

Secondary to this, experience and insights were gained along the way about cold traps and working with these test setups.
The collection efficiency was surprisingly high, despite the shape of the cold trap not being optimized.

5. Conclusion

The challenge of this research project is the lack of data and previous research done in the field of water capture for ISRU. Nevertheless, these outcomes provide a solid foundation for LUWEX and future research. Many different ways to capture water vapour are envisioned, and this work provides an initial overview in some of the possibilities. Future works will investigate what the most optimal way to capture water would be for different scenarios.

Visit https://luwex.space/ or scan the QR code!

This work is part of the DLR internally funded young investigator group "Synergetic Material Utilization" (SMU) established 2021 at the Institute of Space Systems in Bremen, Germany. The group focuses on research and development of ISRU technologies for Moon and Mars exploration.

The project LUWEX is funded through the Horizon Europe framework program of the European Union with the grant number 101081937.

Funded by the European Union

Experimental optimisation of lunar regolith beneficiation for the production of an Ilmenite-rich feedstock

Kunal Kulkarni*[1], Paul Zabel[2]

[1]Technical University of Berlin, Institute of Aeronautics and Astronautics, Berlin, Germany
[2]German Aerospace Center (DLR), Institute of Space Systems, Bremen, Germany
*kunal.kulkarni@dlr.de

1. Introduction

The space industry is moving towards increasing sustainability for operations of a long duration space mission and eventually a permanent space settlement. In-situ resource utilisation (ISRU) technologies will play a major role in realizing this vision. As Moon is the current object of interest, lunar regolith becomes the most abundantly available source of different minerals on the lunar surface. One such mineral is Ilmenite which is an ore of titanium as well as a source for oxygen. Previous research shows that Ilmenite is a more energy efficient source for extraction of oxygen compared to other minerals such as silicates.

However, Ilmenite deposits on the lunar surface are scattered and not as high as the silicate minerals. Therefore, beneficiation of lunar regolith for increasing the Ilmenite concentrations to maintain process efficiency is important for the potential oxygen process chain. The research published in this poster is a part of the lunar regolith beneficiation project undertaken at the German Aerospace Center in Bremen by the Synergetic Material Utilisation research group. A test setup is developed for beneficiation of lunar regolith to separate Ilmenite from the rest of the particles in the lunar regolith and produce an enriched feedstock that can be further used for extraction of oxygen and/or other metals.

2. Beneficiation Test Setup

The beneficiation test setup is a multi-stage processing unit that comprises of gravitational, magnetic and electrostatic beneficiation methods for beneficiation of the input lunar regolith simulant. It starts with a vibratory feeder followed by a horizontal sifter that filters the regolith based on the particle size. The next stage is a permanent magnet rotating drum separator that filters out the ferromagnetic agglutinates and dust particles. The last stage consists of a tribocharging setup with electrostatic plate separator at the bottom which further separates Ilmenite from the other phases present in the simulant. The system schematic and the beneficiation test setup are both shown in the figures below.

3. Experimental Evaluation

The experimental validation and optimisation of the beneficiation test setup is currently in progress. The goal of the optimisation experiments is two fold:

1. Validation of the beneficiation test setup
2. Determination of an optimized configuration of experimental parameters for achieving best possible beneficiation

The different phases of experimental optimisation are shown in the figure 1.

- **Phase 0**
  - Feed rate calibration in conventional units (kg/hr)
  - Magnetic separator operational testing
- **Phase 1**
  - Magnetic separator output v/s regolith feed rate
  - Magnetic separator output v/s rotational speed of the permanent magnet drum separator
- **Phase 2**
  - Electrostatic beneficiation output v/s electrostatic field voltage (wider range of values)
- **Phase 3**
  - Electrostatic beneficiation output v/s electrostatic field voltage (narrower range after results from phase 2)
- **Phase 4**
  - Effect of different simulant systems on the output of the beneficiation test setup

Figure 1: Phases of optimisation experiments

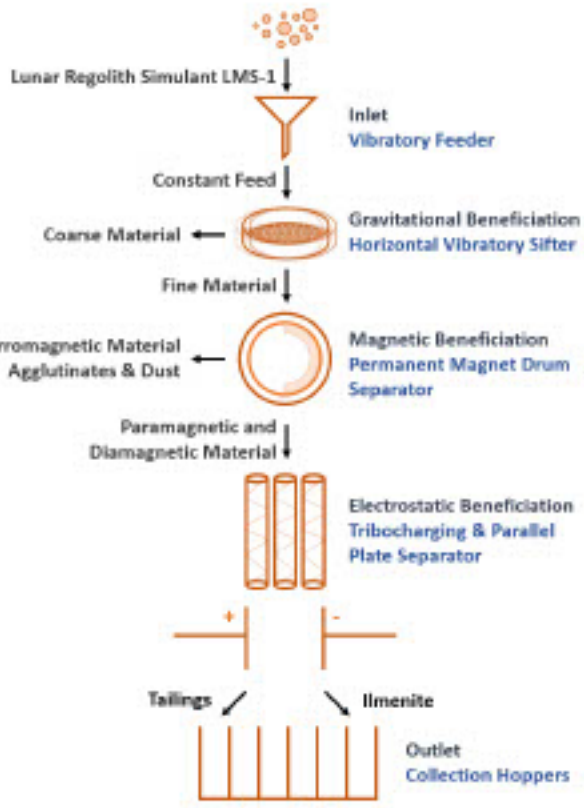

Figure 2: Beneficiation setup system schematic

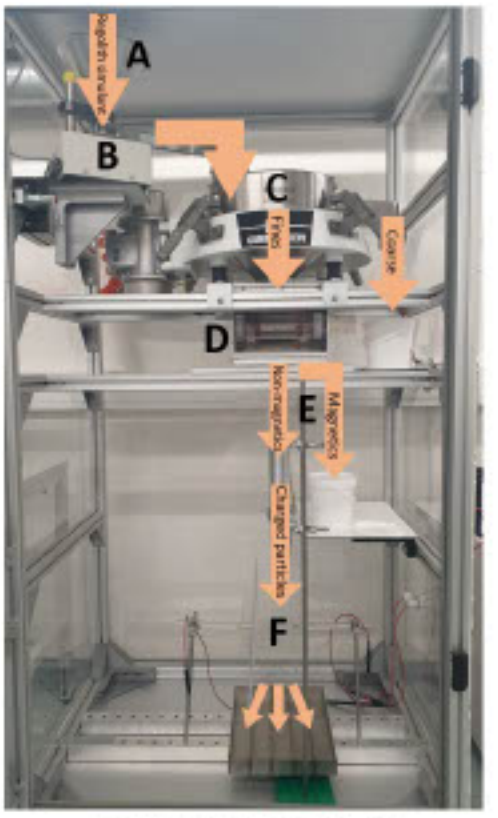

Figure 3: Beneficiation test setup

4. Sample Phase Analysis

The samples collected during optimisation experiments were analysed using X-ray diffractometry (XRD) at the Department of Crystallography in the University of Bremen. The qualitative phase analysis for the samples is done using X'pert HighScore software tool while the quantitative phase analysis is done on TOPAS software that uses Rietveld refinement approach for analysis.

5. Preliminary results

The initial data derived from analysing collected samples is used to calculate the essential beneficiation parameters that give clarity about effectiveness of the test setup. The parameters are yield, recovery, grade and enrichment ratio. All of these are calculated for Ilmenite in the output samples. Each experiment is conducted three times and the average is calculated for further consideration to account for any inconsistencies in the experiments. The results from Phase 1 are illustrated in figure 4 that show relationship between the beneficiation parameters and feed rate of the input regolith. These illustrate the output of magnetic beneficiation stage of the test setup. The equations used for calculation of the beneficiation parameters are given below.

$$\text{Yield} = \frac{\text{Mass of product produced (eg. Ilmenite)}}{\text{Total mass of feedstock}}$$

$$\text{Recovery} = \frac{\text{Mass of the produced product (eg. Ilmenite)}}{\text{Mass of product in raw material (Ilmenite in regolith fed to the beneficiation system)}}$$

$$\text{Grade} = \frac{\text{Mass of product (Ilmenite in feedstock)}}{\text{Mass of stream (Total mass of feedstock)}}$$

$$\text{Enrichment Ratio} = \frac{\text{Grade of given species in the outlet (Ilmenite content in the ore concentrate)}}{\text{Grade of the same species in input (Ilmenite content in raw material)}}$$

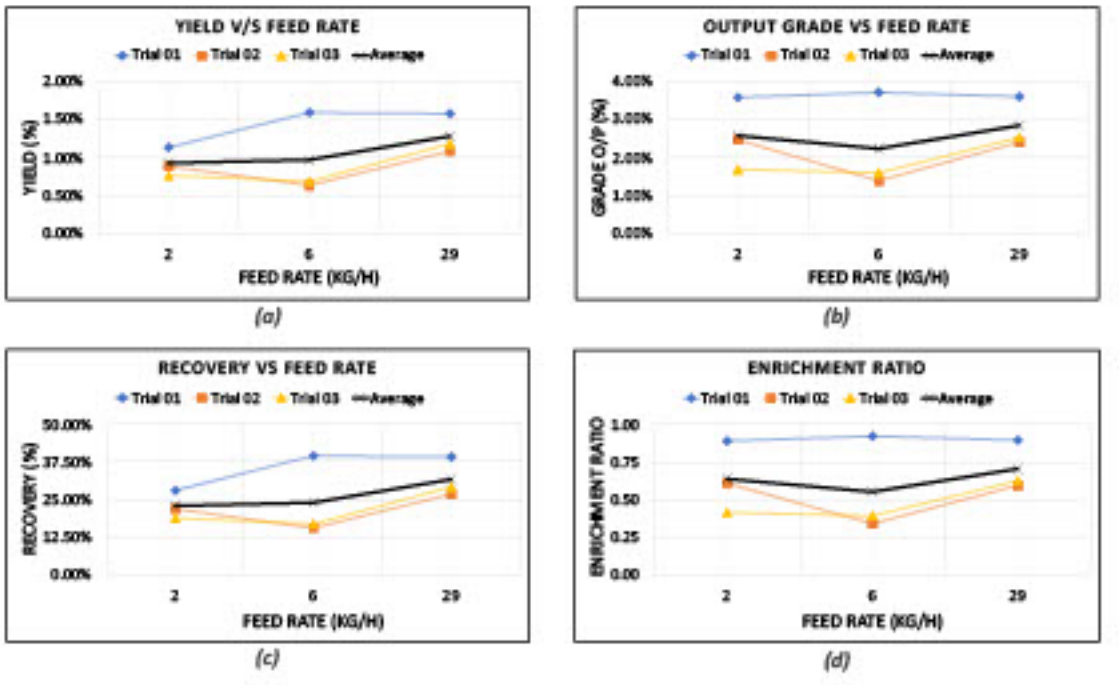

Figure 4: Preliminary results for magnetic beneficiation of LMS-1 lunar mare simulant

6. Conclusion

The phase 1 results show the effectiveness of magnetic beneficiation stage when considered independently. The current efforts are focused on the electrostatic beneficiation stage, particularly on the electrostatic plate separator. The initial results of the electrostatic separation show positive results with enrichment ratios up to 2.9, 33% recovery for ilmenite in output bins and around 12% grade of Ilmenite in the output. Further experiments and optimisation will provide better insights about the effect of electrostatic separator stages on the beneficiation parameters. Eventually, a more comprehensive analysis of results will provide the final optimal configuration such that the best possible beneficiation is achieved while also taking into account secondary parameters such as power consumption, maintenance requirements, etc.

This work is part of the DLR internally funded young investigator group "Synergetic Material Utilization" (SMU) established 2021 at the Institute of Space Systems in Bremen, Germany. The group focuses on research and development of ISRU technologies for Moon and Mars exploration.

Design Investigation of Lunar Water Extraction

Luca Kiewiet[1*], Mart Heitkamp[1], Christoph Kalis[1], and Paul Zabel[1]

[1]German Aerospace Center (DLR), Institute of Space Systems, Bremen, Germany
*luca.kiewiet@dlr.de

1. Introduction

Water is an essential resource for space exploration, for both robotic and human exploration. It is foreseen that in the future, these resources can be used to produce rocket propellant by electrolyzing water into its components Hydrogen and Oxygen or by astronauts for drinking water and breathable oxygen. This Space Resource Utilisation (SRU) would reduce the cost of spacefaring significantly. Recent discoveries have confirmed the presence of ice at the Lunar south pole. In this work, which is a continuation of the work presented in [1], the design parameters of 4 types of methods for thermal water extraction on the Moon are investigated. These methods are the in-situ surface heating method, the in-situ heated rods method, and the crucible method in different variations, as can be seen in figure 1. The goal is to find the most optimal way to extract water from the lunar surface.

Additionally, this poster will present some early results from the EU *LUWEX* project.

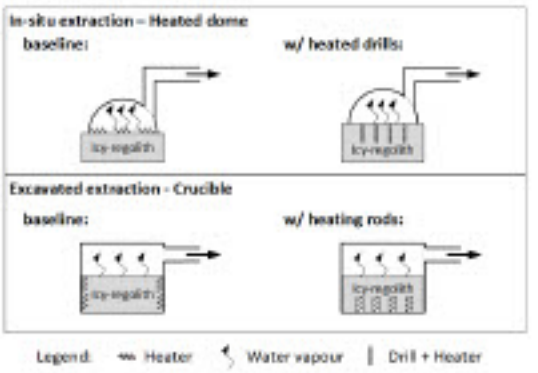

Figure 1: Schematic of examples for thermal water extraction methods.

2. Designs

The methods investigated are the in-situ surface heating, in-situ heated rods and a sealed reaction chamber. The sealed reaction chamber is extended with a dynamic version, a rotating drum. In figure 2 this design illustrates the drum in DEM Simulation software *Becker3D*. In table 1 the parameters investigated in this study are presented.

Table 1: Design parameters for each thermal water extractor design.

In-situ surface heating	In-situ heated rods	Reaction chamber
Power density	Number of rods, length of rods, diameter of rods, spacing between rods	Method of applying heat
Emissivity of dome	Power density, power gradient	Size
Dome size	Dome size	Excavation rate

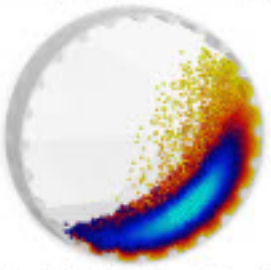

Figure 2: Rotating drum of particles for increasing the effective thermal conductivity; achieving ~10 K / min for significant decrease in water extraction time [2].

3. Methods

COMSOL Multiphysics 6.1 is used to simulate the designs. The designs of figure 1 are implemented where the icy-regolith is modelled as a solid containing ice and regolith. This mixture of ice and regolith contains the phase change material. Heat can be transferred to the ambient environment through radiation. Heat fluxes are applied at the curved surface in figure 3 for the crucible method and at the top surface in figure 4 for the in-situ method. Only when the latent heat of water is surpassed in an element, the ice is sublimated.

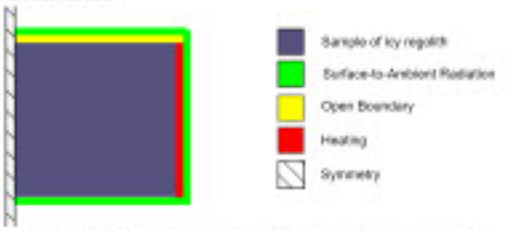

Figure 3: Boundary conditions for heating inside crucible after excavation.

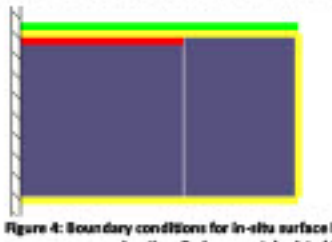

Figure 4: Boundary conditions for in-situ surface heating and in-situ rod heating. Rods are not depicted here.

4. Results

The total time-dependent water yield is shown in figure 5 for the 5% water content in-situ surface heating, in-situ heated drills and the baseline crucible, respectively. In these results, it can be clearly observed that the heated drills and the crucible have much higher yields than the simple in-situ surface heating.

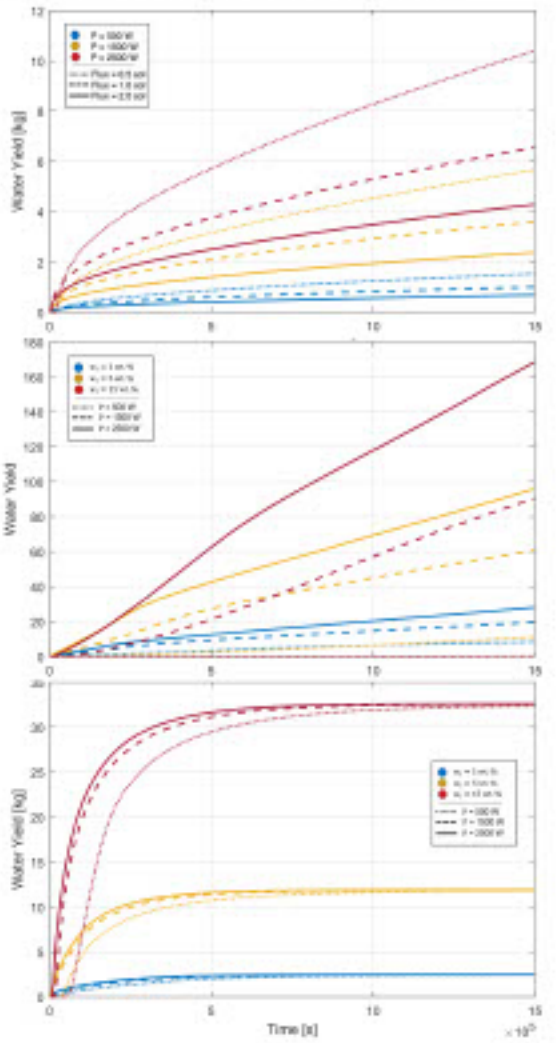

Figure 5: Water yield for in-situ surface heating, in-situ heated drills, and the baseline crucible after excavation [3].

LUWEX - Validation of Lunar Water Extraction and Purification Technologies for In-Situ Propellant and Consumables Production

The *LUWEX* project will use the experience from all the simulations presented in this poster for large scale water extraction experiment in a TVAC. The test will integrate both the water extraction and the water vapour capturing, as well as the water purification. In figure 6, a schematic of the complete test setup is presented, up until the storage after extraction. The hardware inside the dashed line will be surrounded by a could shroud with a temperature of 80 Kelvin, imitating the lunar environment. These tests are scheduled to take place in the summer of 2024.

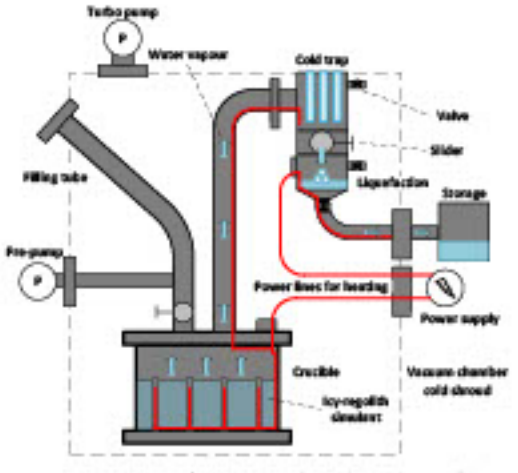

Figure 6: LUWEX Test setup for water extraction and capturing. Crucible dimensions: ϕ = 30 cm, H = 27 cm

Table 2 shows the design parameters for experiment design. For *LUWEX* the number of heated elements, its radii, power distribution and water content are determined to be most contributing and selected as design optimizers. In figure 7 the COMSOL implementation is shown.

Table 2: Design parameters for *LUWEX* thermal water extraction.

Variable		Unit
N	Number of rods	-
R_r	Radius of rod(s)	m
Q	Power	W
C_i	Initial water content	%
a	Coefficient, where $a + b = 1$	-
b	Coefficient, where $a + b = 1$	-

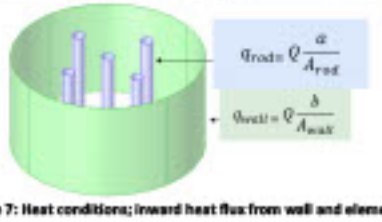

Figure 7: Heat conditions; inward heat flux from wall and elements.

The results in figure 8 show the time of complete extraction decreases when implementing a higher number of heated elements. Integrating design optimization, decreases extraction time with 30% approximately. However, a balance must be struck between what is practical and what is optimal. Increasing Q to 1500 W reduces the extraction time by a factor of about 3, as expected.

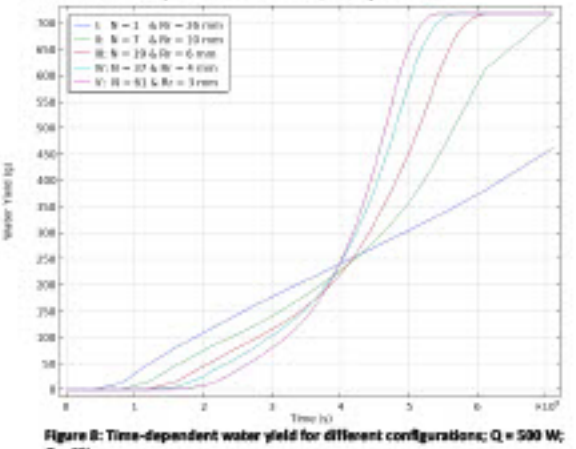

Figure 8: Time-dependent water yield for different configurations; Q = 500 W; C_i = 5%.

References

[1] L. Kiewiet, N.M. Hab, F.M. Marchese, R. Freer and P. Zabel, Trade-off and optimization for thermal Lunar water extraction system. (2022), International Astronautical Federation (IAF).
[2] Becker 3D GmbH, (2023) Heat Transfer. ThreeParticle R6.0.7.
[3] N.M. Hab, Modeling, Simulation and Comparison of Lunar Thermal Water Extraction Methods for Space Resource Utilization LPE-MA 2022/01. (2022), Master's Thesis, German Aerospace Center, DLR.

Visit https://luwex.space/ or scan the QR code!

This work is part of the DLR internally funded young investigator group "Synergetic Material Utilization" (SMU) established 2021 at the Institute of Space Systems in Bremen, Germany. The group focuses on research and development of ISRU technologies for Moon and Mars exploration.

The project LUWEX is funded through the Horizon Europe framework programme of the European Union with the grant number 101081937.

Funded by the European Union

Defining the architecture of the lunar ISRU Pilot Plant using MBSE

Nadia Pougnet [1, 2, 3], Aidan Cowley [3], Alexis Paillet [1]

1 : Centre National d'Études Spatiales (CNES) | 2 : Department of Aerospace Science and Technology, Politecnico di Milano (DAER) | 3 : European Astronaut Centre, European Space Agency (EAC, ESA)

Presenter

Nadia Pougnet

MSc student in space engineering, intern working on space resource utilization at Spaceship FR (CNES) and Spaceship EAC (ESA)

: nadiapougnet@outlook.com
: linkedin.com/in/nadia-pougnet

Introduction

As noted in ISECG's GER [1], In-Situ Resource Utilization (IRSU) will be a key asset for human space exploration. The Spaceship initiative, which is part of ESA's Exploration Preparation, Research and Technology Team (ExPeRT), is dedicated to developing technologies for space exploration, and thus decided to study ISRU. Given the complexity of the system required for ISRU, it is essential to gain experience with demonstration missions. The ISRU Pilot Plant mission aims at testing oxygen extraction from regolith at a relevant scale for crew support.

The goal of this study is to propose an architecture for the ISRU Pilot Plant mission using Model Based System Engineering (MBSE), to identify critical dependencies and requirements to develop a more robust and efficient system architecture.

Methodology

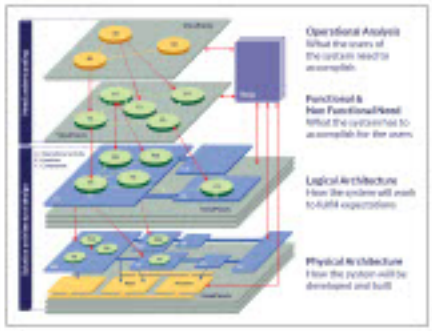

Fig. 1 - The Arcadia method [2]

This study is performed using the Capella tool with the Arcadia method presented in Fig. 1. This methodology can be summarized in 4 steps:

- Define the mission environment
- Define the system's interaction with this environment
- Define the internal structure of the system in terms of functionalities
- Define the internal structure of the system in terms of components

This methodology ensures that the final architecture can be traced back to the mission context and goals, providing a robust approach to system design.

Results

Operational analysis

Inputs:
- Mission stakeholders
- Mission objectives
- Literature review of the environment

Outputs:
- Entities taking part in the mission
- Contribution of these entities to the mission success
- Interaction between these entities
- Mission and environment requirements

System analysis

Inputs:
- Operational analysis
- Technology review
- System specialist

Outputs:
- Capabilities of the system
- External function of the system
- Limit between the system and its environment
- Define the interaction between system and its surrounding actors
- Interface and operational requirements

Logical architecture

Inputs:
- System analysis
- Technology review
- System specialist
- Sub-system specialist

Outputs:
- Internal function of the system
- Sub-system definition
- Function allocation to sub-system
- Functional and operational requirements

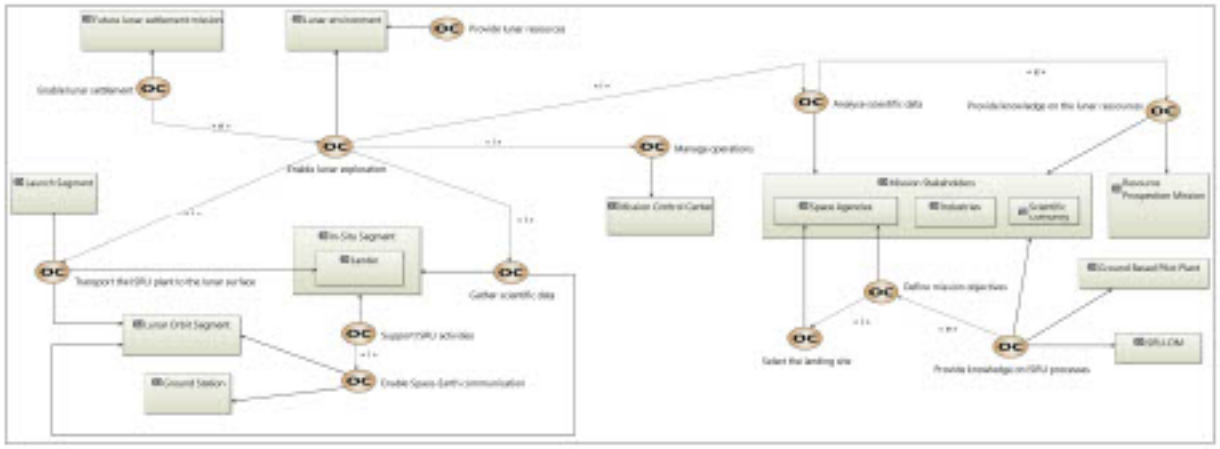

Fig. 2 - Operational Capabilities Breakdown diagram

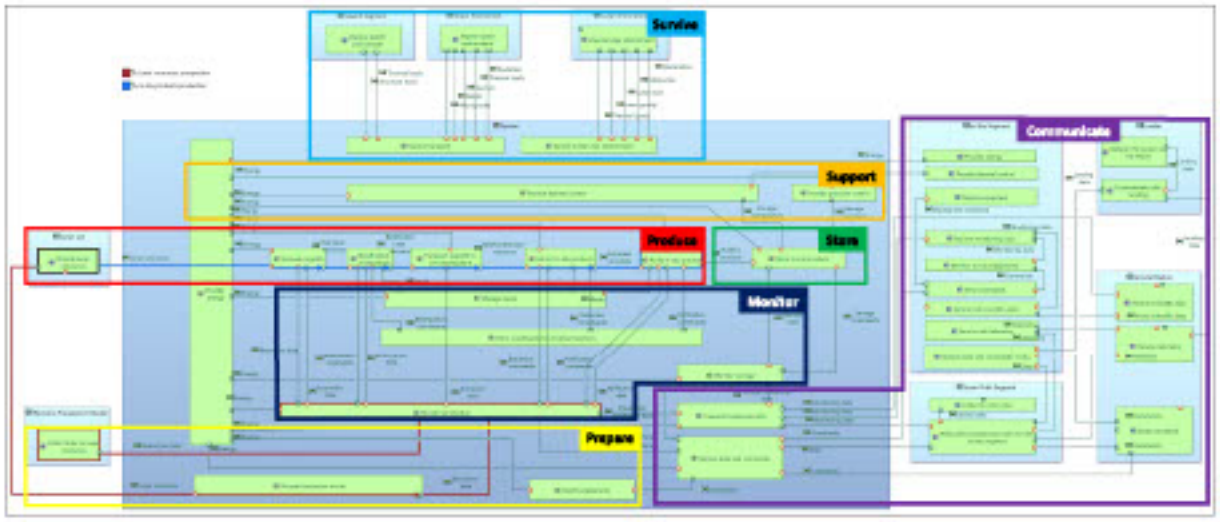

Fig. 3 - System Architecture Blank diagram

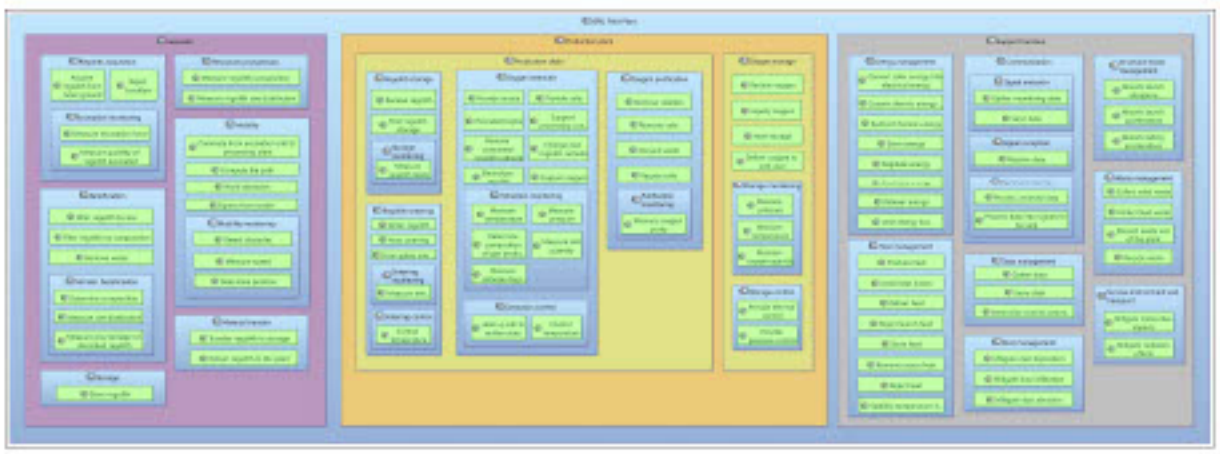

Fig. 4 - Logical Architecture Blank diagram

Conclusion

The main out-takes of the project are:
- Definition of the mission goals and context
- Allocation of the responsibilities among mission stakeholders
- Definition of the interaction between the ISRU Pilot Plant and its environment
- Identification of the minimum required function and subsystem of the ISRU Pilot Plant
- Internal interactions among subsystems
- Identification of several possible architectures, all meeting the initial mission guidelines

Next steps

The next steps of this work are:
- Quantitative trade-off analysis of the different architectures to select the best solution for the mission
- Use the MBSE model as a support of communication for specialists from different fields taking part in the trade-off analysis and system development
- Use the MBSE model as a support for the integration and verification of the final system

Acknowledgment

A special thank you to Alexis Paillet and Aidan Cowley for their support and guidance through this project. A sincere thank you to all the members of the Spaceship FR who contributed to this work and to the experts consulted at CNES and IRAP for their insightful advice and expertise.

Ref. : [1] ISECG Global Exploration Roadmap (2018), [2] Capella website

LUXEMBOURG INSTITUTE OF SCIENCE AND TECHNOLOGY | LIST

On-board eXplainable AI models for in situ Lunar and Martian images

Olivier Parisot, Alexandru-Adrian Tantar

Context and challenges

- Rovers: important role in the exploration of other planetary bodies in Solar System -- especially in areas that would be difficult or impossible (yet) to reach by human exploration.
- Considering calpabilities (landscapes images) and constraints (power / communication / mobility) …
- … can we imagine an on-board approach for pathfinding based on images of the nearby rover environment and on pre-registered maps ?

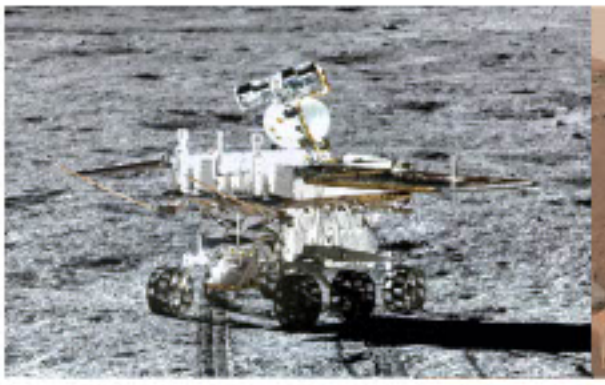

By CSNA/Siyu Zhang/Kevin M. Gill - ChangE-4, Yutu-2, CC BY 2.0, https://commons.wikimedia.org/w/index.php?curid=106500269

By NASA/JPL-Caltech - Perseverance, Public Domain, https://commons.wikimedia.org/w/index.php?curid=102555084

State of the art

- From images captured by **on-board cameras**, AI models can generate **'bird eye views'** from landscape images.
- This technique can be used to observe roads & buildings overall allowing to construct approximate **maps of the landscape** in front.
- Pre-requisite: a dataset with correspondence between landscapes and those views [1].

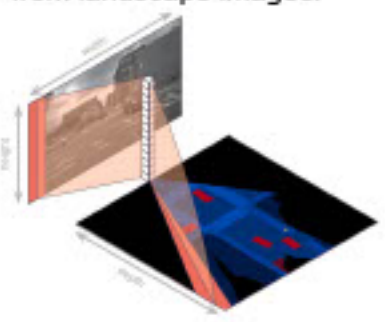

Figure from [1]

LIST Background

- MILAN project ('MachIne Learning for AstroNomy ', funded by FNR): design of **AI models** that process **high-resolution** images on devices with **limited computational resources** [2].
- As such, we will leverage the knowledge gained in developing and deploying such AI models as to enable **on-board** novel functionality in **robotic devices** and extend their **autonomy**.

Telescope: https://www.fnr.lu/research-with-impact-fnr-highlight/fnr-science-image-competition-telescope/

Planned experiments

- The approach can be applied to Moon and Mars landscapes images -- for mapping elements such as hills, craters, block of rocks.

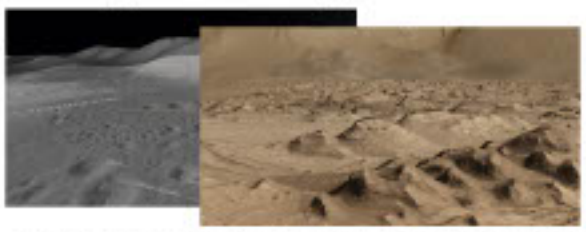

Data **ingestion & processing** from sources (example: *OpenSpace project* [3])

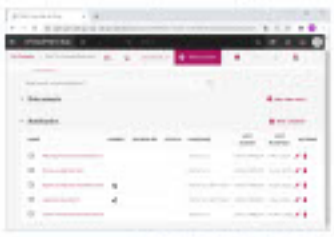

AI models **design & training** on LIST Data Analytics platform

AI models **pruning & deployment** on devices like Raspberry Pi

Perspectives

- A **consistent AI pipeline** from data to models – leading to a technique for geolocalizing planetary landscape pictures.
- Interpretable images processing with **eXplainable AI**, as Trustworthy is essential for reliable space exploration [4].

References

[1] Saha, A., Mendez, O., Russell, C., & Bowden, R. (2022). Translating images into maps. IEEE ICRA 2022 (pp. 9200-9206)

[2] Parisot, O.; Bruneau, P.; Hitzelberger, P.; Krebs, G.; Destruel, C. (2022) Improving Accessibility for Deep Sky Observation. In ERCIM News 130

[3] Bock, A., Hansen, C., & Ynnerman, A. (2018). Openspace: bringing nasa missions to the public. *IEEE computer graphics and applications*, *38*(5), 112-118.

[4] Sanneman, L., & Shah, J. A. (2022). The Situation Awareness Framework for Explainable AI (SAFE-AI) and Human Factors Considerations for XAI Systems. International Journal of HCI, 38(18-20), 1772-1788.

Luxembourg Institute of Science and Technology
5, avenue des Hauts-Fourneaux
L-4362 Esch/Alzette
phone: (+352) 275 888 - 1
fax: (+352) 275 885
olivier.parisot@list.lu
LIST.lu

The Moon Factory

Humankind is striving for further exploration of space and a long-term presence on other celestial bodies like moon or mars. Due to limited payloads of rockets and high transport costs, it is essential to use local available resources. The extraction and use of resources is a complex and interdisciplinary task. After the prospection and exploration of added-value materials, regolith mining is the first process in order to make the mineral raw material available. Four subprocesses are identified. These are part the **Moon Factory Concept**.

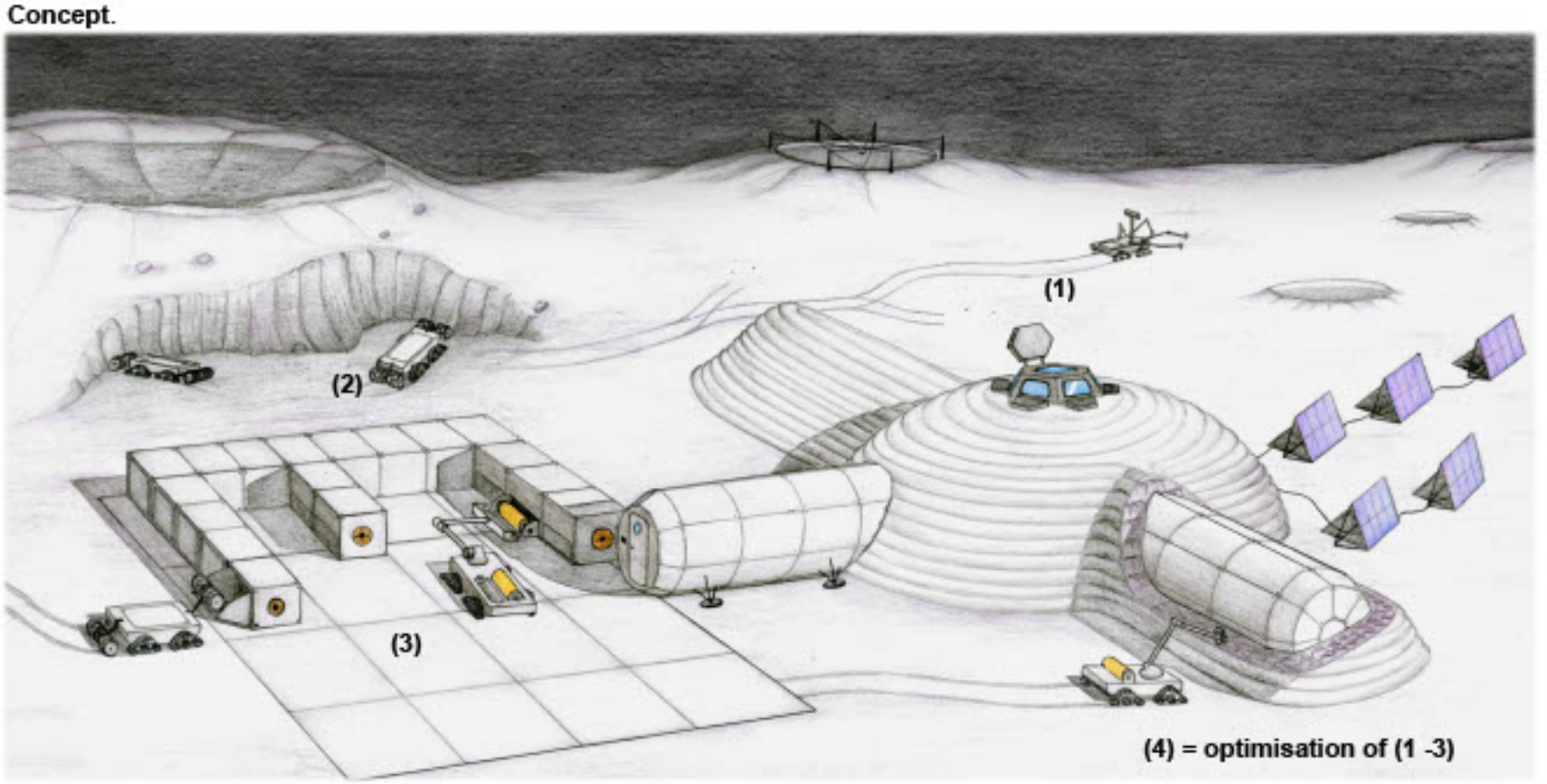

The Moon Factory Concept represents a holistic approach for enabling the use of regolith components for different purposes. The concept encompasses process steps such as extraction operations as well as economic viable logistic solutions on site to enable the manufacturing of consumables based on local raw materials.

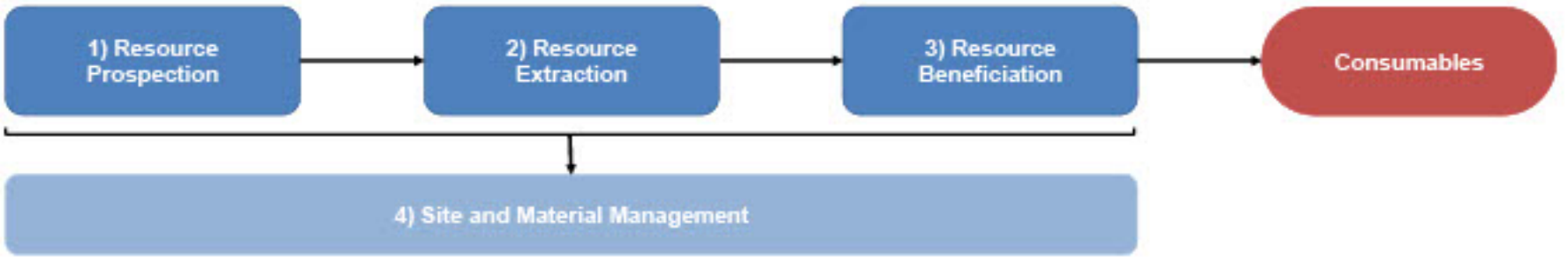

The environmental conditions on the moon, such as reduced gravity or extreme temperatures, pose specific challenges to the extraction and utilisation of the valuable moon minerals being aggregated in the regolith. Consequently, **regolith mining** is a challenging task. For efficiently mining the regolith, it is not sufficient to focus on mechanical solutions to cope with the challenging environmental conditions. Instead, it is also necessary to consider which quantities, of which quality, have to be made available at which time and at which location. Therefore, the Moon Factory Concept not only takes into account mechanical solutions for regolith mining, but also planning and controlling the mining operation.

A key factor for the success of the concept is that it is scalable. This is achieved by using building blocks, each with its own function. Thus, the Moon Factory can not only be scaled in size and tasks, but it gains a unique redundancy that not only increases the safety of the facility but also contributes to higher productivity.

Based on our experience from the iBOSS project, in which a modular and scalable satellite was designed, this is a useful approach to operate machines and apparatus autonomously, reliably, and precisely in the hostile environment of space.

Alexandra Radl, M.Sc.*
Univ.-Prof. Dr.-Ing. Elisabeth Clausen
*aradl@amt.rwth-aachen.de

Stephan Kalapis, M.Sc. M.Sc.*,
Univ.-Prof. Dr.-Ing. Kai-Uwe Schröder
*stephan.kalapis@sla.rwth-aachen.de

Dr.rer.nat. Alexander Niecke*,
Univ.-Prof. Dr.-Ing. Thomas Gries
*alexander.niecke@ita.rwth-aachen.de

Additive Manufacturing using Molten Lunar Regolith - System Progress and First Tests

S. Stapperfend, S. Linke, E. Stoll
Technische Universität Berlin, Chair of Space Technology

Background

Additive manufacturing with molten lunar regolith in vacuum is investigated at TU Berlin

Question

Is it feasible to create structures by pouring molten regolith?

System Progress

- 3-axis Traversing Unit installed and tested
- Vacuum pumps tested
- Vacuum chamber set up for final experiments
- Printhead ordered and arrives soon
  → Vacuum tests can start soon

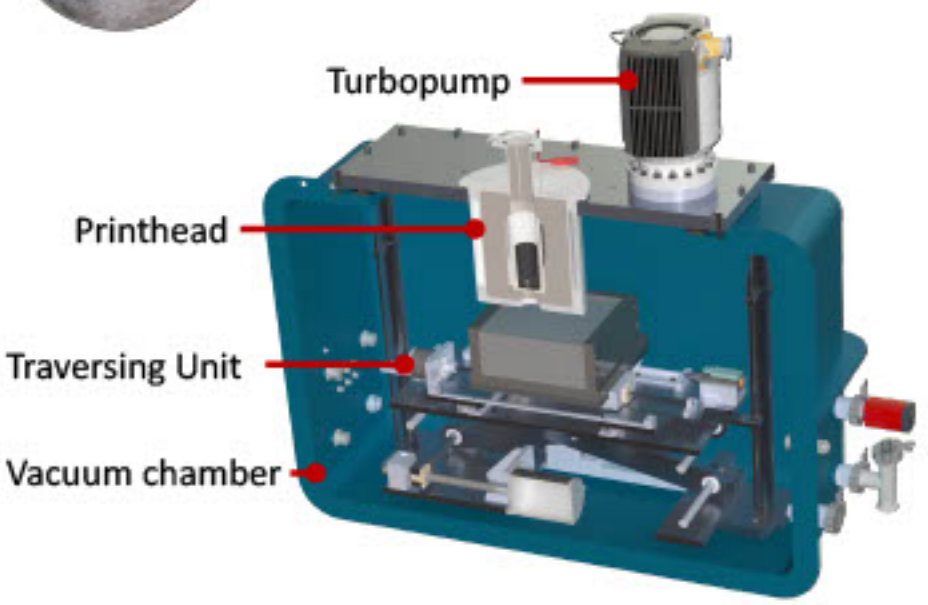

First Tests

- First tests were done to estimate process parameters
- Seven pouring experiments have been performed in air
- Material: TUBS-M (lunar regolith mare simulant)
- Temperatures: 1,300 °C – 1,500 °C
- Substrate: Steel plate and raw regolith (TUBS-M)

Example: TUBS-M at 1400 °C (Test #6)

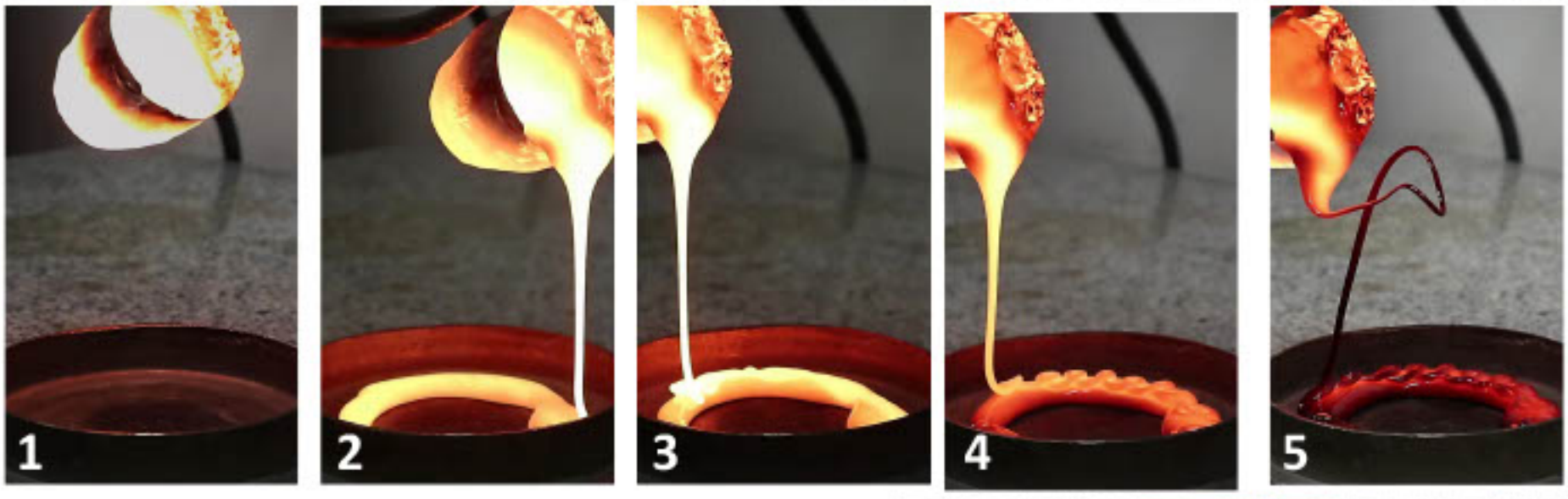

1. TUBS-M is molten in a Pt-crucible at 1,400 °C.
2. First layer: Low viscosity melt is poured by hand and fuses together.
3. Second layer: As the temperature decreases, the viscosity increases. The new applied melt 'sinks' into first layer.
4. Third layer: As the temperature decreases even more, the previous applied layers got more solid, allowing the new material to stay on top. Coiling can be observed.
5. Melt solidifies quickly, resulting in a glassy black material.

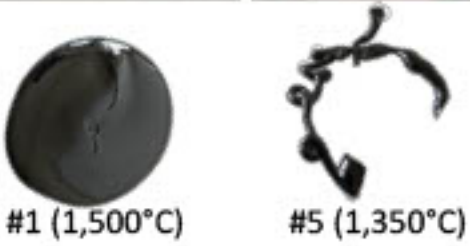

#1 (1,500°C) #5 (1,350°C) #7 (1,300°C)

Supported by:
Federal Ministry for Economic Affairs and Climate Action
on the basis of a decision by the German Bundestag

Acknowledgements

This is funded by the DLR Space Administration with funds provided by the Federal Ministry for Economic Affairs and Climate Action (BMWK) under grant numbers 50WM2057. The authors would like to express their gratitude to Prof. Dingwell and Dr. Hess from Ludwig-Maximilians-University in Munich for their support and for providing the necessary resources to carry out these tests.

Value chain for Pyrite based solar panel production and application

T. Raadik[1*], K. Kristmann[1], J. Ciazela[2], M. Jozefowicz[3], M. Kowalinski[4], A. Sniadkowski[5], J. Bakala[4], M. Steslicki[4], N. Zalewska[4], B. Pieterek[2,6], M. Ciazela[2], D. Marciniak[2], G. Paslawski[2], Z. Szaforz[4], M. Wilgucki[7], A. Woods[8], A. Makaya[9]

[1]Tallinn University of Technology
[2]Institute of Geological Sciences
[3]European Space Foundation
[4]Space Research Centre
[5]SKA Polska
[6]Institute of Geology, Adam Mickiewicz University
[7]Four Point
[8]Astrostrom GmbH
[9]ESA – ESTEC

*Corresponding author
Dr. Taavi Raadik, taavi.raadik@taltech.ee

Introduction

Energy is essential to establishing a sustainable presence on the Moon. The most efficient and reliable technologies for energy production should therefore come from in-situ resources. One such resource is pyrite (FeS_2) which can be used in unique monograin layer solar cells to provide electrical power for lunar operations. This poster demonstrates the value chain for pyrite, from detection to application like lunar settlements, lunar rover coverage, SBSP stations.

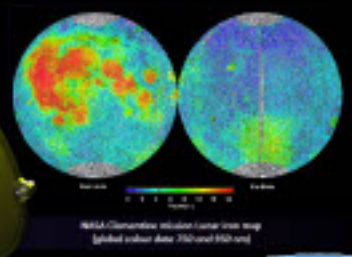

Detection

Mining

Extraction

Solar cell fabrication

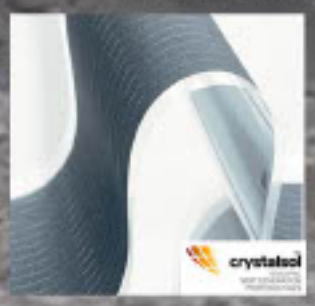

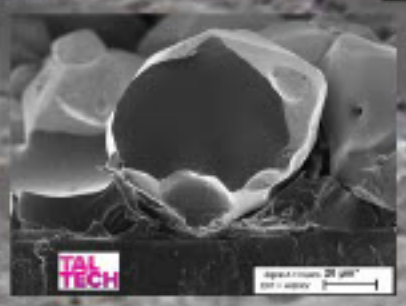

Application

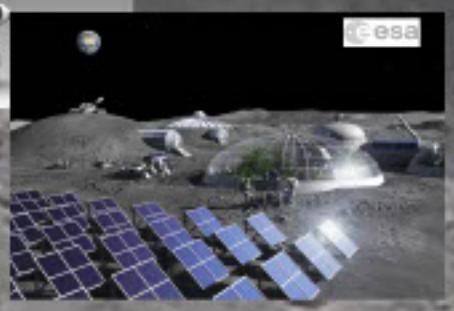

TAL TECH

CBK

esa

ASTROSTROM

SKA Polska

ING PAN

AUTONOMOUS TRANSPORT PLATFORM

Acknowledgment
The work has been supported by Estonian research Council grant PRG 1815, European Space Agency Discovery programme under Contract no. 4000134676, European Regional Development Fund Project TK141.

Logistical Infrastructure for an ISRU-based Sunshade Concept to Support Climate Action

T. MAHESWARAN[1], J. GANZMANN[1], D. ACKER[1], S. FASOULAS[1]
[1]Institute of Space Systems, University of Stuttgart, maheswarant@irs.uni-stuttgart.de

Supported by
AIRBUS DEFENCE & SPACE
ariane GROUP
esa

Low Earth Orbit (LEO)

Earth - Moon Lagrange Point 2 (EML2)

Sun-Earth Lagrange Point 1 (SEL1)

Launch Vehicle
SpaceX Starship
Lunar Electromagnetic Launcher (LEM)
Total Mass: 21 Mt
Total Launches: 280
Chemical Tug (one way): 4.68 t

Launch Vehicle
SpaceX Starship
Lunar Electromagnetic Launcher (LEM)
Total Mass: 13.8 Mt
Total Launches: 1.62 Mio.
Chemical Tug (one way): 11.2 t

Launch Vehicle
SpaceX Starship
Lunar Electromagnetic Launcher (LEM)
Total Mass: 13.8 Mt
Total Launches: 1.62 Mio.
Chemical Tug (one way): 11.2 t

Launch Vehicle
SpaceX Starship
Sunshades per Launch: 47
Launches: 6.6 Mio.

Launch Vehicle
SpaceX Starship
Option 1: Chemical Tug
Total Tug Mass: 4.1 Mt
Total Launches: 4.3 Mio.
Option 2: Electrical Tug
Total Tug Mass: 90.3 Mt
Total Launches: 904 k

Launch Vehicle
SpaceX Starship
Launch Payload: 100 t
Launches: 1.47 Mio.

Launch Vehicle
SpaceX Starship
Option 1: Chemical Tug
Total Tug Mass: 400 Mt
Total Launches: 4.00 Mio.
Option 2: Electrical Tug
Total Tug Mass: 33.2 Mt
Total Launches: 332 k

Launch Vehicle
SpaceX Starship
Launch Payload: 100 t
Launches: 1.17 Mio.

Launch Vehicle
SpaceX Starship
Option 1: Chemical Tug
Total Tug Mass: 340 Mt
Total Launches: 3.4 Mio.
Option 2: Electrical Tug
Total Tug Mass: 27 Mt
Total Launches: 270 k

Launch Vehicle
SpaceX Starship
Launch Payload: 100 t
Launches: 468 k

Launch Vehicle
SpaceX Starship
Option 1: Chemical Tug
Total Tug Mass: 197 Mt
Total Launches: 1.97 Mio.
Option 2: Electrical Tug
Total Tug Mass: 16.2 Mt
Total Launches: 162 k

Launch Vehicle
SpaceX Starship
Launch Payload: 100 t
Launches: 468 k

Launch Vehicle
SpaceX Starship
Option 1: Chemical Tug
Total Tug Mass: 197 Mt
Total Launches: 1.97 Mio.
Option 2: Electrical Tug
Total Tug Mass: 16.2 Mt
Total Launches: 162 k

Transfer Vehicle
IPSS Space Tug
Payload per Tug: 420 kg
Option 1: Chemical Tug (one way)
Total Tug Mass: 47.5 Mt
Total Tugs: 339 Mio.
Option 2: Electrical Tug*
Total Tug Mass: 90.3 Mt
Total Tugs: 10.8 Mio.
*Orbital refueling included

Launch + Transfer Vehicle
SpaceX Starship
Sunshades per Launch: 47
Launches*: 17.5 Mio.
Mass Occupancy: 40 %
*Orbital refueling included

Transfer Vehicle
IPSS Space Tug
Payload per Tug: 300 kg
Option 1: Chemical Tug (one way)
Total Tug Mass: 4.00 Mt
Total Tugs: 294 Mio.
Option 2: Electrical Tug*
Total Tug Mass: 34.2 Mt
Total Tugs: 11.3 Mio.
*Orbital refueling included

Transfer Vehicle
IPSS EML 1
Payload per Launch: 100 kg
Total Payload Mass: 46.8 Mt
Total Launches: 496 Mio.

Refueling Vehicle
IPSS Fuel Tug
Payload per Tug: 100 kg
Option 1: Chemical Tug
Total Tug Mass: 190 kt
Total Tugs: 19 M
Option 2: Electrical Tug*
Total Tug Mass: 43.0 t
Total Tugs: 430
*Orbital refueling included

Transfer Vehicle
IPSS EML 2
Payload per Launch: 100 kg
Total Tug Mass: 118 Mt
Total Launches: 1.18 Mio.

Refueling Vehicle
IPSS Fuel Tug
Payload per Tug: 100 kg
Option 1: Chemical Tug
Total Tug Mass: 44 kt
Total Tugs: 444 k
Option 2: Electrical Tug*
Total Tug Mass: 9.09 kt
Total Tugs: 2170
*Orbital refueling included

Transfer Vehicle
IPSS EML 2
Payload per Launch: 100 kg
Total Tug Mass: 118 Mt
Total Launches: 1.18 Mio.

Refueling Vehicle
IPSS Fuel Tug
Payload per Tug: 100 kg
Option 1: Chemical Tug
Total Tug Mass: 44 kt
Total Tugs: 444 k
Option 2: Electrical Tug*
Total Tug Mass: 9.09 kt
Total Tugs: 2170
*Orbital refueling included

Transfer Vehicle
IPSS Space Tug
(EML2 - SEL1)
Payload per Tug: 100 kg
Option 1: Chemical Tug*
Total Tug Mass: 18.62 kt
Total Tugs: 90 k
Option 2: Electrical Tug*
Total Tug Mass: 4.09 kt
Total Tugs: 13.7 k
*Orbital refueling included

Transfer Vehicle
IPSS Space Tug
(LEO - SEL1)
Payload per Tug: 100 kg
Option 1: Chemical Tug (one way)
Total Tug Mass: 360 Mt
Total Tugs: 3.6 Mio.
Option 2: Electrical Tug*
Total Tug Mass: 27 Mt
Total Tugs: 10.8 Mio.
*Orbital refueling included

Transfer Vehicle
IPSS Space Tug
(EML2 - SEL1)
Payload per Tug: 100 kg
Option 1: Chemical Tug*
Total Tug Mass: 394.8 kt
Total Tugs: 2.0 k
Option 2: Electrical Tug*
Total Tug Mass: 33 kt
Total Tugs: 7.6 k
*Orbital refueling included

Transfer Vehicle
IPSS Space Tug
(LEO - SEL1)
Payload per Tug: 100 kg
Option 1: Chemical Tug (one way)
Total Tug Mass: 196 Mt
Total Tugs: 1.96 Mio.
Option 2: Electrical Tug*
Total Tug Mass: 14.7 Mt
Total Tugs: 5.9 Mio.
*Orbital refueling included

Transfer Vehicle
IPSS Space Tug
(EML2 - SEL1)
Payload per Tug: 100 kg
Option 1: Chemical Tug*
Total Tug Mass: 394.8 kt
Total Tugs: 2.0 k
Option 2: Electrical Tug*
Total Tug Mass: 33 kt
Total Tugs: 7.6 k
*Orbital refueling included

Transfer Vehicle
IPSS Space Tug
(LEO - SEL1)
Payload per Tug: 100 kg
Option 1: Chemical Tug (one way)
Total Tug Mass: 196 Mt
Total Tugs: 1.96 Mio.
Option 2: Electrical Tug*
Total Tug Mass: 14.7 Mt
Total Tugs: 5.9 Mio.
*Orbital refueling included

Launch Vehicle
IPSS EML 1
Total Mass: 570 kt
Total Railguns: 10
Lunar Mass Fraction: 99 %
Power: 200 MW
Energy per Launch: 95 MWh
Solar Park Area: 2.66 km²

Launch Vehicle
IPSS EML 2
Total Mass: 2.81 Mt
Total Railguns: 63
Lunar Mass Fraction: 99 %
Power: 2.73 GW
Energy per Launch: 95 MWh
Solar Park Area: 13.28 km²

Terrestrial Concept

Total Mass:	147 Mt
Amount of Sunshades:	118 Mio.
Sunshade Area:	0.01 km²
Sunshade Mass:	1.25 t
Resources:	
Terrestrial	100 %
Lunar	0 %
Total Launches:	
Chemical Tug:	17.5 Mio.

Terrestrial Concept 2

Total Mass:	147 Mt
Amount of Sunshades:	118 Mio.
Sunshade Area:	0.01 km²
Sunshade Mass:	1.25 t
Resources:	
Terrestrial	100 %
Lunar	0 %
Total Launches:	
Chemical Tug:	5.95 Mio.
Electrical Tug:	1.80 Mio.

Lunar - ISMA Concept 1

Total Mass:	212.5 Mt
Amount of Sunshades:	25 Mio.
Sunshade Area:	0.04 km²
Sunshade Mass:	8.5 t
Resources:	
Terrestrial	55 %
Lunar	45 %
Total Launches:	
Chemical Tug:	4.77 Mio.
Electrical Tug:	1.44 Mio.

Lunar - ISMA Concept 2

Total Mass:	580 Mt
Amount of Sunshades:	952k
Sunshade Area:	1.05 km²
Sunshade Mass:	580 t
Resources:	
Terrestrial	11 %
Lunar	89 %
Total Launches:	
Chemical Tug:	2.62 Mio.
Electrical Tug:	787 k

Lunar - ISMA Concept 3

Total Mass:	580 Mt
Amount of Sunshades:	952k
Sunshade Area:	1.05 km²
Sunshade Mass:	580 t
Resources:	
Terrestrial	11 %
Lunar	89 %
Total Launches:	
Chemical Tug:	2.62 Mio.
Electrical Tug:	787 k

Efficiency Level
Chemical vs. Electrical Tug

1	2.4	1.1	3.7	1.4	4.6	2.5	8.4	2.5	8.4

Advances in metal extraction from highland regolith using molten salt electrolysis

T. Schild[1], B. Lomax[2], K. Hadler[1], M. Conti[2], D. Harries[1], G. Aridon[3], A. Lecossais[3]

1: European Space Resources Innovation Centre, 2: European Space Agency, 3: Airbus Defence & Space

LUXEMBOURG SPACE RESOURCES WEEK

INTRODUCTION

Context:

Molten salt electrolysis (MSE) is studied for the ***In Situ*** **production of oxygen on the Moon** [1]. It uses the principle of electro-deoxidation to reduce the oxygen-rich minerals present in lunar regolith. Oxygen bearing gas is evolved, **leaving solid remnants rich in useful metallic elements** (e.g. Al, Si, Ca, Fe).

Project objectives:

- Investigate the **refinement of metallic compounds obtained by MSE** of highland regolith simulants.
- **Produce alloy feedstock in sufficient quality and quantity to allow additive manufacturing** of demonstration parts, using Airbus' Metal3D process.

Main research questions:

- What is the expected **range of compositions of the solid products** from highland regolith MSE?
- What metallurgical techniques can be applied to **derive usable alloys from those products**?
- How do the obtained feedstock compositions affect the **Metal3D additive manufacturing process**?

MATERIALS & METHODS

Molten Salt Electrolysis process

Experiments are conducted with MSE reactor as described by Lomax et al. [1], using:

- **Feedstock:** LHS-1 regolith simulant [2], ca. 25g sintered pellet
- **Salt:** 800g $CaCl_2$ + 5g CaO, molten at 950°C
- **Electrolysis parameters:** 3.2V constant voltage for 24 hours
- **Atmosphere:** Inert atmosphere, Argon 5.0
- **Anode material:** Graphite, CO/CO2 evolving
- **Other materials:** Inconel, alumina, stainless steel, molybdenum

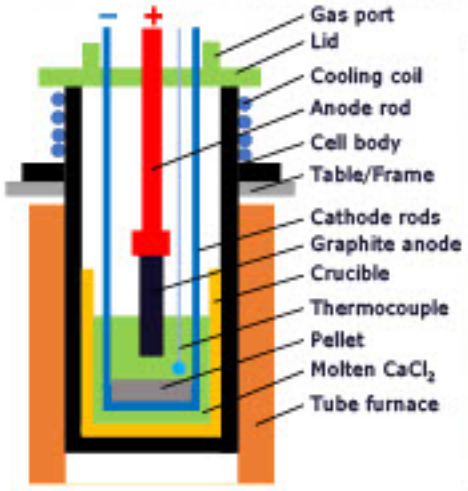

Fig. 1 – Schematic view of MSE cell

Fig. 2 – Electrodes before and after MSE run

Material processing & characterization

The solid material recovered at the cathode is processed as follows:

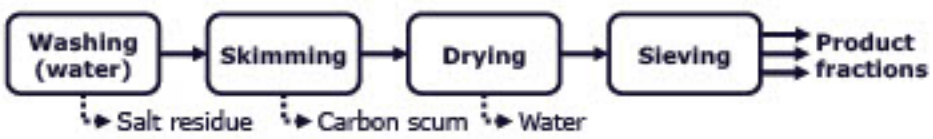

The obtained material samples are ground to a powder and uses to determine:

- **Remaining oxygen content**, using inert gas fusion ONH analysis
- **Average metal content**, using large area SEM-EDX scans
- **Phase composition**, using point-by-point analysis of SEM-EDX maps (Fig. 3)

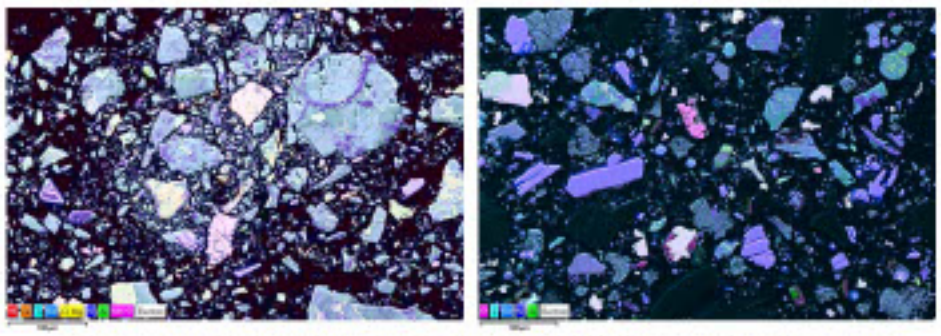

Fig. 3 – SEM-EDX compositional maps of reduced LHS-1 (left: >600µm, right: <75µm)

PRELIMINARY RESULTS

Preliminary results are from 3 comparable LHS-1 reduction runs (A, B & C)

Average oxygen & metal content

- **Total O content of ca. 6 wt.%** in solid product from run C
- O content is higher in smaller particles
- Mass of material is concentrated in largest size fraction

} **Fig. 4**

- **Main components: Al, Si, Ca & Fe** (+Mg, Ti, Cr, Mn, Ni & Mo)
- Product **depleted in Si & Al but enriched in Fe**, compared to LHS-1
- **Ca & Fe content varies significantly** between the 2 runs

} **Fig. 5**

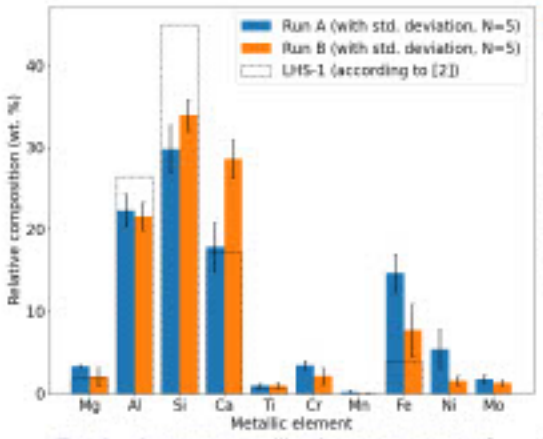

Fig. 4 – Average metallic element content of LHS-1 & corresponding MSE products

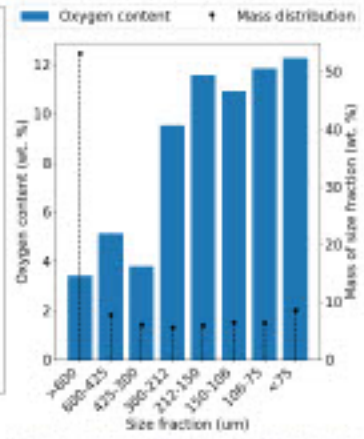

Fig. 5 – Mass & oxygen distribution in sieved product fractions (run C)

Local composition

- Strong **negative correlation between Ca & Fe** content
- Strong **positive correlation between Fe & Mn, Ni** content

} **Fig. 6**

- Presence of **Al-Si-Ca, Al-Si-Fe, Al-rich & Si-rich phases**
- Absence of pure Ca phases

} **Fig. 7**

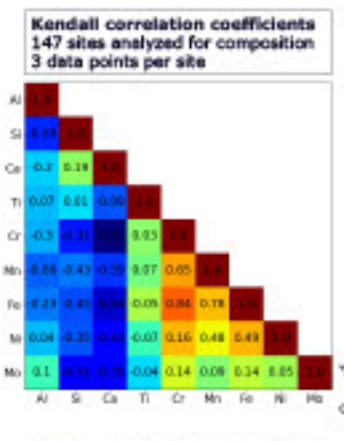

Fig. 6 – Correlation between metal content in analyzed sites

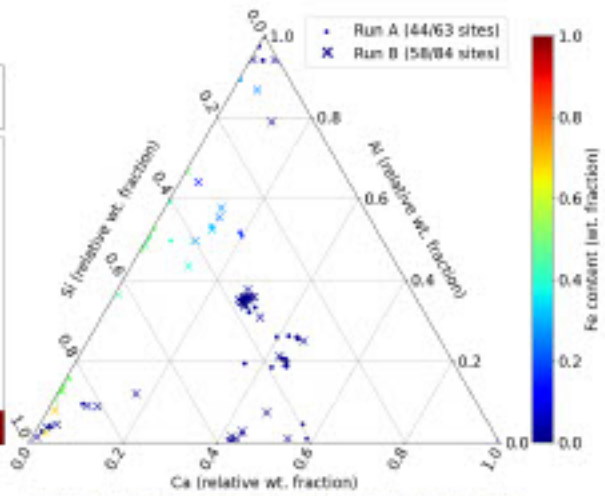

Fig. 7 – Local composition of Al-Si-Ca-Fe rich sites (sites with Al + Si +Ca + Fe >80wt.%)

FINDINGS & NEXT STEPS

The preliminary results show that:

- The main metallic compounds produce are in the **Al-Ca-Si-Fe system.**
- **Material transfers take place** between cathode structure and reduced material

The next steps to be undertaken are:

- **Confirm the present results** with additional material analyses
- Study **spatial distribution of phases** (pure vs. heterogeneous particles)
- **Define beneficiation & refinement strategies** to yield usable alloy feedstocks from MSE products
- Study **impact of regolith feedstock variation** on final material composition

REFERENCES

[1] B. A. Lomax et al., 'Proving the viability of an electrochemical process for the simultaneous extraction of oxygen and production of metal alloys from lunar regolith', Planetary and Space Science, vol. 180, p. 104748, Jan. 2020

[2] Exolith lab, 'LHS-1 Lunar Highlands Simulants - Fact sheet', Dec. 2022.

esric · esa · LUXEMBOURG SPACE AGENCY · LUXEMBOURG INSTITUTE OF SCIENCE AND TECHNOLOGY | LIST · AIRBUS

Advances in metal extraction from highland regolith using molten salt electrolysis

T. Schild[1], B. Lomax[2], K. Hadler[1], M. Conti[2], D. Harries[1], G. Aridon[3], A. Lecossais[3]

1: European Space Resources Innovation Centre, 2: European Space Agency, 3: Airbus Defence & Space

LUXEMBOURG SPACE RESOURCES WEEK

INTRODUCTION

Context:

Molten salt electrolysis (MSE) is studied for the ***In Situ*** **production of oxygen on the Moon** [1]. It uses the principle of electro-deoxidation to reduce the oxygen-rich minerals present in lunar regolith. Oxygen bearing gas is evolved, **leaving solid remnants rich in useful metallic elements** (e.g. Al, Si, Ca, Fe).

Project objectives:

- Investigate the **refinement of metallic compounds obtained by MSE** of highland regolith simulants.
- **Produce alloy feedstock in sufficient quality and quantity to allow additive manufacturing** of demonstration parts, using Airbus' Metal3D process.

Main research questions:

- What is the expected **range of compositions of the solid products** from highland regolith MSE?
- What metallurgical techniques can be applied to **derive usable alloys from those products**?
- How do the obtained feedstock compositions affect the **Metal3D additive manufacturing process**?

MATERIALS & METHODS

Molten Salt Electrolysis process

Experiments are conducted with MSE reactor as described by Lomax et al. [1], using:

- **Feedstock:** LHS-1 regolith simulant [2], ca. 25g sintered pellet
- **Salt:** 800g $CaCl_2$ + 5g CaO, molten at 950°C
- **Electrolysis parameters:** 3.2V constant voltage for 24 hours
- **Atmosphere:** Inert atmosphere, Argon 5.0
- **Anode material:** Graphite, CO/CO2 evolving
- **Other materials:** Inconel, alumina, stainless steel, molybdenum

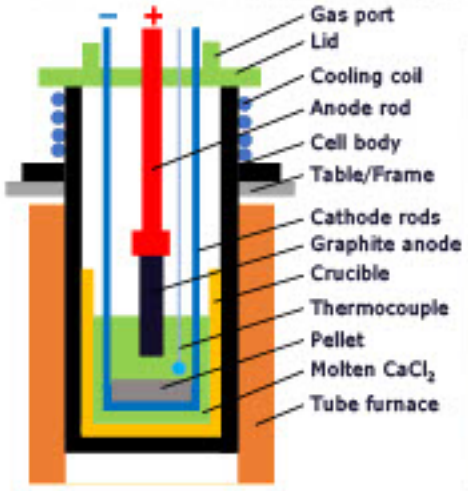

Fig. 1 – Schematic view of MSE cell

Fig. 2 – Electrodes before and after MSE run

Material processing & characterization

The solid material recovered at the cathode is processed as follows:

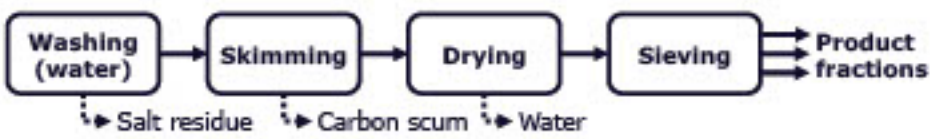

The obtained material samples are ground to a powder and uses to determine:

- **Remaining oxygen content**, using inert gas fusion ONH analysis
- **Average metal content**, using large area SEM-EDX scans
- **Phase composition**, using point-by-point analysis of SEM-EDX maps (Fig. 3)

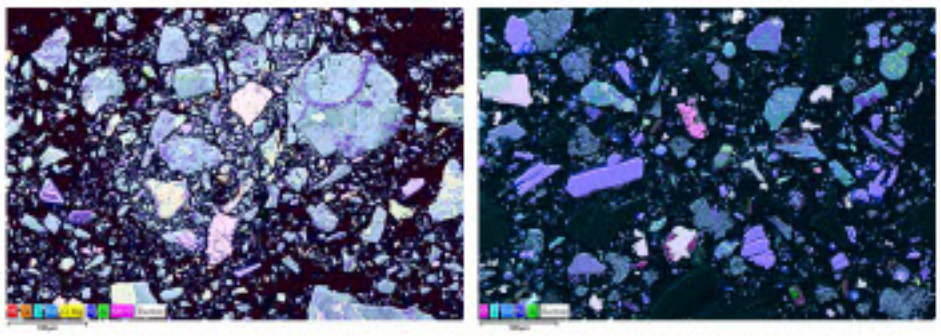

Fig. 3 – SEM-EDX compositional maps of reduced LHS-1 (left: >600µm, right: <75µm)

PRELIMINARY RESULTS

Preliminary results are from 3 comparable LHS-1 reduction runs (A, B & C)

Average oxygen & metal content

- **Total O content of ca. 6 wt.%** in solid product from run C
- O content is higher in smaller particles
- Mass of material is concentrated in largest size fraction

} **Fig. 4**

- **Main components: Al, Si, Ca & Fe** (+Mg, Ti, Cr, Mn, Ni & Mo)
- Product **depleted in Si & Al but enriched in Fe**, compared to LHS-1
- **Ca & Fe content varies significantly** between the 2 runs

} **Fig. 5**

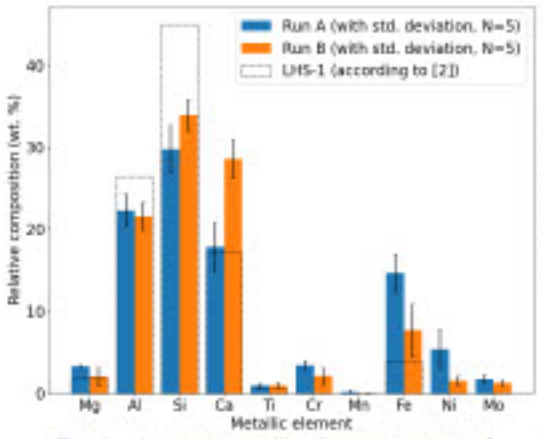

Fig. 4 – Average metallic element content of LHS-1 & corresponding MSE products

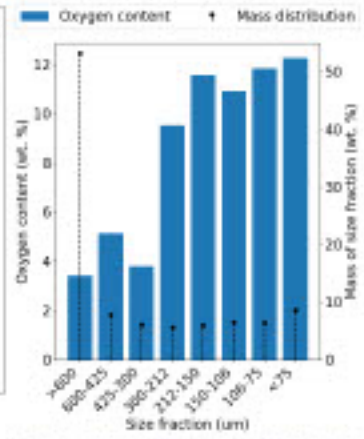

Fig. 5 – Mass & oxygen distribution in sieved product fractions (run C)

Local composition

- Strong **negative correlation between Ca & Fe** content
- Strong **positive correlation between Fe & Mn, Ni** content

} **Fig. 6**

- Presence of **Al-Si-Ca, Al-Si-Fe, Al-rich & Si-rich phases**
- Absence of pure Ca phases

} **Fig. 7**

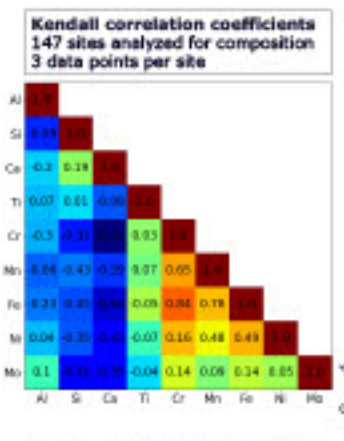

Fig. 6 – Correlation between metal content in analyzed sites

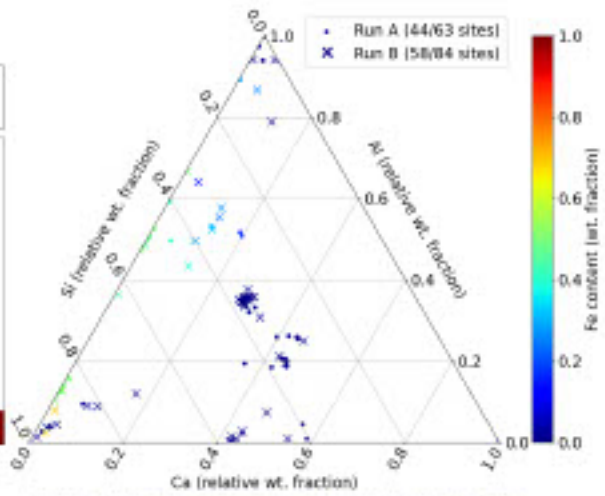

Fig. 7 – Local composition of Al-Si-Ca-Fe rich sites (sites with Al + Si +Ca + Fe >80wt.%)

FINDINGS & NEXT STEPS

The preliminary results show that:

- The main metallic compounds produce are in the **Al-Ca-Si-Fe system.**
- **Material transfers take place** between cathode structure and reduced material

The next steps to be undertaken are:

- **Confirm the present results** with additional material analyses
- Study **spatial distribution of phases** (pure vs. heterogeneous particles)
- **Define beneficiation & refinement strategies** to yield usable alloy feedstocks from MSE products
- Study **impact of regolith feedstock variation** on final material composition

REFERENCES

[1] B. A. Lomax et al., 'Proving the viability of an electrochemical process for the simultaneous extraction of oxygen and production of metal alloys from lunar regolith', Planetary and Space Science, vol. 180, p. 104748, Jan. 2020

[2] Exolith lab, 'LHS-1 Lunar Highlands Simulants - Fact sheet', Dec. 2022.

esric · esa · LUXEMBOURG SPACE AGENCY · LUXEMBOURG INSTITUTE OF SCIENCE AND TECHNOLOGY | LIST · AIRBUS

TOWARDS ADOPTING RGB-THERMAL FUSION TECHNIQUES FOR SPACE APPLICATIONS

Leo Pauly*, Wassim Rharbaoui* , Vincent Gaudillière, Arunkumar Rathinam, Nilotpal Sinha, Abd El Rahman Shabayek, Anis Kacem and Djamila Aouada (*equal contribution)
SnT, University of Luxembourg
leo.pauly@uni.lu

CVI2 Research Group
cvi2.uni.lu

ABSTRACT

- Deep Learning (DL) based computer vision algorithms are gaining attention in space applications
- DL algorithms for space applications rely on RGB (visible) images → Sensitivity to extreme illumination conditions (e.g., sun glare and shadows)

- Use **thermal** imagery to complement visible images
- Improved performance with DL when fusing multiple modalities [1]
- DL model for **RGB & thermal data fusion** for space applications is an ongoing research effort

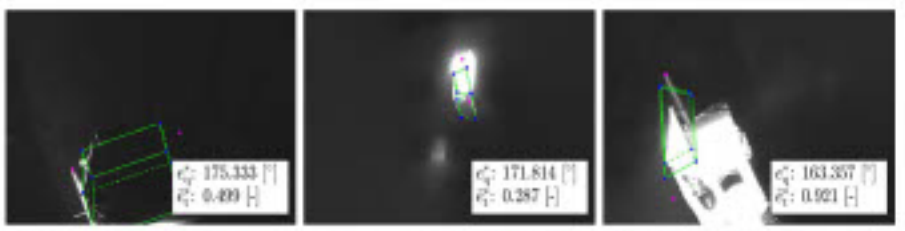

Inaccurate predictions of current vision-based algorithms due to extreme lighting conditions, which is a major limitation in space [2]

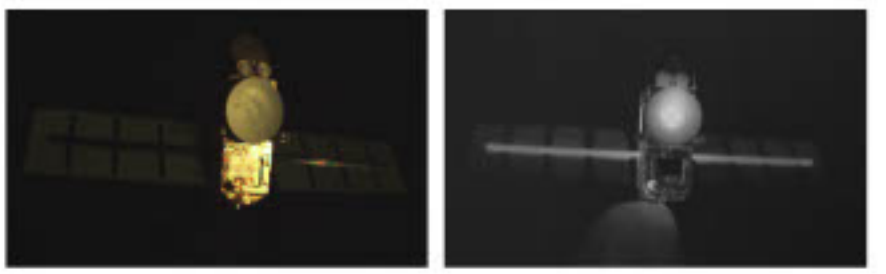

Illustration of RGB and thermal images from the Jason-1 dataset [3]

DATASETS

- **Lack of publicly available large real-world datasets** for training the data-hungry DL algorithms
- **Spatial and temporal miss-alignment** in the current datasets
- **Difficulty in generating synthetic datasets** due to the complexity of modelling heat signatures, material properties, heat equations etc., for different objects in a space environment

CHALLENGES

Given the current research trends, several challenges arise in the **algorithm design** and the **datasets** used.

ALGORITHM DESIGN

- **Computational complexity** of current algorithms requires extensive computational and memory resources, making them unsuitable for space applications
- **Lack of fusion strategies** for effectively combining modality-specific (contextual) and common (structural) features

CONCLUSION

- Fusing RGB and thermal images has the potential to mitigate the performance drop of vision algorithms under extreme illumination conditions in space
- Several challenges exist in algorithm design and dataset collection, providing interesting future directions for research

References
[1] Chen, Yi-Ting, et al. "Multimodal object detection via probabilistic ensembling." *ECCV*. 2022.
[2] Park, Tae Ha, et al. "Satellite Pose Estimation Competition 2021: Results and analyses." *Acta Astronautica*. 2023.
[3] Hogan, Maxwell, et al. "Using Convolutional Neural Networks for Relative Pose Estimation of a Non-Cooperative Spacecraft with Thermal Infrared Imagery." *arXiv preprint arXiv:2105.13789*. 2021.

CURRENT TRENDS IN RGB & THERMAL FUSION

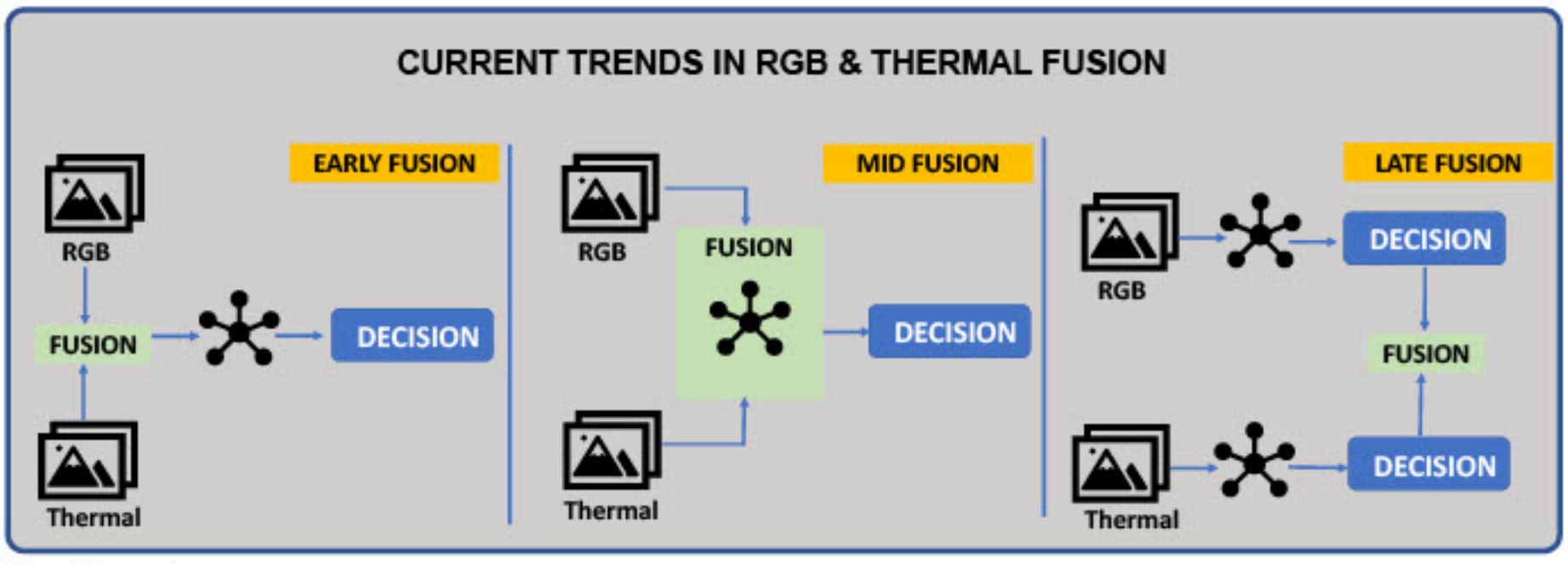

Acknowledgement:
This work was funded by the Luxembourg National Research Fund (FNR), under the project reference BRIDGES2020/IS/14755859/MEETA/Aouada, and by LMO (https://www.lmo.space).

V. Petrov, S. Filippychev, etc.
Mission Space S.a.r.l., corresponding address: v@mission.space

Mission Space's system for space weather now- and forecasting

In recent years, there has been a drastic increase in the use of near-Earth space: the number of satellites in LEO and the dependance on space-based services have grown exponentially. All these ground, air and space-based infrastructure and services are much more vulnerable to the space weather events of different kinds.

We present a solution:

A complex system for monitoring, analysis and notification about space weather events

On-ground data processing:

- Reconstruction of the near-Earth radiation full picture,
- Real-time data analysis,
- User interface & APIs

Our goal is to collect data from space in real time, transform it into predictive analytics, value added insights, alert notifications and sell it to the customers

Using multi-point measurements on LEO our system will extrapolate the dynamics to the whole near-Earth space, taking into account the environmental asymmetry effects.

After full deploy our model will be able to:
- Constantly monitor local space weather conditions,
- Have real-time monitoring features,
- Reconstruct the environment during the event

Constellation of up to 24 LEO-based instruments

Short-term prognosis of incoming events

A set of detectors:

- Three independent units,
- Unified design and flexible adaptation,
- Less than 1.5 kg / 1.5U in total,
- < 0.5 W per unit,
- First launch: Q3/2023

Parameters	PL-1b	PL-1g	PL-2
Dimension, mm	85 x 50 x 46	95 x 95 x 52	147 x 94 x 30
Mass, no more than, kg	0.5	0.6	0.750
Power consumption, W	< 0.5	< 0.5	< 0.5
Data produced, MiB/day *	1..70	1..70	0.5..50
FoV, °	30..65	30..65	Omni
Information interface	Under the agreement with the developer of the spacecraft		

Ground and orbital parts of the system will be deployed gradually and simultaneously to be fully available in the next several years:

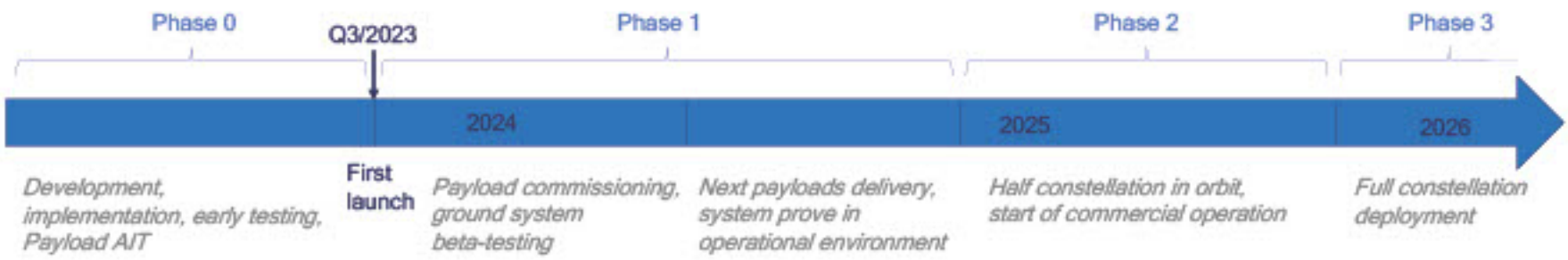

Conclusion:

Mission Space develops a complex system for monitoring, analysis and notification about Space Weather events. The system consists of orbital constellation of *cosmic radiation detectors* and ground facilities for *data collection, processing, analysis and storage* + web-based *user interface.*
First set of instruments is ready for launch in Q3/2023, alongside the opening of the ground system.

European Union
European Regional Development Fund
Investing in your future
TAL TECH
Luxembourg Space Resources Week 2023
esric
powered by LSA, ESA & LIST

We will need to make solar cells in space. There is a solid way to do it.

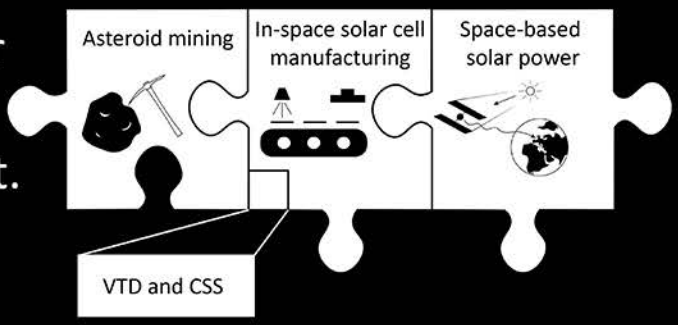

Physical methods of thin-film solar cell absorbers deposition for extraterrestrial applications

Mykhailo Koltsov, Nicolae Spalatu

Laboratory for Thin Film Energy Materials, Department of Materials and Environmental Technology, Tallinn University of Technology

Expected timeline for space-based solar power industry development + space mining

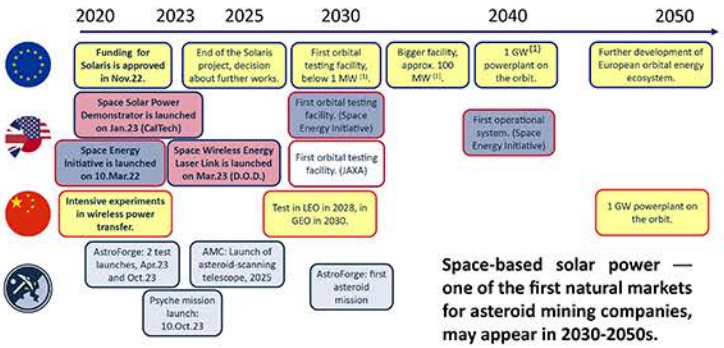

Space-based solar power — one of the first natural markets for asteroid mining companies, may appear in 2030-2050s.

Some concentrations of the main thin-film-PV elements

Element	In carbonaceous asteroids, ppm	In metallic asteroids, ppm	In Earth's crust, ppm
Cd [2,5]	~1 (in CI)	0.01-0.02	0.1-0.5
Te [3]	<3	0.45	0.001-0.01
Sb [4]	0.1-0.2	0.02-0.3	0.2-0.5
Se [3]	6.5-27	100	0.05
Ga [3]	3.3-9.8	89	10-19
As [5]	1.8-2.2	3.7	1.5-2.1
S [6,7]	<60000	10000-185000	260-520

Advantages and disadvantages of VTD/CSS family of methods

Advantages	Disadvantages
Comparative simplicity of the main method	Need for high vacuum (easier in space)
High purity of the deposited material	High energy consumption (easier to satisfy in space, than high material needs)
High and controllable speed of deposition (0.1-15 μm/min)	
May work without any carrier gas, just in vacuum	
Comparatively low demand for additional materials/precursors.	

Vapor transport deposition (VTD): material is vaporized, goes to the substrate, condenses there, forming a thin film.
Close-spaced sublimation (CSS): subclass of VTD with little distance between source and substrate, kept in "semi-ampoule" conditions.

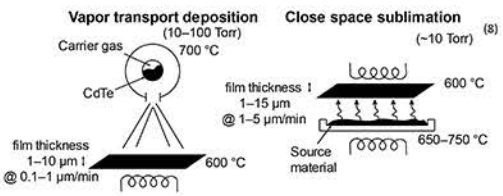

Efficiencies (for CdTe): 22% (top), up to 19% (market).
Related companies: First Solar (USA), CTF Solar (EU).

Thin-film solar cell structure (example CdTe cell): (9)

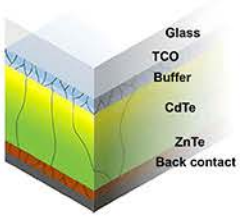

Principal scheme of industrial VTD application (10)

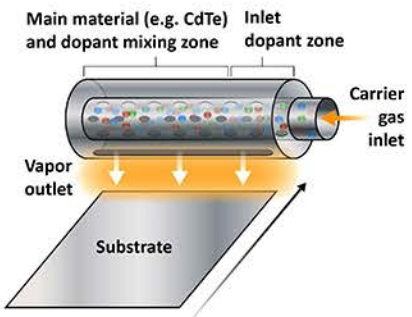

Potential timeline:

1. Technology adaptation and development – the sooner the better;
2. First practical implications – after first asteroid mining missions with suitable (by)products;
3. Specific solar cell technology (CdTe, GaAs, Sb_2S_3, Sb_2Se_3) depends on its stability in space and on the material availability in mined bodies/supply chains.

Adaptation of VTD/CSS technologies for extraterrestrial environment may be an important step towards greener future for Earth and faster growth for space economy.

Acknowledgements:

This study was funded by the Estonian Research Council projects PRG627 "Antimony chalcogenide thin films for next-generation semi-transparent solar cells applicable in electricity producing windows", PSG689 "Bismuth Chalcogenide Thin-Film Disruptive Green Solar Technology for Next Generation Photovoltaics", and the European Union's Horizon2020 programme under the ERA Chair project 5GSOLAR grant agreement No 952509.

References:

1. Sanjay Vijendran interview, Insider's guide to energy podcast, 3.Apr.23
2. F. Wombacher, M. Rehkämper, K. Metzger, A. Bischoff and C. Münker, Geochim. Cosmochim. Acta, 2008, 72, 646–667.
3. J. A. Dallas, S. Raval, S. Saydam and A. G. Dempster, Acta Astronaut., 2021, 186, 74–86.
4. S. D. Ross, Near-Earth Asteroid Mining, 2001.
5. X. Duan and M. Regelous, *J. Anal. At. Spectrom.*, 2014, **29**, 2379–2387.
6. R. Burgess, I. P. Wright and C. T. Pillinger, Meteoritics, 1991, 26, 55–64.
7. N. L. Chabot, *Geochim. Cosmochim. Acta*, 2004, **68**, 3607–3618.
8. N. Spalatu, Development of CdTe absorber layer for thin-film solar cells, TUT Press, Tallinn, 2017.
9. D. Suthar, S. Chuhadiya , R. Sharma, Himanshu and M. S. Dhaka, Mater. Adv., 2022, 3, 8081-8107
10. B. E. McCandless, W. A. Buchanan, C. P. Thompson, G. Sriramagiri, R. J. Lovelett, J. Duenow, D. Albin, S. Jensen, E. Colegrove, J. Moseley, H. Moutinho, S. Harvey, M. Al-Jassim and W. K. Metzger, *Sci. Reports 2018 81*, 2018, **8**, 1–13.

Characterisation of Water contaminated by Lunar Regolith and Selection of an associated Water Purification System

Victoria Pesch*[1,2], Rieke Freer[1], Luca Kiewiet[1] and Paul Zabel[1]

[1]German Aerospace Center (DLR), Institute of Space Systems, Bremen, Germany
[2]City University of Applied Sciences Bremen/Hochschule Bremen, Bremen, Germany
*Victoria.pesch@web.de

1. Introduction

In future lunar habitats, the contact between lunar dust and liquid water will be inevitable, as reported in the In-Situ Resource Utilization Gap Assessment Report, 2021 and the Dust Mitigation Gap Assessment Report, 2016. It is therefore necessary to understand and characterise water contaminated by lunar regolith. The experimental results provide a basis for the development of a lunar water simulant and associated water purification system.

2. Dissolution Experiments

The dust dissolution experiments were conducted using three different *ExoLith Lab* regolith simulants. For the dissolution experiments, 250mL of the aqueous solution was mixed with a defined simulant mass on an overhead shaker. After a specified time (two minutes up to three days) a sample was taken for measurement of pH and elemental concentrations of aluminium, calcium, iron, potassium, magnesium, manganese, sulphur, silicon, and titanium by inductively coupled plasma optical emission spectrometry (ICP-OES).
The experimental results are the element concentrations in the solution and the pH as a function of time. After three days, the turbidity of the solutions was also measured. The following figure gives an overview of the different experimental parameters. In total, 17 different test batches were performed and correlated in order to develop a water simulant and a possible water treatment system.

3. Test Batch Parameters of Lunar Regolith Dissolution Experiments

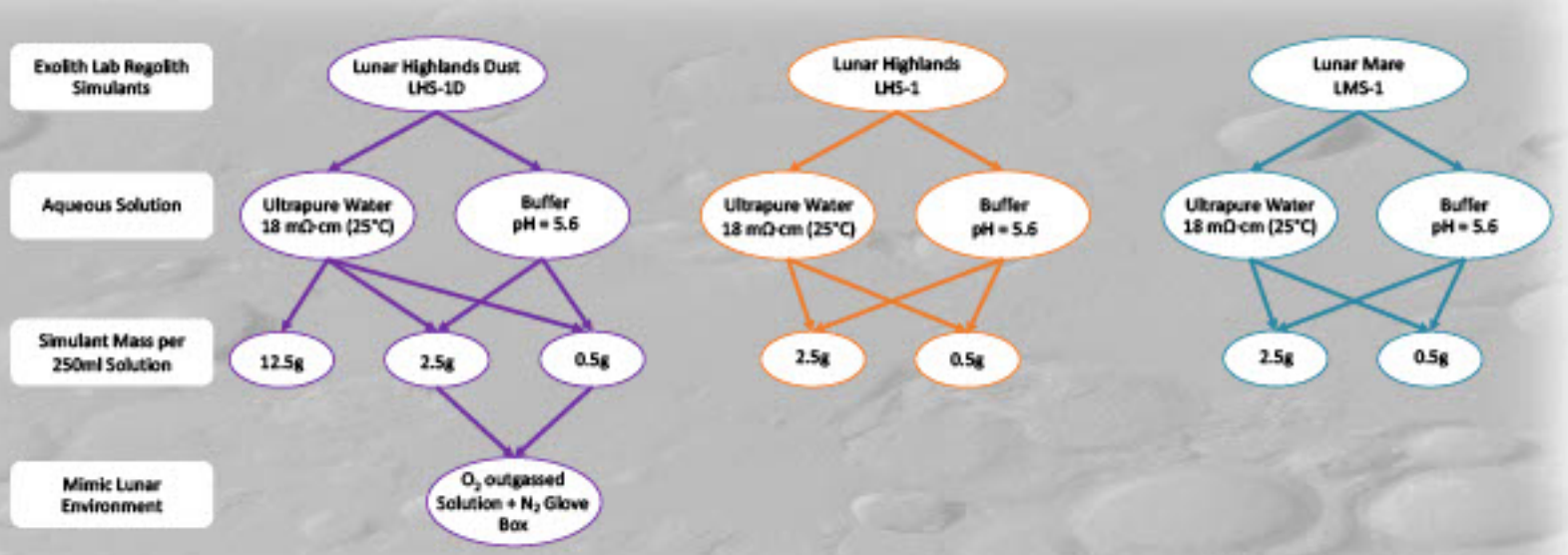

The experimental results are used to develop lunar water simulants and a water purification system.

4. Lunar Water Purification System

A schematic drawing of the lunar water purification system is shown on the right, with a picture of the experimental set-up below.

Steps of lunar water purification:

- Sedimentation in infusion bag
- Büchner vacuum filtration
- Precision pump pumps maximum possible amount of water into evaporation flask inside heating bath
- Steam condenses in condensator, cooled by chiller unit
- Distillate is collected in receiver flask
- Woulff bottle is used to protect vacuum pump and controller from polluted water
- Vacuum controller ensures correct pressure level
- Vacuum pump conveys liquid and steam

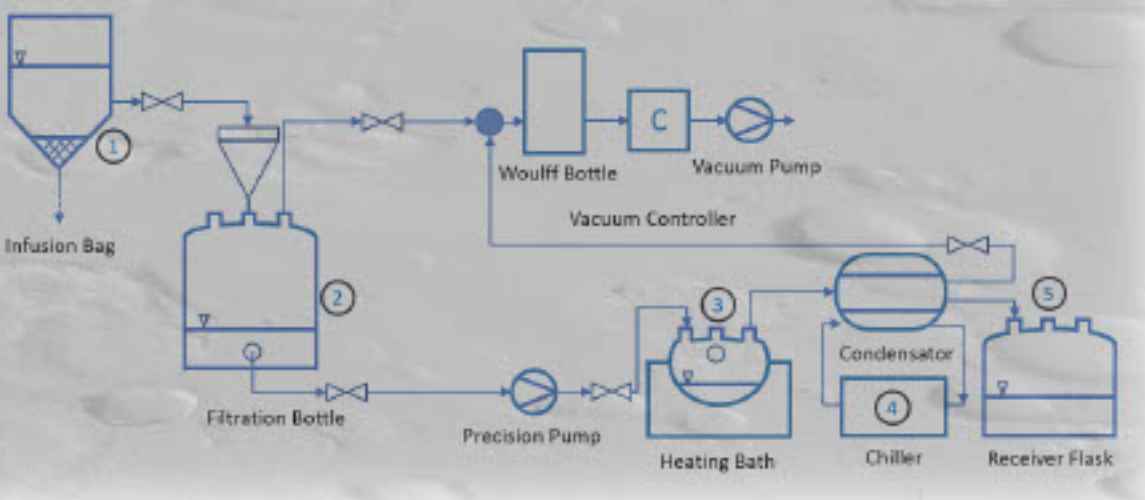

5. Measuring Points

The numbers in the schematic drawing in section 4 indicate the measuring points. Measuring point (1) is inside the infusion bag to determine the pH value and the electric conductivity. The second measuring point (2) is inside the filtration bottle, to determine the filling level. This is to protect the downstream precision pump from sucking in air. Inside the evaporation flask inside the heating bath (3) the temperature, the pH value, and the electric conductivity are measured. As a safety measurement to ensure proper function, the temperature of the cooling fluid inside the chiller (4) is measured. The last measuring point (5) is inside the receiver flask where the temperature, pH, and electric conductivity are measured.

Turbidity samples, from left to right: LMS-1 1:100, LMS-1 1:500, LHS-1 1:100, LHS-1 1:500

6. Outlook

In the future, the purification system can be optimised in terms of hardware and software. A system to control the sedimentation will be developed. At this stage, the sedimentation is determined via a time constant instead of using a sensor. Filters with different filter material or different mesh size can be used for Büchner vacuum filtration, resulting in different water purities. The temperature of the heating bath can be adjusted to optimise the distillation. To investigate different volatiles, simulants with different compositions, particle sizes and additional elements can be tested to simulate LCROSS volatiles. This will bring the lunar water purification system as close as possible to real lunar operating conditions.

This work is part of the DLR internally funded young investigator group "Synergetic Material Utilization" (SMU) established 2021 at the Institute of Space Systems in Bremen, Germany. The group focuses on research and development of ISRU technologies for Moon and Mars exploration.

Development of PtNi Catalyst for Reversible Fuel Cells for Space Applications

Vishnu PULLANGATIL[1,2,3], Vincent ROGE[2], Adrian Marie PHILLIPE[2], Jérôme GUILLOT[2], Christèle VERGNE[2], Emanuele BARBORINI[2], Marc MICHEL[2]

1. *European Space Resources Innovation Centre (esric.lu)*
2. *Luxembourg Institute of Science and Technology (list.lu)*
3. *University of Luxembourg (uni.lu)*

LUXEMBOURG SPACE RESOURCES WEEK

Introduction

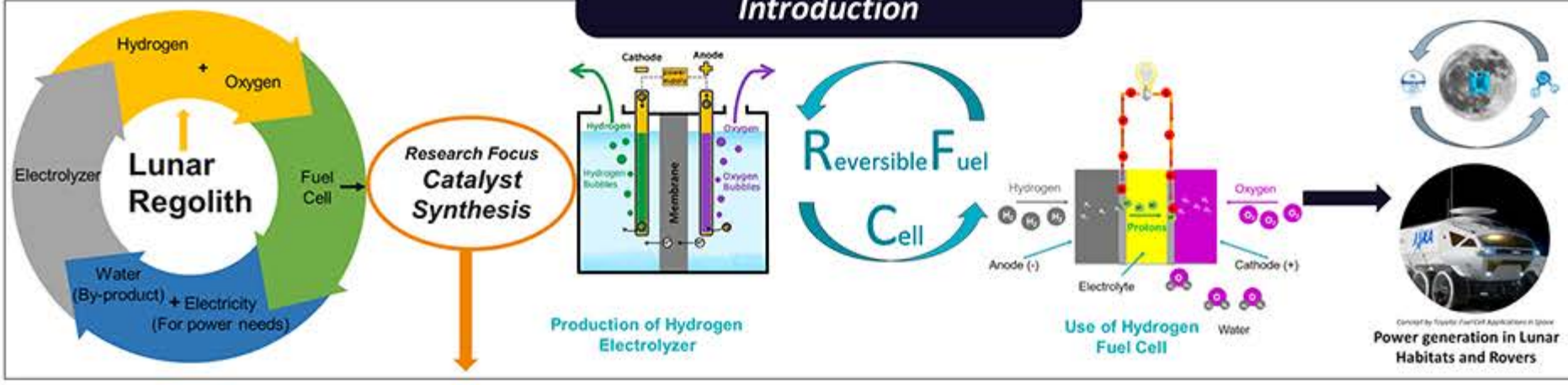

Catalyst Synthesis Methodology

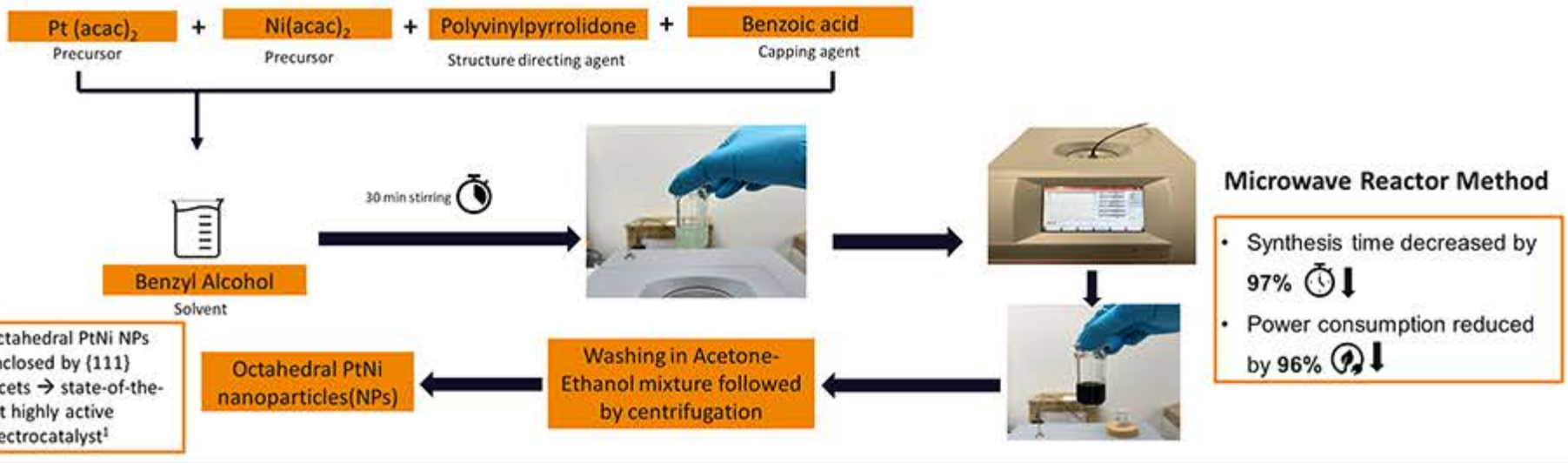

Results

Structural Characterization

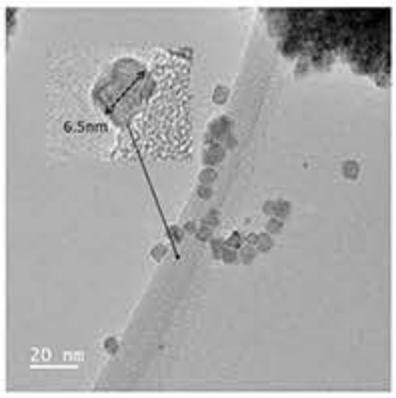

TEM micrographs hinting the Octahedral morphology of the catalyst NPs

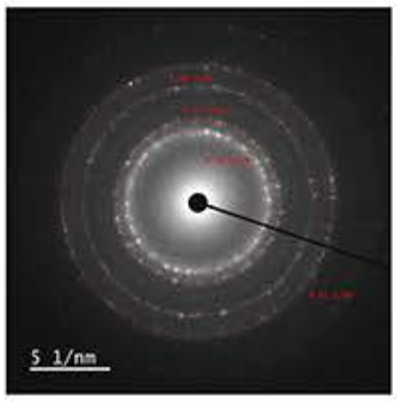

Selected Area Electron Diffraction(SAED) showing the polycrystallinity of NPs

Elemental Composition-XPS

Sample	C 1s %	Ni 2p %	O 1s %	Pt 4d %	Si 2p %	Ni:Pt
PtNi 220C	48.7	12.9	36.9	1.1	0.5	12.3
PtNi 240C	33.3	16.5	37.5	4.3	8.4	3.8

- Synthesis temperature plays a role in the relative Ni and Pt content

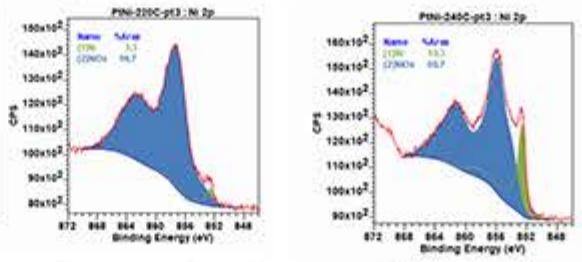

- Temperature has an impact on Oxidation state of Ni in catalyst

Cyclic Voltammetry

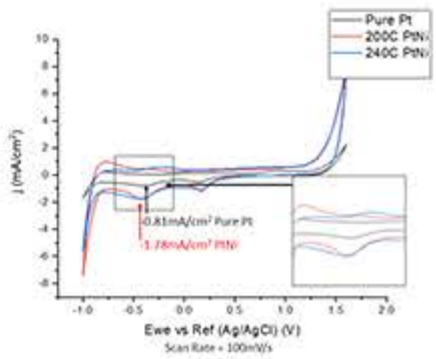

- Catalytic activity observed in PtNi alloy
- Intensity of current observed in PtNi> Pt thin film

Conclusion

- Fast PtNi Nanoparticles (NPs) synthesis in Microwave Reactor
- NPs have Crystalline Structure with an avg. particle size 6.5nm
- Improved Pt utilization
- Evidence of catalytic activity in PtNi catalyst

Next Steps

- Reducing NiO_x content to Ni metal in alloy
- Supporting the Catalyst on a Carbon support
- Studying Electrochemical Surface Area of PtNi

References

- *1. Jue Wang et al, Electrochimicia Acta, 2018*
- *Markus Nesselberger et al, JACS, 2011*

Vishnu P

esric

esric · esa · LUXEMBOURG SPACE AGENCY · LUXEMBOURG INSTITUTE OF SCIENCE AND TECHNOLOGY | LIST

April 2023